IV. Signal Processing

IV. Signal Processing

1. Continuous Signals

Assume a sinusoidal signal with a frequency of 1 kHz and an amplitude of $1\,\mu\mathrm{V}$.

If the amplifier has $\Delta f = 1\ \mathrm{MHz}$ bandwidth and an equivalent input noise of $e_n = 1\ \mathrm{nV}/\sqrt{\mathrm{Hz}}$, the total noise level

$$v_n = e_n\sqrt{\Delta f_n} = e_n\sqrt{\frac{p}{2}\Delta f} = 1.3\ m\mathrm{V}$$

and the signal-to-noise ratio is 0.8.

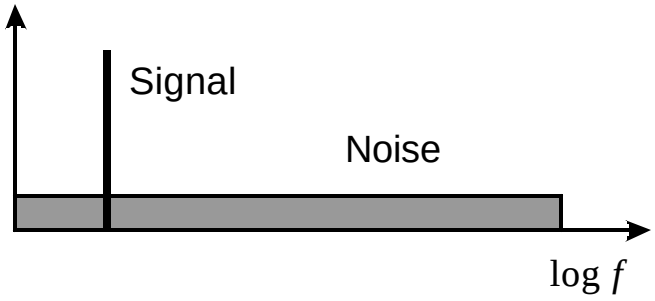

The bandwidth of 1 MHz is much greater than needed, as the signal is at 1 kHz, so we can add a simple RC low-pass filter with a cutoff frequency of 2 kHz. Then the total noise level

$$v_n = e_n\sqrt{\Delta f_n} = e_n\sqrt{\frac{p}{2}\Delta f} = 56\ \mathrm{nV}$$

and the signal-to-noise ratio is 18.

Since the signal is at a discrete frequency, one can also limit the lower cut-off frequency, i.e. use a narrow bandpass filter centered on the signal frequency.

For example, if the noise bandwidth is reduced to 100 Hz, the signal-to-noise ratio becomes 100.

How small a bandwidth can one use?

The bandwidth affects the settling time, i.e. the time needed for the system to respond to changes in signal amplitude.

Note that a signal of constant amplitude and frequency carries no information besides its presence. Any change in transmitted information requires either a change in amplitude, phase or frequency.

Recall from the discussion of the simple amplifier that a bandwidth limit corresponds to a response time

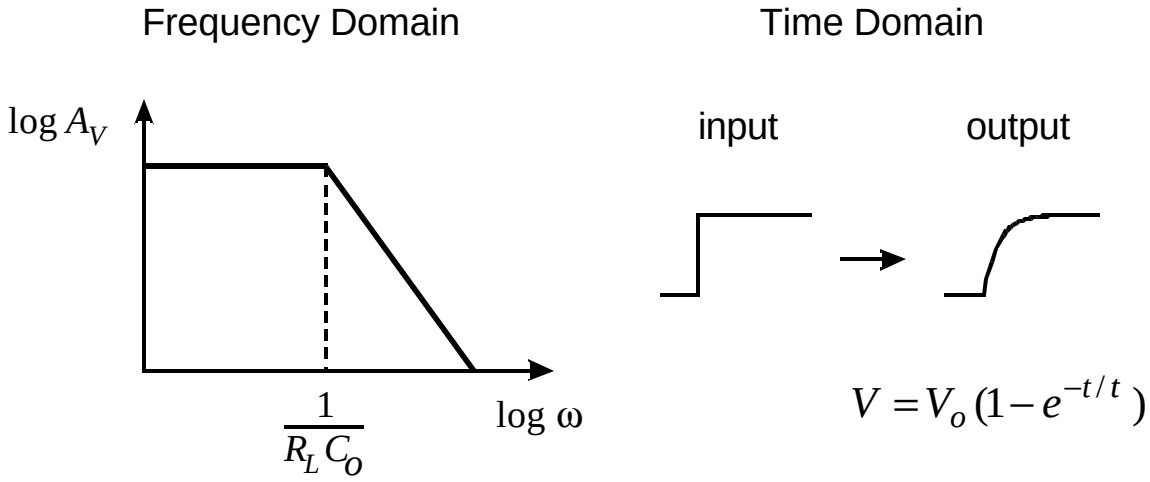

The time constant t corresponds to the upper cutoff frequency

$$t = \frac{1}{2p\ f_u}$$

This also applied to a bandpass filter. For example, consider a simple bandpass filter consisting of a series LC resonant circuit. The circuit bandwidth is depends on the dissipative loss in the circuit, i.e. the equivalent series resistance.

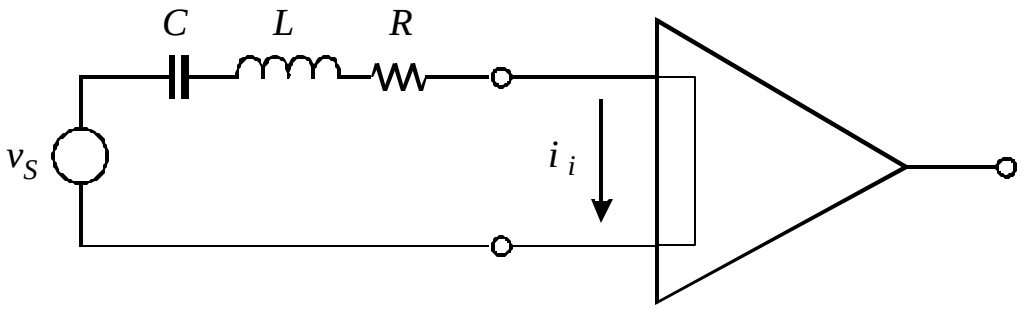

The bandwidth

$$\Delta w = \frac{w_0}{Q}$$

where

$$Q = \frac{w_0 L}{R}$$

To a good approximation the settling time

$$t = \frac{1}{\Delta w / 2}$$

Half the bandwidth enters, since the bandwidth is measured as the full width of the resonance curve, rather then the difference relative to the center frequency.

and the time dependence

$$I = I_o(1 - e^{-t/t})$$

The figure below shows a numerical simulation of the response when a sinusoidal signal of $w = 10^7$ radians is abruptly switched on and passed through an LC circuit with a bandwidth of 2 kHz
(i.e the dark area is formed by many cycles of the sinusoidal signal).

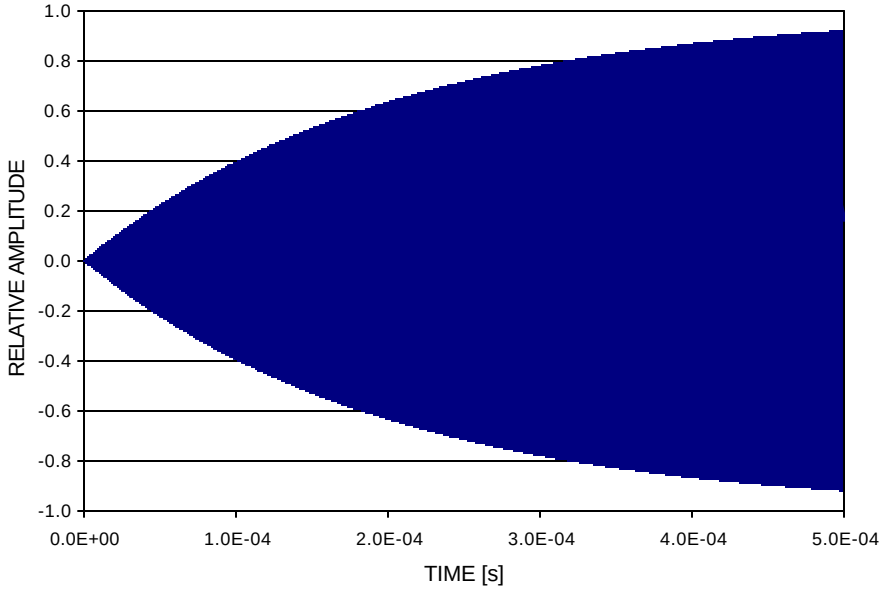

The signal attains 99% of its peak value after $4.6t$. For a bandwidth Δf = 2 kHz, $\Delta w = 4p \cdot 10^3$ radians and the settling time t = 160 μs.

Correspondingly, for the example used above a possible bandwidth Δf = 20 Hz for which the settling time is 16 ms.

- The allowable bandwidth is determined by the rate of change of the signal

2. Pulsed Signals

Two conflicting objectives:

1. Improve Signal-to-Noise Ratio S/N

   Restrict bandwidth to match measurement time

   ⇒ Increase pulse width

   Typically, the pulse shaper transforms a narrow detector current pulse to

   a broader pulse
   (to reduce electronic noise),

   with a gradually rounded maximum at the peaking time T_P
   (to facilitate measurement of the amplitude)

Detector Pulse ⇒ Shaper Output

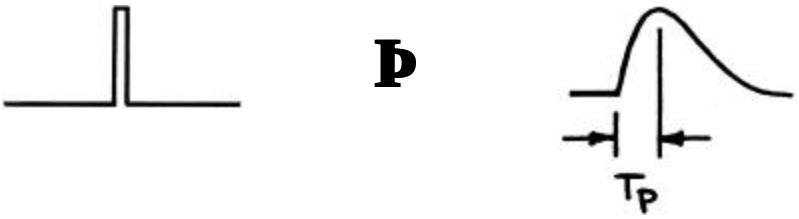

If the shape of the pulse does not change with signal level, the peak amplitude is also a measure of the energy, so one often speaks of pulse-height measurements or pulse height analysis. The pulse height spectrum is the energy spectrum.

2. Improve Pulse Pair Resolution

- Decrease pulse width

Pulse pile-up distorts amplitude measurement

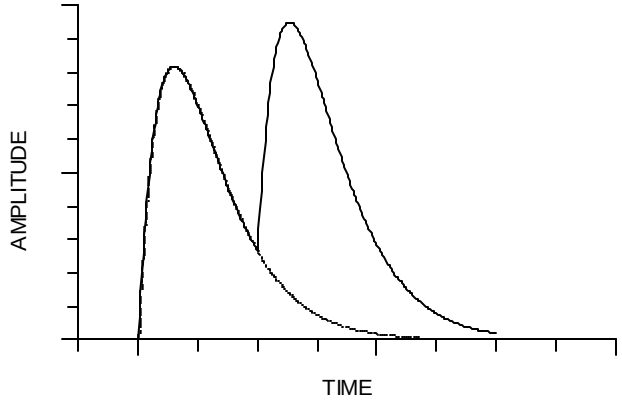

Reducing pulse shaping time to 1/3 eliminates pile-up.

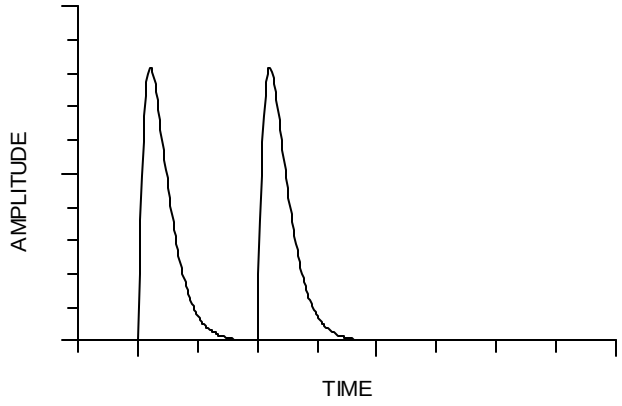

Necessary to find balance between these conflicting requirements. Sometimes minimum noise is crucial, sometimes rate capability is paramount.

Usually, many considerations combined lead to a "non-textbook" compromise.

- *"Optimum shaping" depends on the application!*

- Shapers need not be complicated –
  Every amplifier is a pulse shaper!

Simple Example: CR-RC Shaping

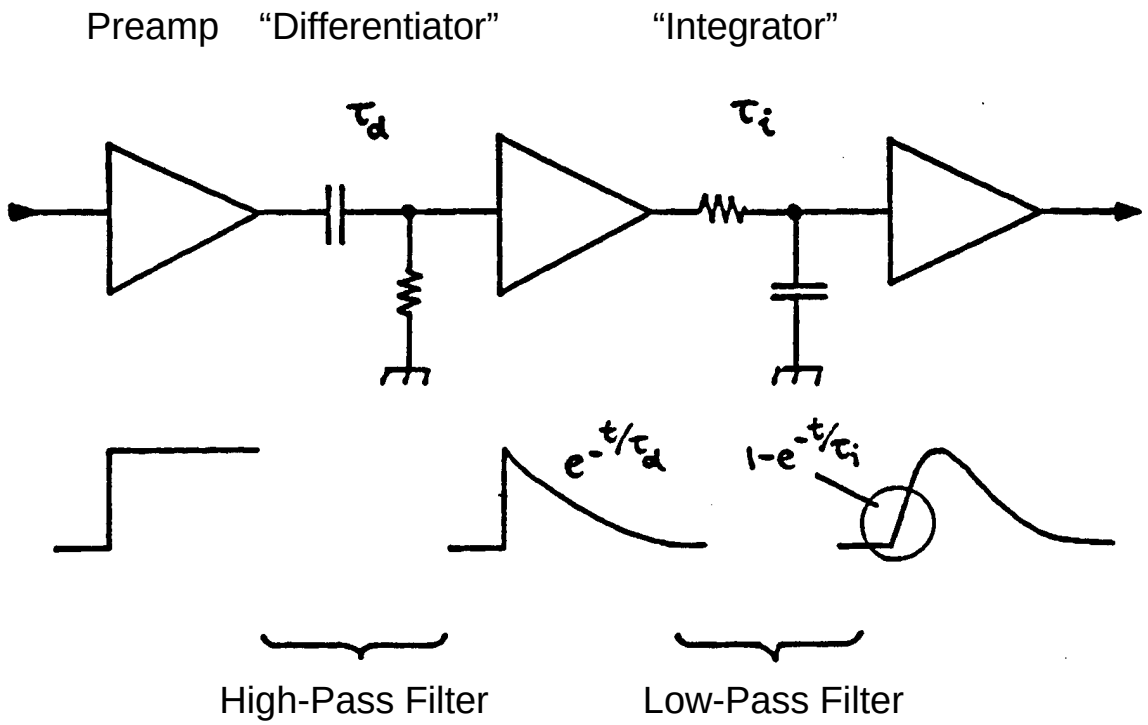

Simple arrangement: Noise performance only 36% worse than optimum filter with same time constants.

Þ Useful for estimates, since simple to evaluate

Key elements

- lower frequency bound
- upper frequency bound
- signal attenuation

important in all shapers.

Pulse Shaping and Signal-to-Noise Ratio

Pulse shaping affects both the

- total noise

and

- peak signal amplitude

at the output of the shaper.

Equivalent Noise Charge

Inject known signal charge into preamp input
(either via test input or known energy in detector).

Determine signal-to-noise ratio at shaper output.

Equivalent Noise Charge $\equiv$ Input charge for which $S/N = 1$

Effect of relative time constants

Consider a *CR-RC* shaper with a fixed differentiator time constant of 100 ns.

Increasing the integrator time constant lowers the upper cut-off frequency, which decreases the total noise at the shaper output.

However, the peak signal also decreases.

CR-RC SHAPER
FIXED DIFFERENTIATOR TIME CONSTANT = 100 ns
INTEGRATOR TIME CONSTANT = 10, 30 and 100 ns

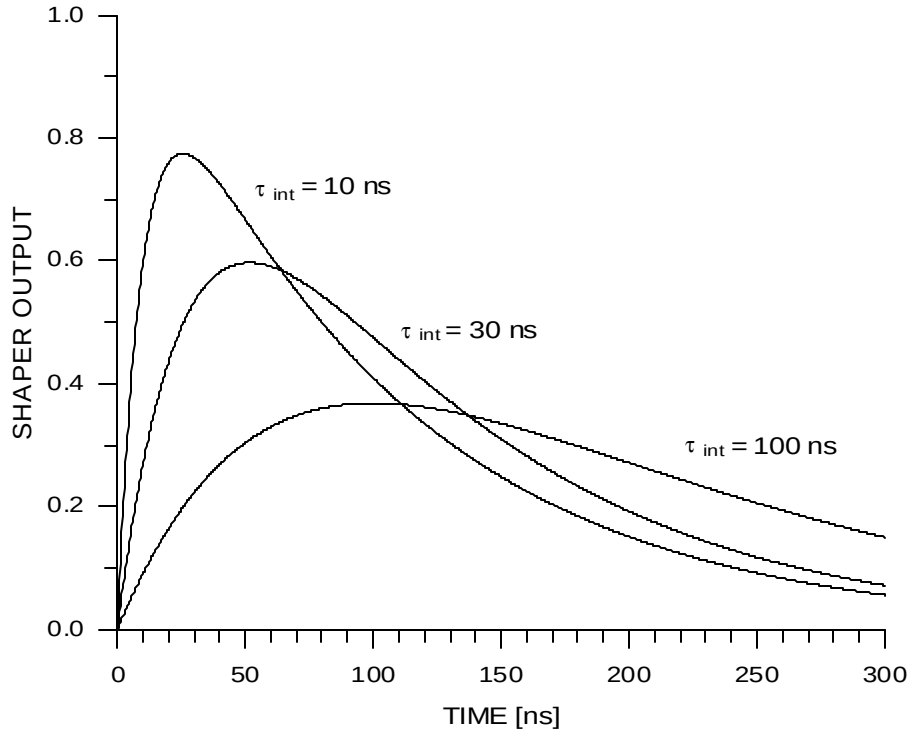

Still keeping the differentiator time constant fixed at 100 ns, the next set of graphs shows the variation of output noise and peak signal as the integrator time constant is increased from 10 to 100 ns.

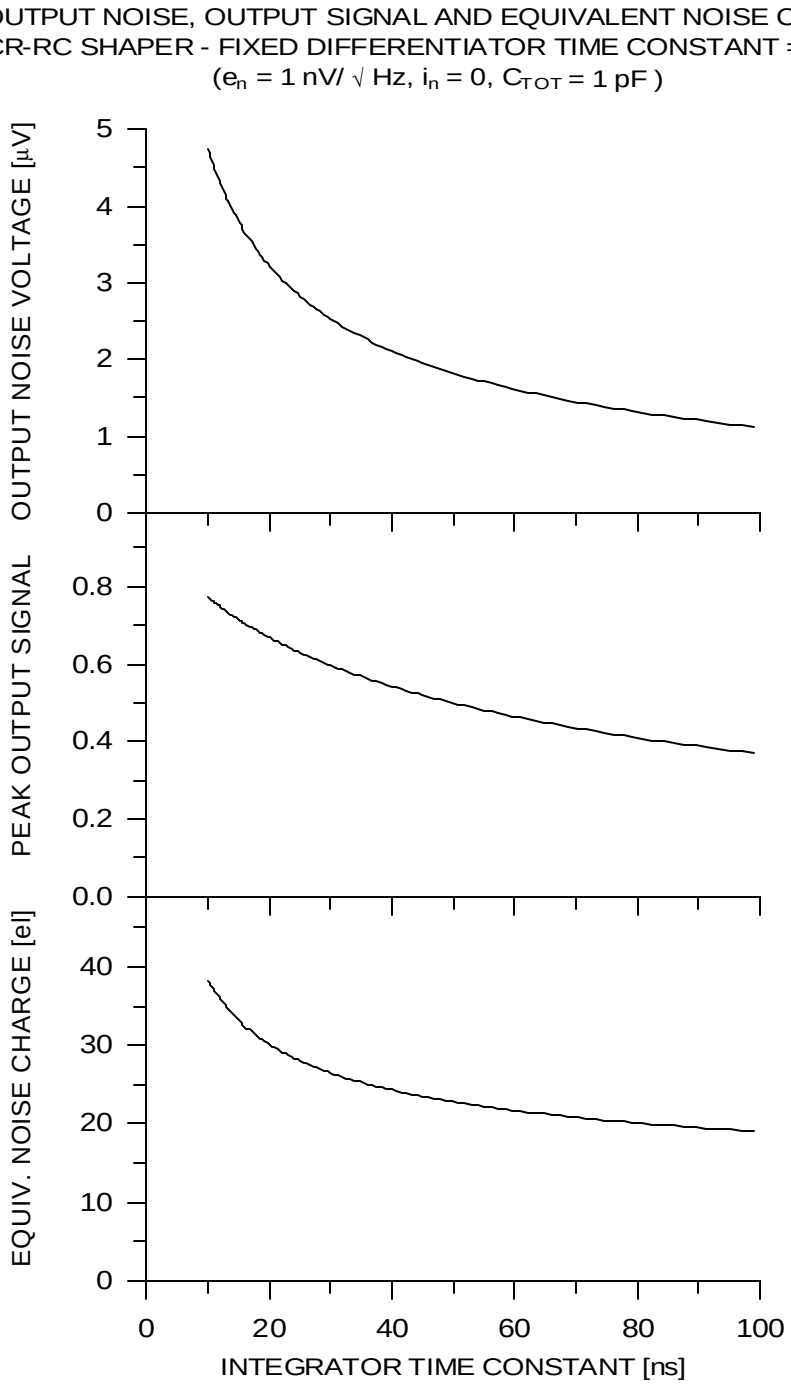

$$\frac{V_{no}(100\,\text{ns})}{V_{no}(10\,\text{ns})} = \frac{1}{4.2}$$

$$\frac{V_{so}(100\,\text{ns})}{V_{so}(10\,\text{ns})} = \frac{1}{2.1}$$

The roughly 4-fold decrease in noise is partially compensated by the 2-fold reduction in signal, so that

$$\frac{Q_n(100\,\text{ns})}{Q_n(10\,\text{ns})} = \frac{1}{2}$$

For comparison, consider the same *CR-RC* shaper with the integrator time constant fixed at 10 ns and the differentiator time constant variable.

As the differentiator time constant is reduced, the peak signal amplitude at the shaper output decreases.

CR-RC SHAPER
FIXED INTEGRATOR TIME CONSTANT = 10 ns
DIFFERENTIATOR TIME CONSTANT = ∞, 100, 30 and 10 ns

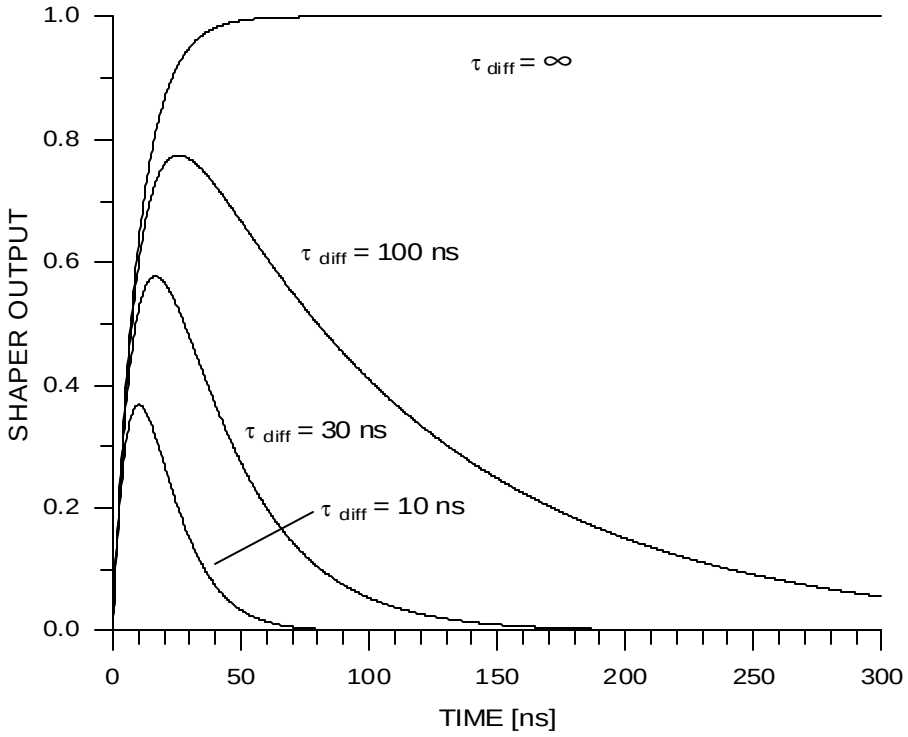

Note that the need to limit the pulse width incurs a significant reduction in the output signal.

Even at a differentiator time constant t_{diff} = 100 ns = 10 t_{int} the output signal is only 80% of the value for $t_{diff} = \infty$, i.e. a system with no low-frequency roll-off.

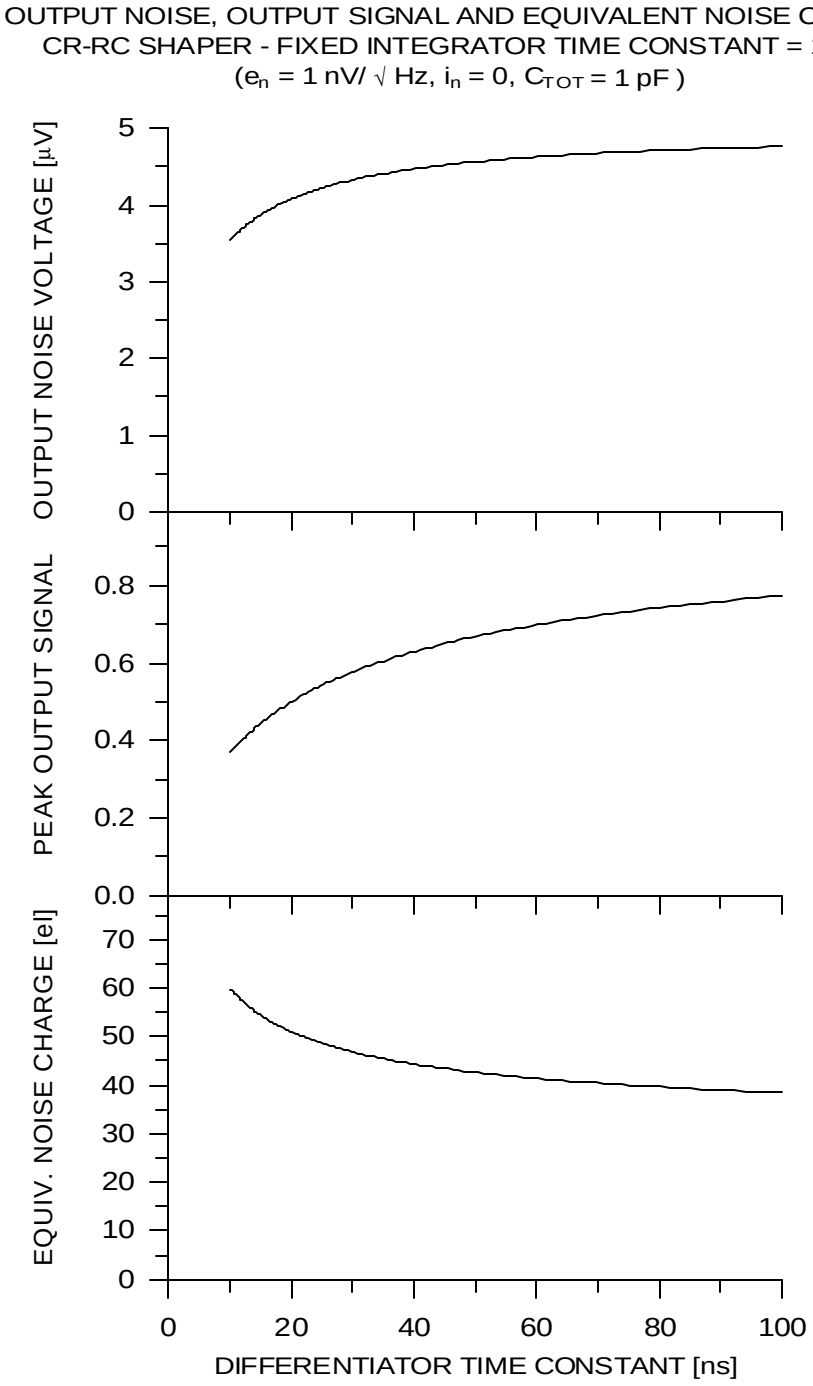

$$\frac{V_{no}(100\,\text{ns})}{V_{no}(10\,\text{ns})} = 1.3$$

$$\frac{V_{so}(100\,\text{ns})}{V_{so}(10\,\text{ns})} = 2.1$$

Although the noise grows as the differentiator time constant is increased from 10 to 100 ns, it is outweighed by the increase in signal level, so that the net signal-to-noise ratio improves.

$$\frac{Q_n(100\,\text{ns})}{Q_n(10\,\text{ns})} = \frac{1}{1.6}$$

Summary

To evaluate shaper noise performance

- Noise spectrum alone is inadequate

Must also

- Assess effect on signal

Signal amplitude is also affected by the relationship of the shaping time to the detector signal duration.

If peaking time of shaper < collection time

- signal loss (“ballistic deficit”)

Ballistic Deficit

Loss in Pulse Height (and Signal-to-Noise Ratio) if Peaking Time of Shaper < Detector Collection Time

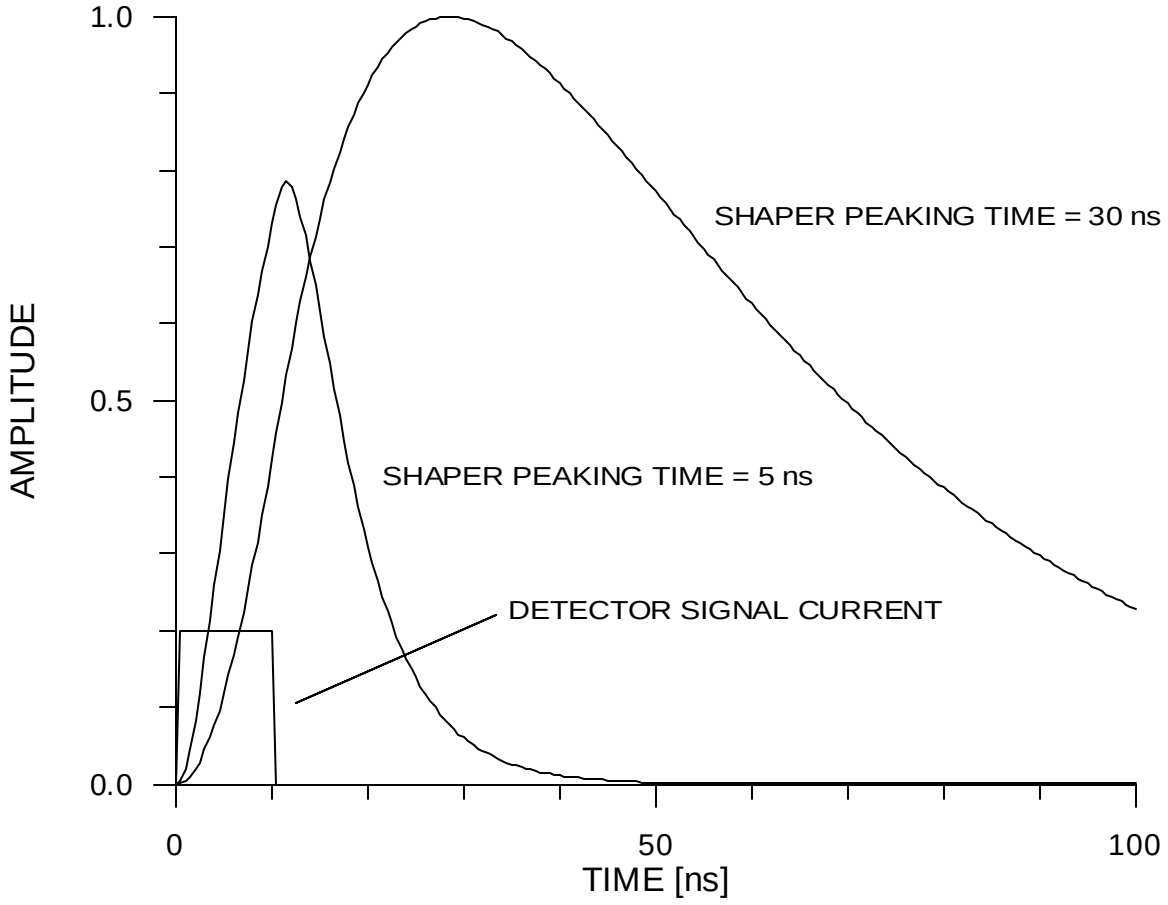

Note that although the faster shaper has a peaking time of 5 ns, the response to the detector signal peaks after full charge collection.

3. Evaluation of Equivalent Noise Charge

A. Experiment

Inject an input signal with known charge using a pulse generator set to approximate the detector signal (possible ballistic deficit). Measure the pulse height spectrum.

peak centroid ⇒ signal magnitude

peak width ⇒ noise (FWHM= 2.35 rms)

If pulse-height digitization is not practical:

1. Measure total noise at output of pulse shaper
   a) measure the total noise power with an rms voltmeter of sufficient bandwidth
      or
   b) measure the spectral distribution with a spectrum analyzer and integrate (the spectrum analyzer provides discrete measurement values in N frequency bins Df_n)

$$V_{no} = \sqrt{\sum_{n=0}^{N} \left(v_{no}^2(n) \cdot \Delta f \right)}$$

The spectrum analyzer shows if "pathological" features are present in the noise spectrum.

2. Measure the magnitude of the output signal V_{so} for a known input signal, either from detector or from a pulse generator set up to approximate the detector signal.

3. Determine signal-to-noise ratio $S/N = V_{so} / V_{no}$

   and scale to obtain the equivalent noise charge

$$Q_n = \frac{V_{no}}{V_{so}} Q_s$$

B. Numerical Simulation (e.g. SPICE)

This can be done with the full circuit including all extraneous components. Procedure analogous to measurement.

1. Calculate the spectral distribution and integrate

$$V_{no} = \sqrt{\sum_{n=0}^{N} v_{no}^2(n) \cdot \Delta f}$$

2. Determine the magnitude of output signal V_{so} for an input that approximates the detector signal.

3. Calculate the equivalent noise charge

$$Q_n = \frac{V_{no}}{V_{so}} Q_s$$

C. Analytical Simulation

1. Identify individual noise sources and refer to input
2. Determine the spectral distribution at input for each source k

$$v_{ni,k}^2(f)$$

3. Calculate the total noise at shaper output ($G(f)$ = gain)

$$V_{no} = \sqrt{\int_0^\infty |G(f)|^2 \left(\sum_k v_{ni,k}^2(f) \right) df} \equiv \sqrt{\int_0^\infty |G(w)|^2 \left(\sum_k v_{n\,i,k}^2(w) \right) dw}$$

4. Determine the signal output V_{so} for a known input charge Q_s and realistic detector pulse shape.
5. Equivalent noise charge

$$Q_n = \frac{V_{no}}{V_{so}} Q_s$$

Analytical Analysis of a Detector Front-End

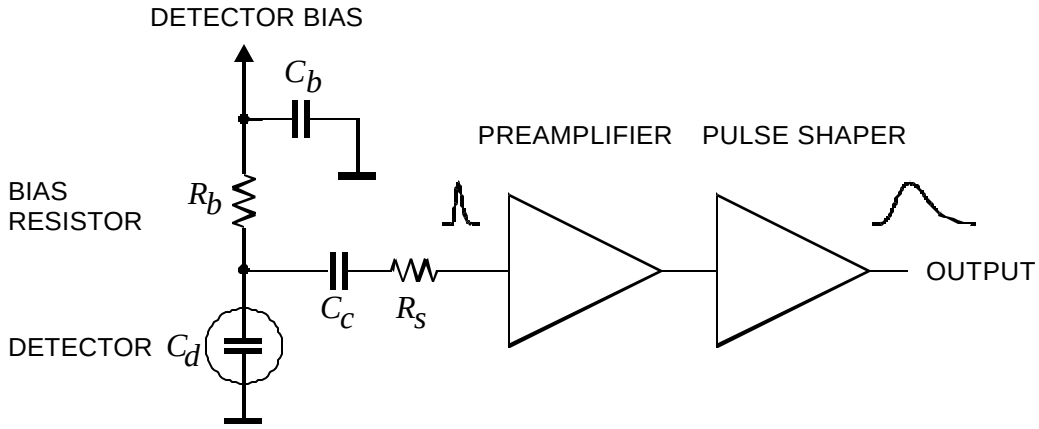

Detector bias voltage is applied through the resistor R_B. The bypass capacitor C_B serves to shunt any external interference coming through the bias supply line to ground. For AC signals this capacitor connects the "far end" of the bias resistor to ground, so that R_B appears to be in parallel with the detector.

The coupling capacitor C_C in the amplifier input path blocks the detector bias voltage from the amplifier input (which is why a capacitor serving this role is also called a "blocking capacitor").

The series resistor R_S represents any resistance present in the connection from the detector to the amplifier input. This includes

- the resistance of the detector electrodes
- the resistance of the connecting wires
- any resistors used to protect the amplifier against large voltage transients ("input protection")
- ... etc.

Equivalent circuit for noise analysis

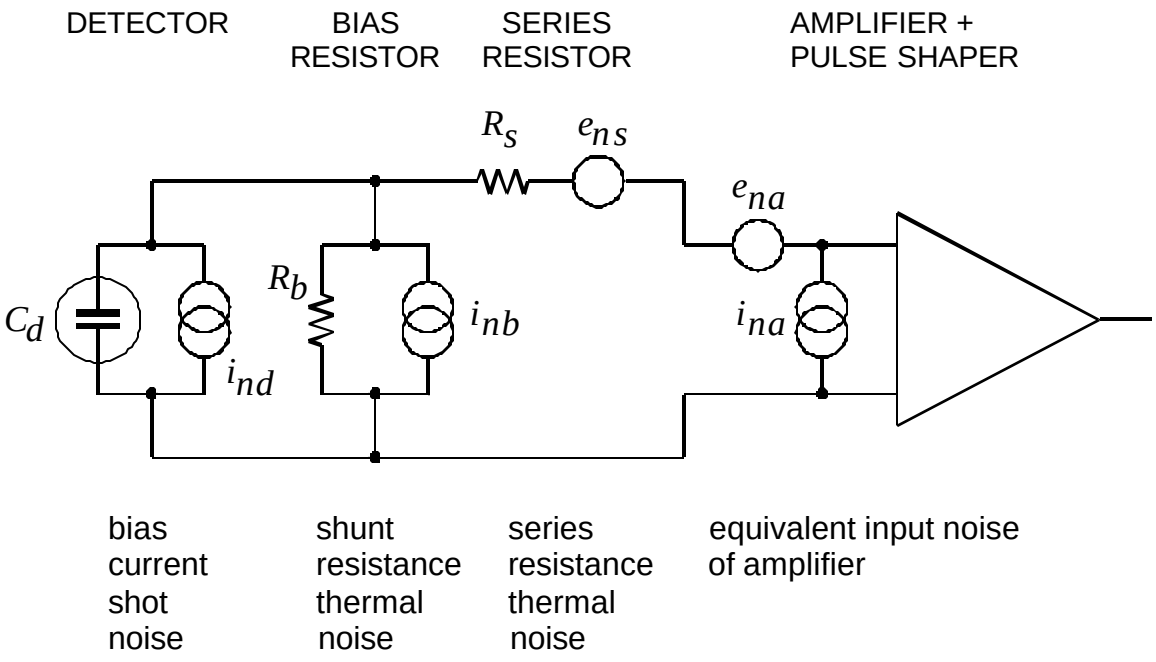

In this example a voltage-sensitive amplifier is used, so all noise contributions will be calculated in terms of the noise voltage appearing at the amplifier input.

Resistors can be modeled either as voltage or current generators.

- Resistors in parallel with the input act as current sources
- Resistors in series with the input act as voltage sources.

Steps in the analysis:

1. Determine the frequency distribution of the noise voltage presented to the amplifier input from all individual noise sources
2. Integrate over the frequency response of a CR-RC shaper to determine the total noise output.
3. Determine the output signal for a known signal charge and calculate equivalent noise charge (signal charge for S/N= 1)

Noise Contributions

1. Detector bias current

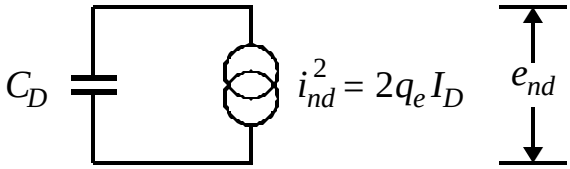

This model results from two assumptions:

1. The input impedance of the amplifier is infinite

2. The shunt resistance R_P is much larger than the capacitive reactance of the detector in the frequency range of the pulse shaper.

   Does this assumption make sense?

   If R_P is too small, the signal charge on the detector capacitance will discharge before the shaper output peaks. To avoid this

$$R_P C_D >> t_P \approx \frac{1}{w_P}$$

   where w_P is the midband frequency of the shaper. Therefore,

$$R_P >> \frac{1}{w_P C_D}$$

   as postulated.

Under these conditions the noise current will flow through the detector capacitance, yielding the voltage

$$e_{nd}^2 = i_{nd}^2 \frac{1}{(w\,C_D)^2} = 2q_e I_D \frac{1}{(w\,C_D)^2}$$

- the noise contribution decreases with increasing frequency (shorter shaping time)

  Note: Although shot noise is "white", the resulting noise spectrum is strongly frequency dependent.

In the time domain this result is more intuitive. Since every shaper also acts as an integrator, one can view the total shot noise as the result of "counting electrons".

Assume an ideal integrator that records all charge uniformly within a time T. The number of electron charges measured is

$$N_e = \frac{I_D T}{q_e}$$

The associated noise is the fluctuation in the number of electron charges recorded

$$s_n = \sqrt{N_e} \propto \sqrt{T}$$

Does this also apply to an AC-coupled system, where no DC current flows, so no electrons are "counted"?

Since shot noise is a fluctuation, the current undergoes both positive and negative excursions. Although the DC component is not passed through an AC coupled system, the excursions are. Since, on the average, each fluctuation requires a positive and a negative zero crossing, the process of "counting electrons" is actually the counting of zero crossings, which in a detailed analysis yields the same result.

2. Parallel Resistance

Any shunt resistance R_P acts as a noise current source. In the specific example shown above, the only shunt resistance is the bias resistor R_b.

Additional shunt components in the circuit:

1. bias noise current source
   (infinite resistance by definition)
2. detector capacitance

The noise current flows through both the resistance R_P and the detector capacitance C_D.

- equivalent circuit

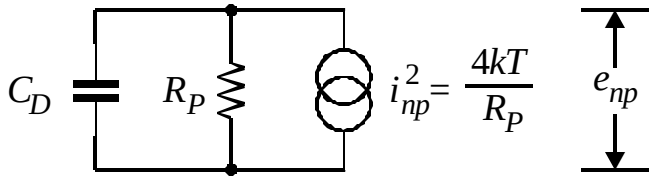

The noise voltage applied to the amplifier input is

$$e_{np}^2 = \frac{4kT}{R_P}\left(\frac{R_P \cdot -i/wC_D}{R_P - i/wC_D}\right)^2$$

$$e_{np}^2 = 4kTR_P \frac{1}{1+(w R_P C_D)^2}$$

Comment:

Integrating this result over all frequencies yields

$$\int_0^\infty e_{np}^2(w)dw = \int_0^\infty \frac{4kTR_P}{1+(w\,R_PC_D)^2}\,dw = \frac{kT}{C_D}$$

which is independent of R_P. Commonly referred to as "kTC" noise, this contribution is often erroneously interpreted as the "noise of the detector capacitance".

An ideal capacitor has no thermal noise; all noise originates in the resistor.

So, why is the result independent of R_P?

R_P determines the primary noise, but also the noise bandwidth of this subcircuit. As R_P increases, its thermal noise increases, but the noise bandwidth decreases, making the total noise independent of R_P.

However,
If one integrates e_{np} over a bandwidth-limited system

$$E_n^2 = \int_0^\infty 4kTR_P \left|\frac{G(iw)}{1-iw\,R_PC_D}\right|^2 dw$$

the total noise decreases with increasing R_P.

3. Series Resistance

The noise voltage generator associated with the series resistance R_S is in series with the other noise sources, so it simply contributes

$$e_{nr}^2 = 4kTR_S$$

4. Amplifier input noise

The amplifier noise voltage sources usually are not physically present at the amplifier input. Instead the amplifier noise originates within the amplifier, appears at the output, and is referred to the input by dividing the output noise by the amplifier gain, where it appears as a noise voltage generator.

$$e_{na}^2 = e_{nw}^2 + \frac{A_f}{f}$$

↑ “white noise”

↑ $1/f$ noise (can also originate in external components)

This noise voltage generator also adds in series with the other sources.

- Amplifiers generally also exhibit input current noise, which is physically present at the input. Its effect is the same as for the detector bias current, so the analysis given in 1. can be applied.

Determination of equivalent noise charge

1. Calculate total noise voltage at shaper output
2. Determine peak pulse height at shaper output for a known input charge
3. Input signal for which S/N=1 yields equivalent noise charge

First, assume a simple CR-RC shaper with equal differentiation and integration time constants $t_d = t_i = t$, which in this special case is equal to the peaking time.

The equivalent noise charge

$$Q_n^2 = \left(\frac{e^2}{8}\right)\left[\left(2q_e I_D + \frac{4kT}{R_P} + i_{na}^2\right)\cdot t + \left(4kTR_S + e_{na}^2\right)\cdot\frac{C_D^2}{t} + 4A_f C_D^2\right]$$

current noise	voltage noise	$1/f$ noise
$\propto t$	$\propto 1/t$	independent
independent of C_D	$\propto C_D^{\,2}$	of t
		$\propto C_D^{\,2}$

- Current noise is independent of detector capacitance, consistent with the notion of “counting electrons”.
- Voltage noise increases with detector capacitance (reduced signal voltage)
- $1/f$ noise is independent of shaping time.
  In general, the total noise of a $1/f$ source depends on the ratio of the upper to lower cutoff frequencies, not on the absolute noise bandwidth. If t_d and t_i are scaled by the same factor, this ratio remains constant.

The equivalent noise charge Q_n assumes a minimum when the current and voltage noise contributions are equal.

Typical Result

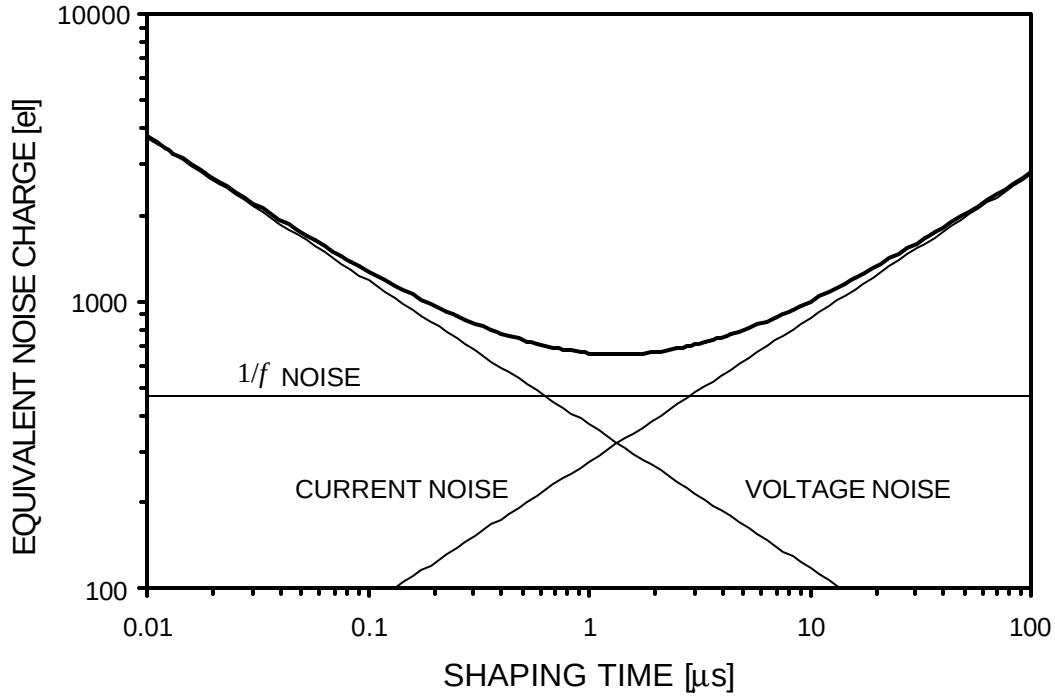

dominated by voltage noise current noise

For a CR-RC shaper the noise minimum obtains for $t_d = t_i = t$.

This criterion does not hold for more sophisticated shapers.

Caution: Even for a CR-RC shaper this criterion only applies when the differentiation time constant is the primary parameter, i.e. when the pulse width must be constrained.

When the rise time, i.e. the integration time constant, is the primary consideration, it is advantageous to make $t_d > t_i$, since the signal will increase more rapidly than the noise, as was shown previously

Numerical expression for the noise of a CR-RC shaper
(amplifier current noise negligible)

(note that some units are "hidden" in the numerical factors)

$$Q_n^2 = 12\, I_B\, t \;+\; 6\cdot 10^5 \frac{t}{R_P} + \; 3.6\cdot 10^4\, e_n^2 \frac{C^2}{t} \quad [\text{rms electrons}^2]$$

where

t shaping time constant [ns]

I_B detector bias current + amplifier input current [nA]

R_P input shunt resistance [kΩ]

e_n equivalent input noise voltage spectral density [nV/√Hz]

C total input capacitance [pF]

Q_n= 1 el corresponds to 3.6 eV in Si
2.9 eV in Ge

(see Spieler and Haller, IEEE Trans. Nucl. Sci. **NS-32** (1985) 419)

Note:

For sources connected in parallel, currents are additive.

For sources connected in series, voltages are additive.

- In the detector community voltage and current noise are often called “series” and “parallel” noise.

  The rest of the world uses equivalent noise voltage and current.

  Since they are physically meaningful, use of these widely understood terms is preferable.

CR-RC Shapers with Multiple Integrators

a. Start with simple CR-RC shaper and add additional integrators (n= 1 to n= 2, ... n= 8) with the same time constant t .

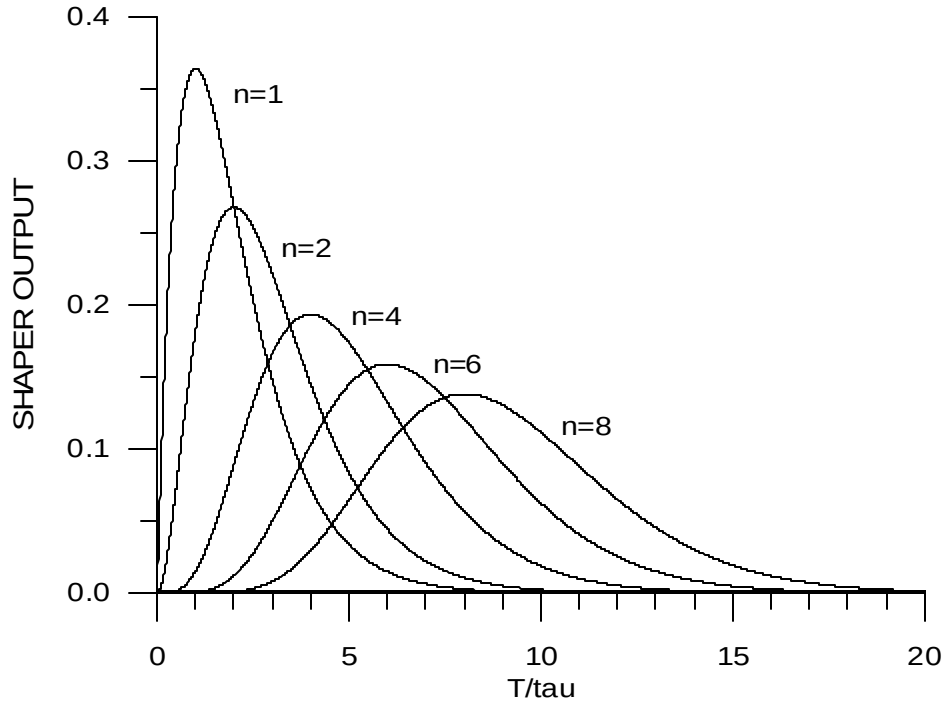

With additional integrators the peaking time T_p increases

$$T_p = n\,t$$

b) Time constants changed to preserve the peaking time
($t_n = t_{n=1}/n$)

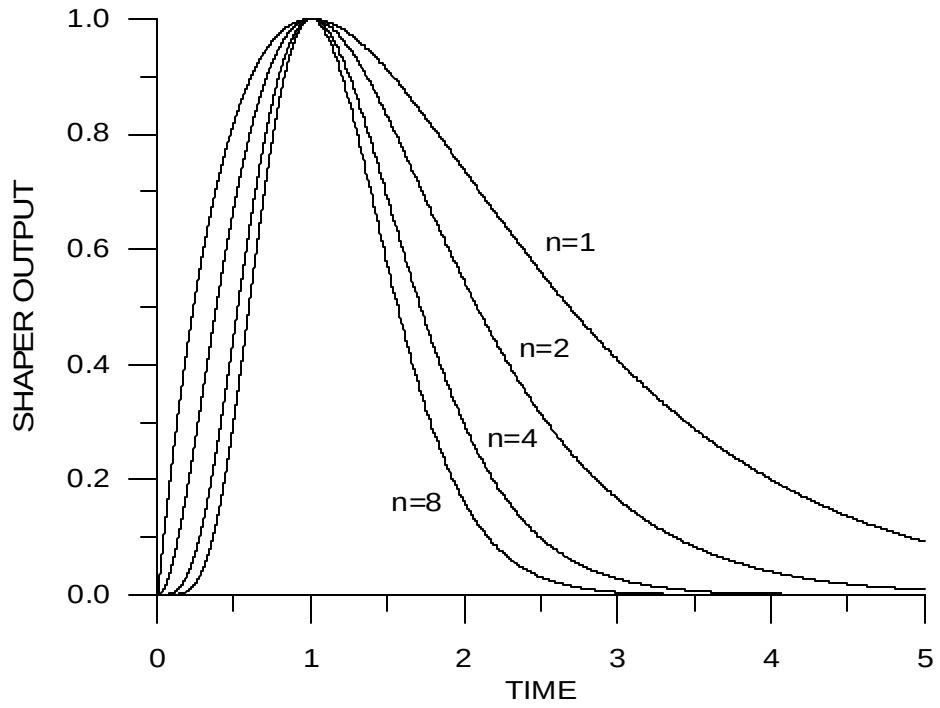

Increasing the number of integrators makes the output pulse more symmetrical with a faster return to baseline.

- improved rate capability at the same peaking time

Shapers with the equivalent of 8 RC integrators are common. Usually, this is achieved with active filters (i.e. circuitry that synthesizes the bandpass with amplifiers and feedback networks).

Examples

1. Photodiode Readout

(S. Holland, N. Wang, I. Kipnis, B. Krieger, W. Moses, LBNL)

Medical Imaging (Positron Emission Tomography)

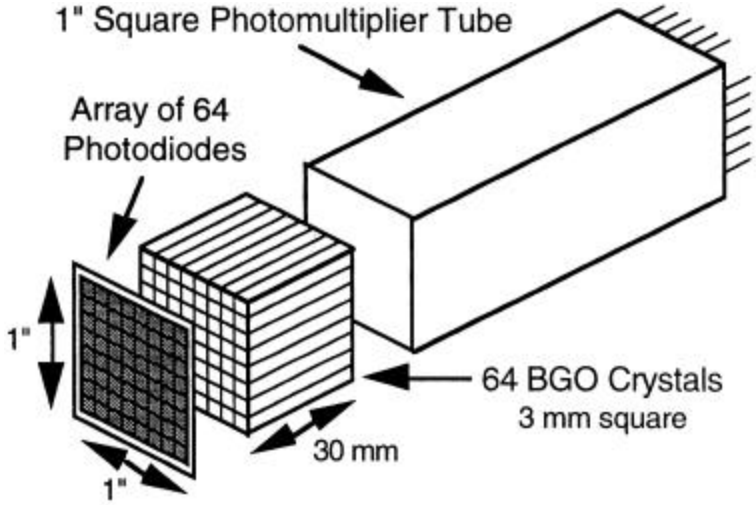

Read out 64 BGO crystals with one PMT (timing, energy) and tag crystal by segmented photodiode array.

Requires thin dead layer on photodiode to maximize quantum efficiency.

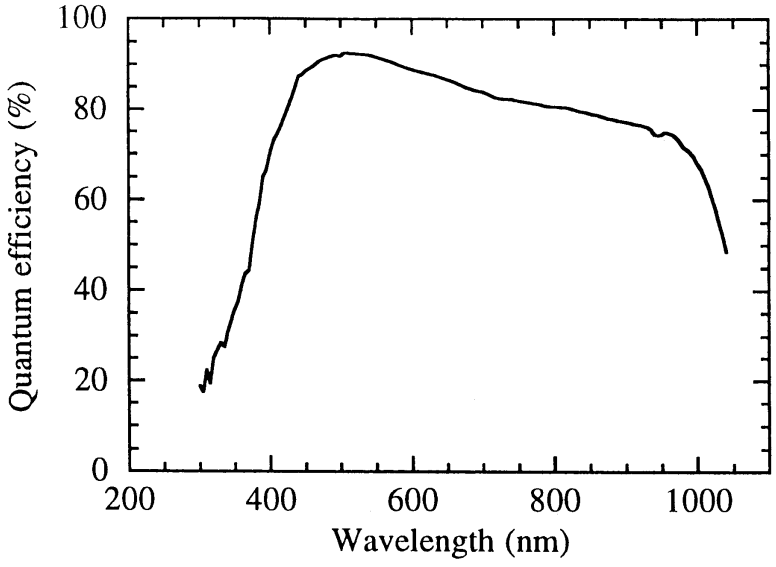

Thin electrode must be implemented with low resistance to avoid significant degradation of electronic noise.

Furthermore, low reverse bias current critical to reduce noise.

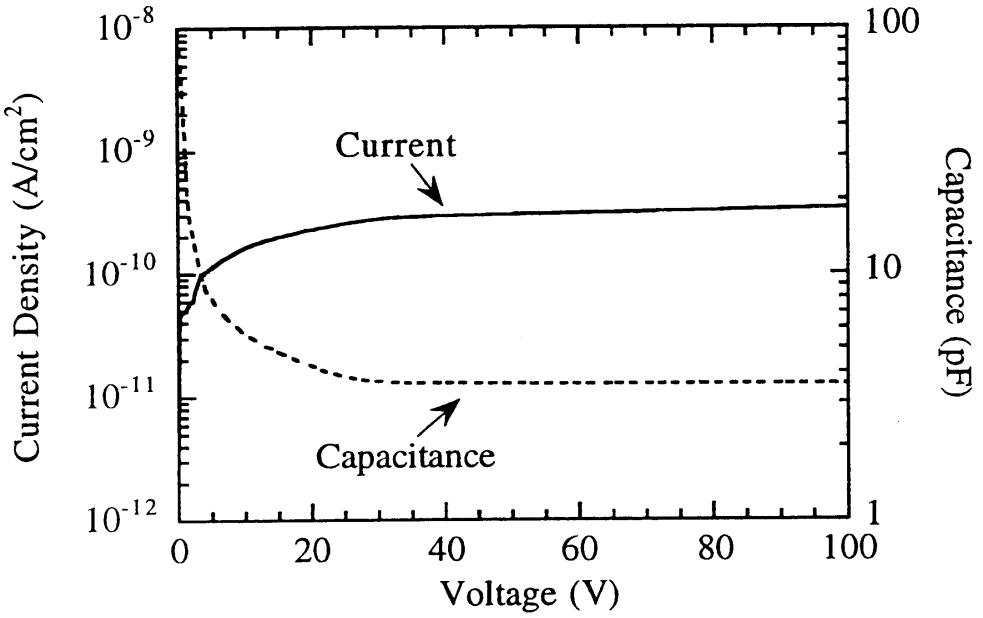

Photodiodes designed and fabricated in LBNL Microsystems Lab.

Front-end chip (preamplifier + shaper):

16 channels per chip

die size: 2 x 2 mm^2,
1.2 µm CMOS

continuously adjustable shaping time (0.5 to 50 µs)

gain: 100 mV per 1000 el.

Noise vs. shaping time

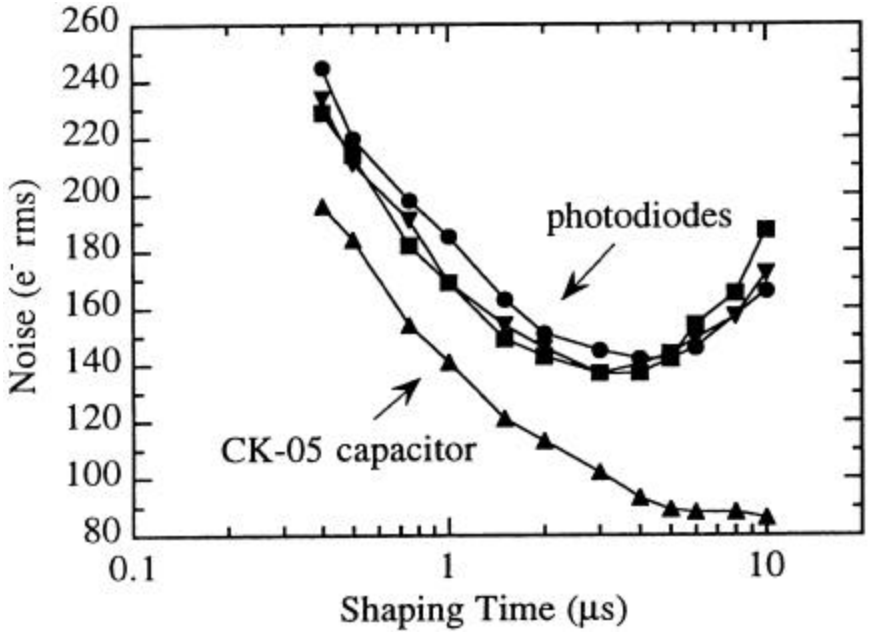

Energy spectrum with BGO scintillator

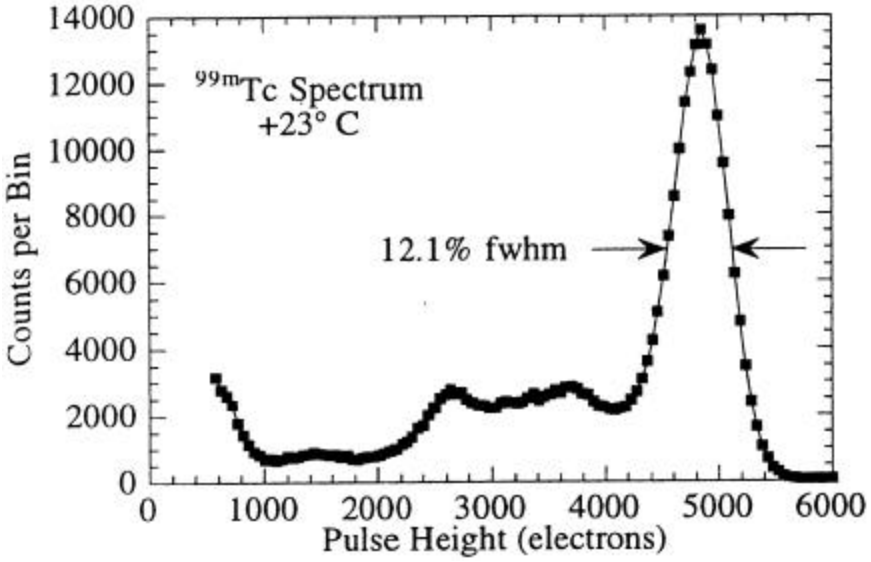

2. High-Rate X-Ray Spectroscopy

(B. Ludewigt, C. Rossington, I. Kipnis, B. Krieger, LBNL)

Use detector with multiple strip electrodes

not for position resolution

but for

segmentation ⇒ distribute rate over many channels

⇒ reduced capacitance

⇒ low noise at short shaping time

⇒ higher rate per detector element

For x-ray energies 5 – 25 keV ⇒ photoelectric absorption dominates
(signal on 1 or 2 strips)

Strip pitch: 100 µm Strip Length: 2 mm (matched to ALS)

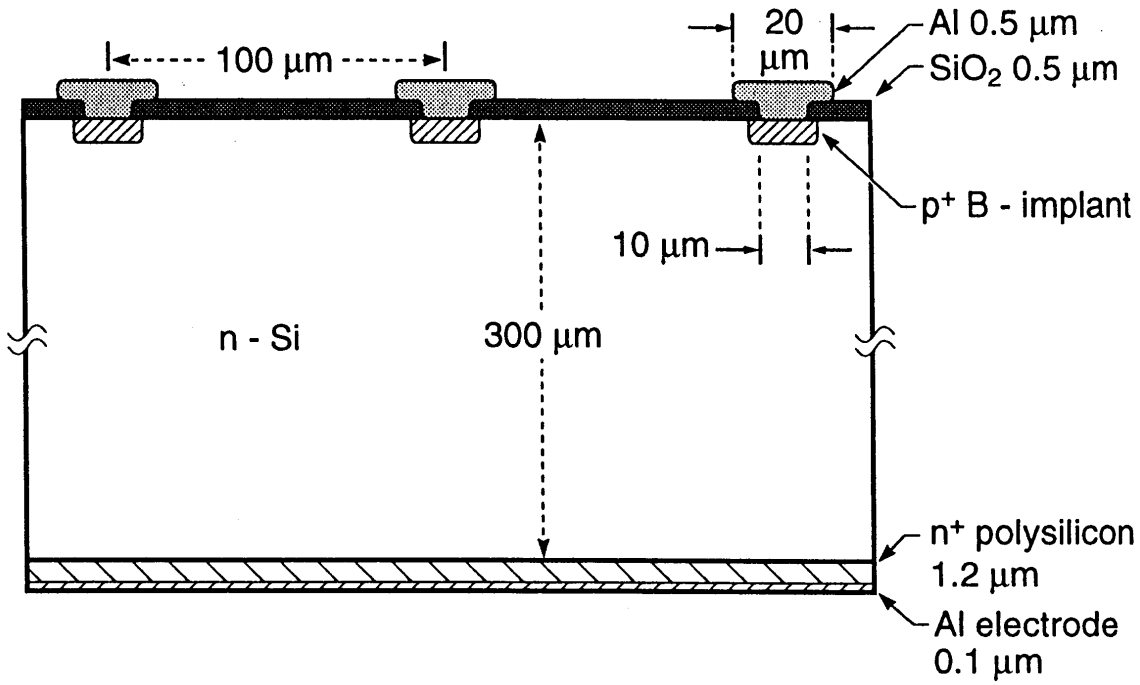

Readout IC tailored to detector

Preamplifier + CR-RC^2 shaper + cable driver to bank of parallel ADCs
(M. Maier + H. Yaver)

Preamplifier with pulsed reset.

Shaping time continuously variable 0.5 to 20 µs.

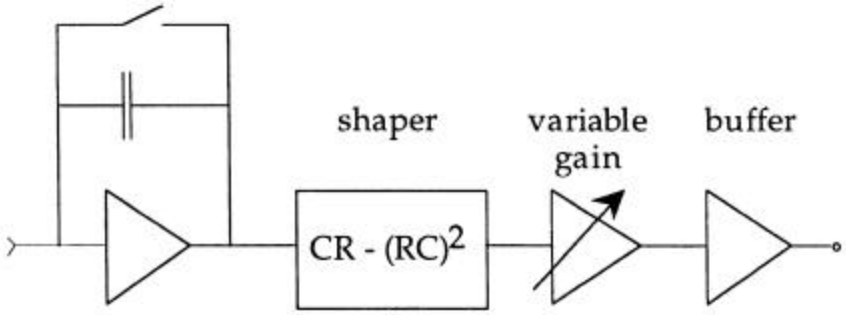

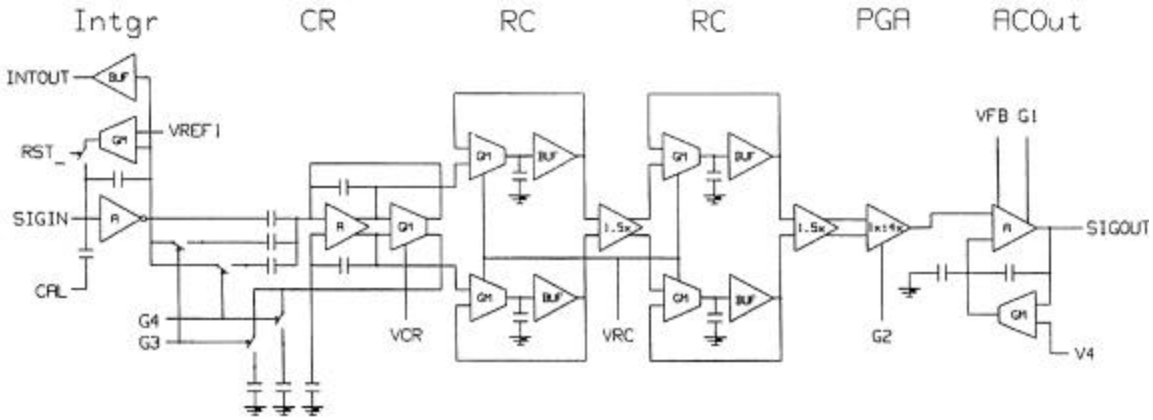

Chip wire-bonded to strip detector

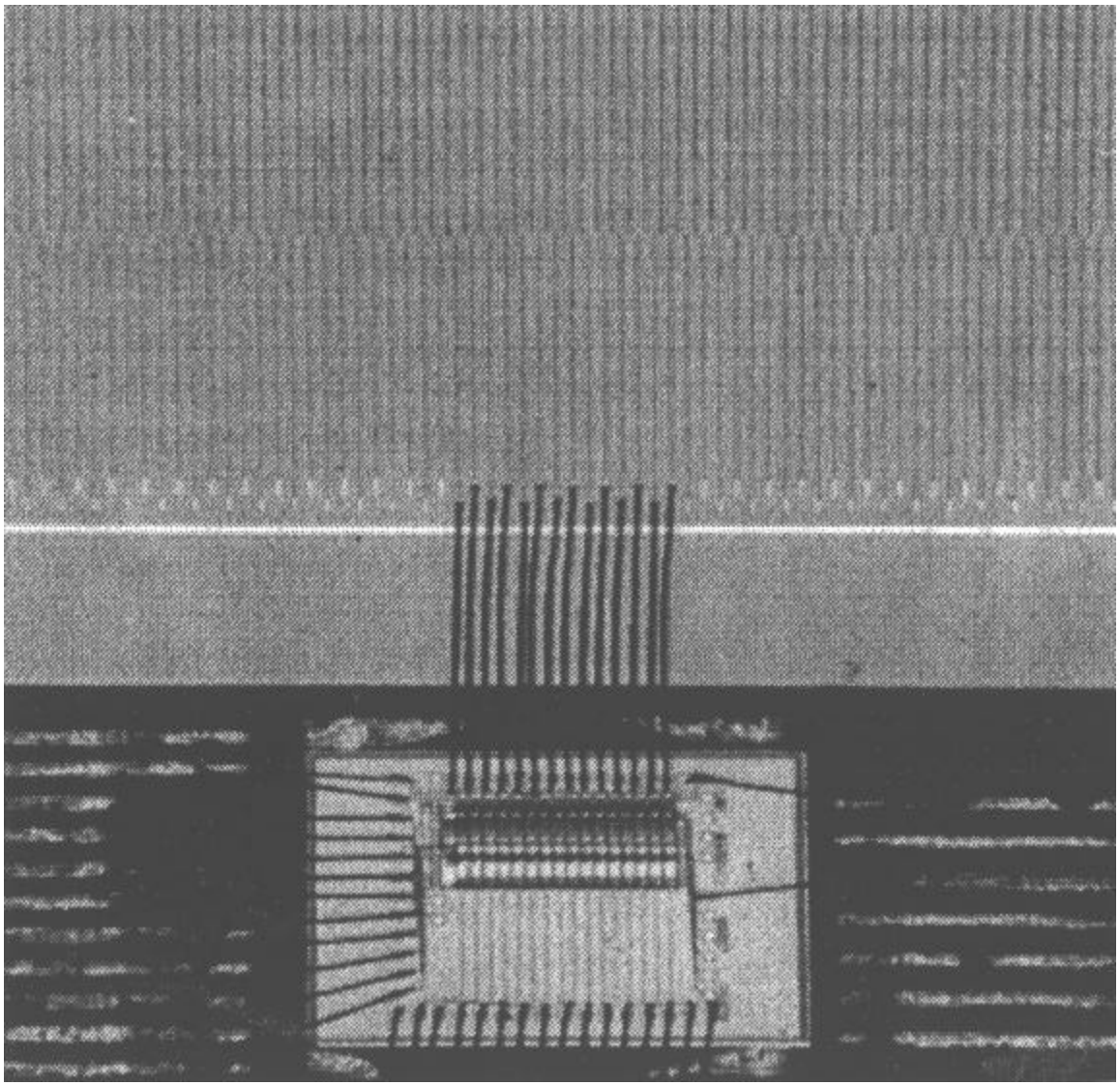

Initial results

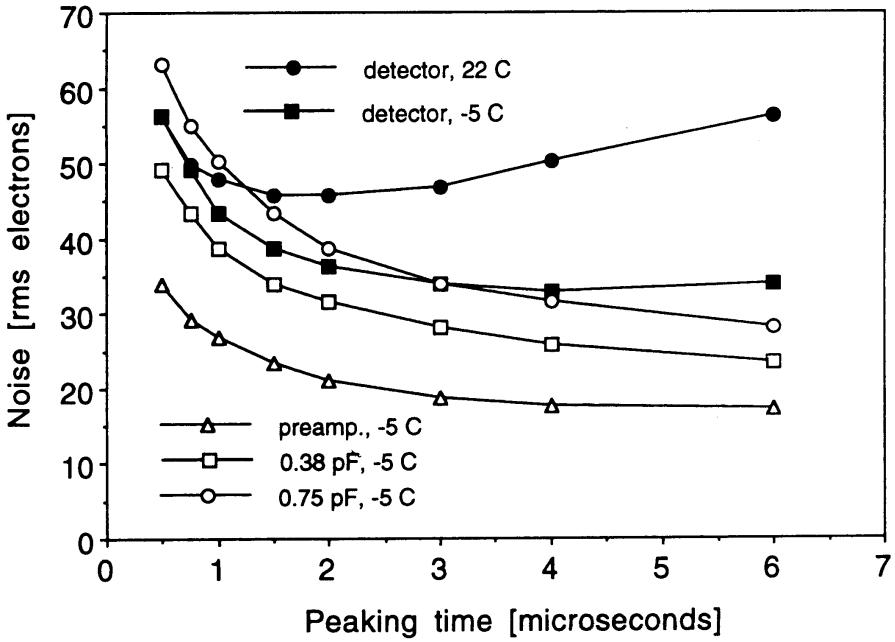

Connecting detector increases noise because of added capacitance and detector current (as indicated by increase of noise with peaking time). Cooling the detector reduces the current and noise improves.

Second prototype

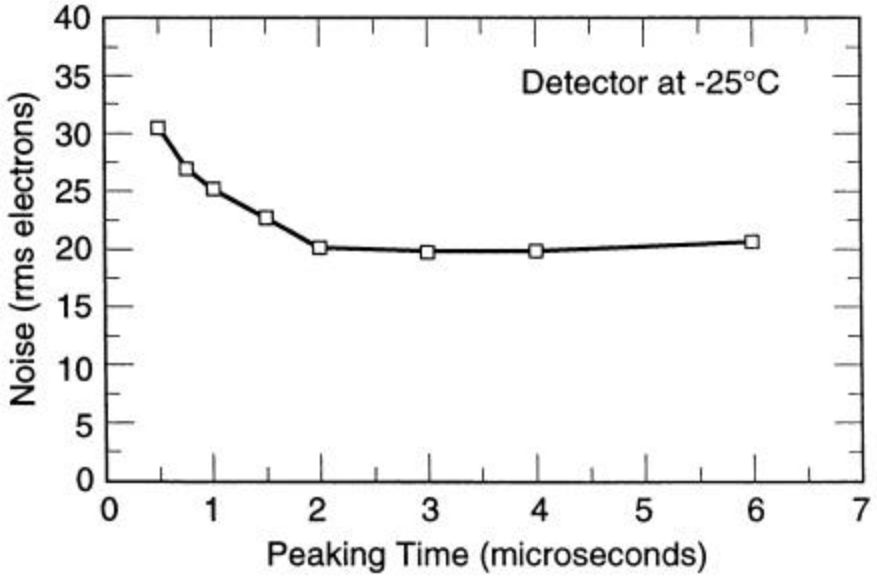

Current noise negligible because of cooling –
"flat" noise vs. shaping time indicates that 1/*f* noise dominates.

Measured spectra

^{55}Fe

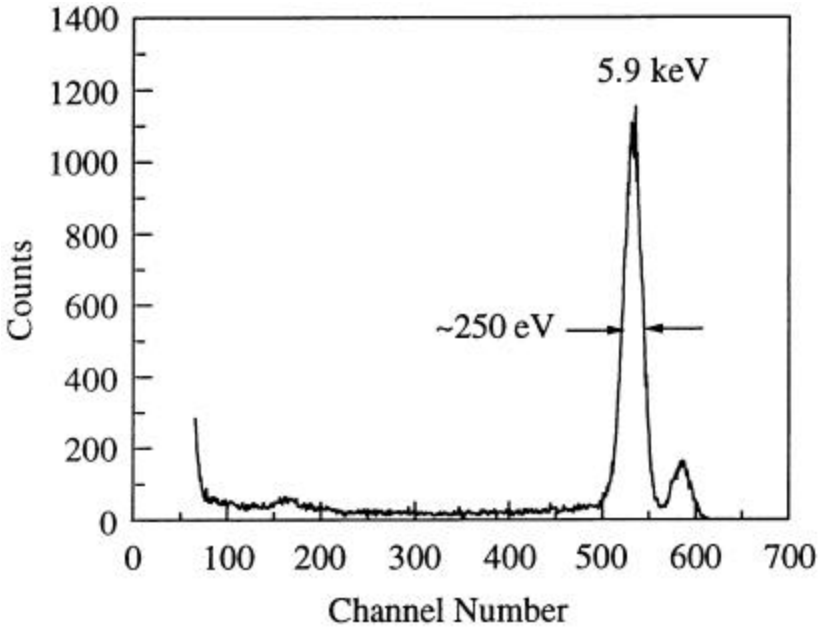

^{241}Am

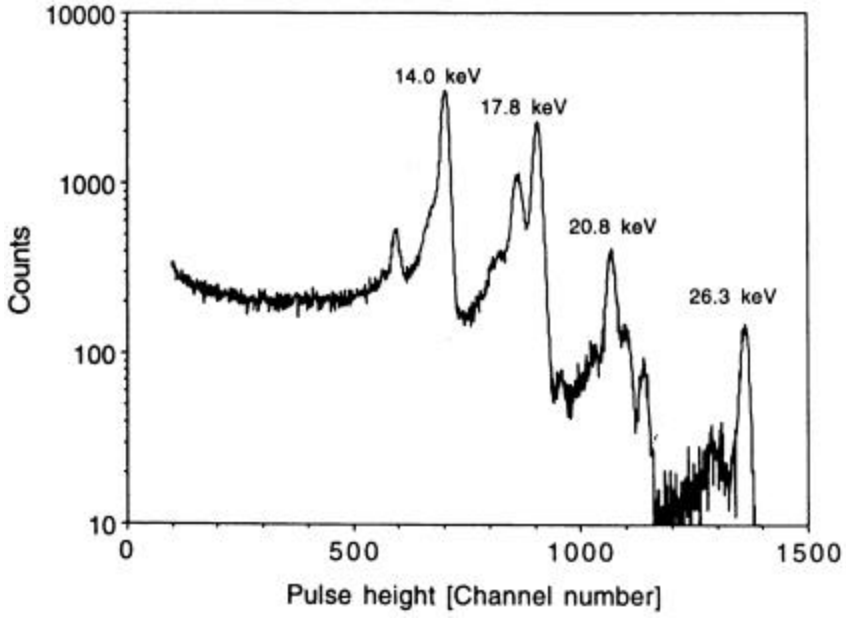

Noise Analysis in the Time Domain

The noise analysis of shapers is rather straightforward if the frequency response is known.

On the other hand, since we are primarily interested in the pulse response, shapers are often designed directly in the time domain, so it seems more appropriate to analyze the noise performance in the time domain also.

Clearly, one can take the time response and Fourier transform it to the frequency domain, but this approach becomes problematic for time-variant shapers.

The CR-RC shapers discussed up to now utilize filters whose time constants remain constant during the duration of the pulse, i.e. they are time-invariant.

Many popular types of shapers utilize signal sampling or change the filter constants during the pulse to improve pulse characteristics, i.e. faster return to baseline or greater insensitivity to variations in detector pulse shape.

These time-variant shapers cannot be analyzed in the manner described above. Various techniques are available, but some shapers can be analyzed only in the time domain.

The basis of noise analysis in the time domain is Parseval's Theorem

$$\int_0^\infty \left|A(f)\right|^2 df = \int_{-\infty}^{\infty} \left[F(t)\right]^2 dt \ ,$$

which relates the spectral power distribution of a signal in the frequency domain to its time dependence.

First an example of a time-variant shaper:

A commonly used time-variant filter is the correlated double-sampler. This shaper can be analyzed exactly only in the time domain.

Correlated Double Sampling

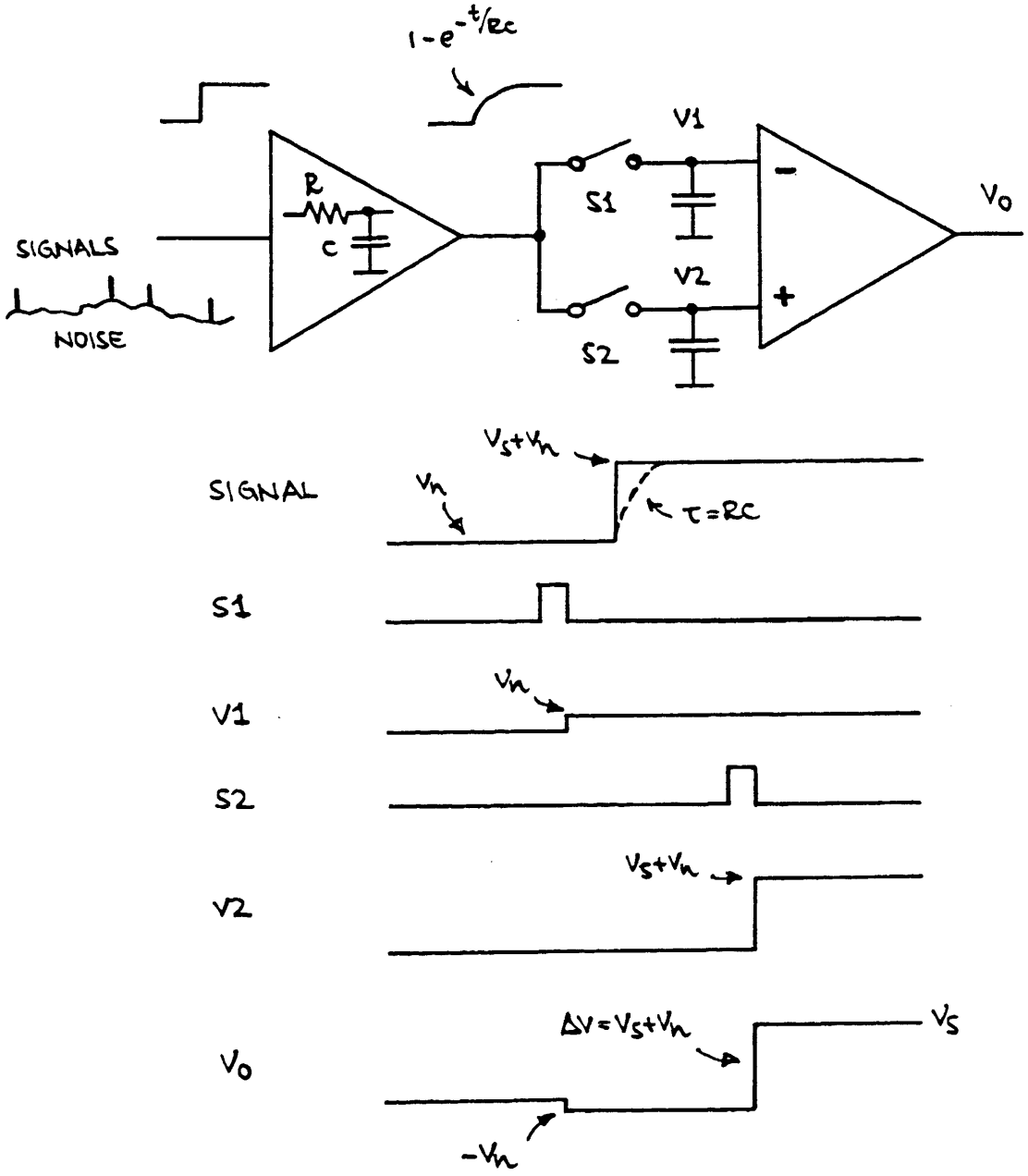

1. Signals are superimposed on a (slowly) fluctuating baseline
2. To remove baseline fluctuations the baseline is sampled prior to the arrival of a signal.
3. Next, the signal + baseline is sampled and the previous baseline sample subtracted to obtain the signal

The noise analysis in the time domain yields the following general result.

$$Q_n^2 = \frac{1}{2}\, i_n^2 \int_{-\infty}^{\infty} [W(t)]^2\, dt \;+\; \frac{1}{2}\, C^2\, e_n^2 \int_{-\infty}^{\infty} [W'(t)]^2\, dt$$

current noise — voltage noise

W(t) is the "weighting function", equivalent to the noise bandwidth in the frequency domain and normalized to the output signal amplitude.

By applying Parseval's Theorem this translates directly to the result obtained in the frequency domain.

W(t) is easy to determine: it is the pulse appearing at the output of the shaper with a step input.

After recording the output with a digitizing oscilloscope one can integrate over $[W(t)]^2$ and its time derivative $[W'(t)]^2$.

For a derivation and examples see
www-physics.LBL.gov/~spieler, "Heidelberg Lectures" IV, p. 42

Since the integrals scale linearly with time, one can express the weighting function in terms of a characteristic time T, so $t \rightarrow t/T$. The characteristic time can be chosen to be a convenient measure of a specific shaper, e.g. the peaking time or the pre-filter integration time constant in a correlated double-sampler.

This yields the general result

$$Q_n^2 = \frac{1}{2}\, i_n^2\; T \int_{-\infty}^{\infty} [W(t)]^2\, dt \;+\; \frac{1}{2}\, C^2\, e_n^2\; \frac{1}{T} \int_{-\infty}^{\infty} [W'(t)]^2\, dt$$

Now the weighting function depends only on the *pulse shape*, i.e. one can determine the weighting function (or "noise index") for any shaping time and easily scale it to other shaping times.

5. Detector Noise Summary

Two basic noise mechanisms: input noise current i_n
input noise voltage e_n

Equivalent Noise Charge:

$$Q_n^2 = \underset{\text{front end}}{i_n^2 \; T_s \; F_i} + \underset{\text{front end}}{C^2 \; e_n^2 \; \frac{F_v}{T_s}} + \underset{\text{front end}}{C^2 \; A_f \; F_{vf}}$$

(shaper) (shaper) (shaper)

where T_s Characteristic shaping time (*e.g.* peaking time)

F_i, F_v, F_{vf} "Shape Factors" that are determined by the shape of the pulse.

They can be calculated in the frequency or time domain.

C Total capacitance at the input node (detector capacitance + input capacitance of preamplifier + stray capacitance + …)

A_f $1/f$ noise intensity

- Current noise contribution increases with T
- Voltage noise contribution decreases with increasing T

  Only for "white" voltage noise sources + capacitive load

  "$1/f$" voltage noise contribution constant in T

The shape factors F_i, F_v are easily calculated

$$F_i = \frac{1}{2T_S}\int_{-\infty}^{\infty}\left[W(t)\right]^2 dt\ , \qquad F_v = \frac{T_S}{2}\int_{-\infty}^{\infty}\left[\frac{dW(t)}{dt}\right]^2 dt$$

where for time invariant pulse shaping $W(t)$ is simply the system's impulse response (the output signal seen on an oscilloscope) with the peak output signal normalized to unity.

Typical values of F_i, F_v

CR-RC shaper	F_i = 0.924	F_v = 0.924
CR-$(RC)^4$ shaper	F_i = 0.45	F_v = 1.02
CR-$(RC)^7$ shaper	F_i = 0.34	F_v = 1.27
CAFE chip	F_i = 0.4	F_v = 1.2

Note that $F_i < F_v$ for higher order shapers. Shapers can be optimized to reduce current noise contribution relative to the voltage noise (mitigate radiation damage!).

"$1/f$" noise contribution depends on the ratio of the upper to lower cutoff frequencies, so for a given shaper it is independent of shaping time.

1. Equivalent Noise Charge vs. Pulse Width

Current Noise vs. T

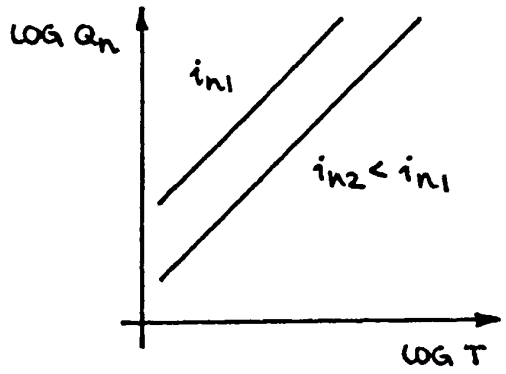

Voltage Noise vs. T

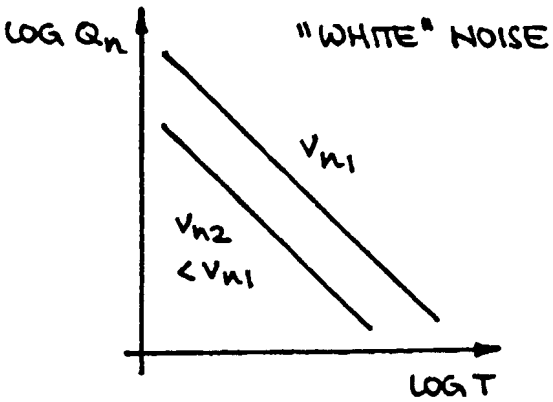

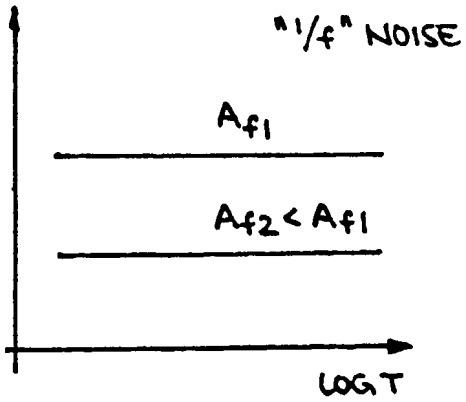

Total Equivalent Noise Charge

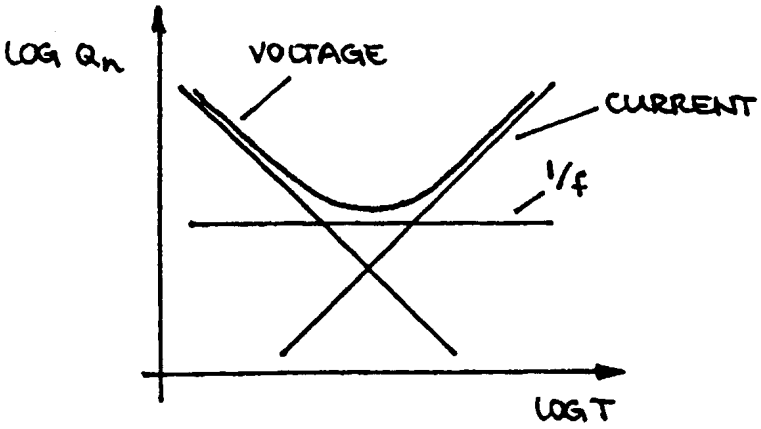

2. Equivalent Noise Charge vs. Detector Capacitance ($C = C_d + C_a$)

$$Q_n = \sqrt{i_n^2 F_i T + (C_d + C_a)^2 e_n^2 F_v \frac{1}{T}}$$

$$\frac{dQ_n}{dC_d} = \frac{2C_d e_n^2 F_v \frac{1}{T}}{\sqrt{i_n^2 F_i T + (C_d + C_a)^2 e_n^2 F_v \frac{1}{T}}}$$

If current noise $i_n^2 F_i T$ is negligible

$$\frac{dQ_n}{dC_d} \approx 2e_n \cdot \sqrt{\frac{F_v}{T}}$$

↑ input stage ↑ shaper

Zero intercept

$$Q_n\big|_{C_d=0} = C_a e_n \sqrt{F_v / T}$$

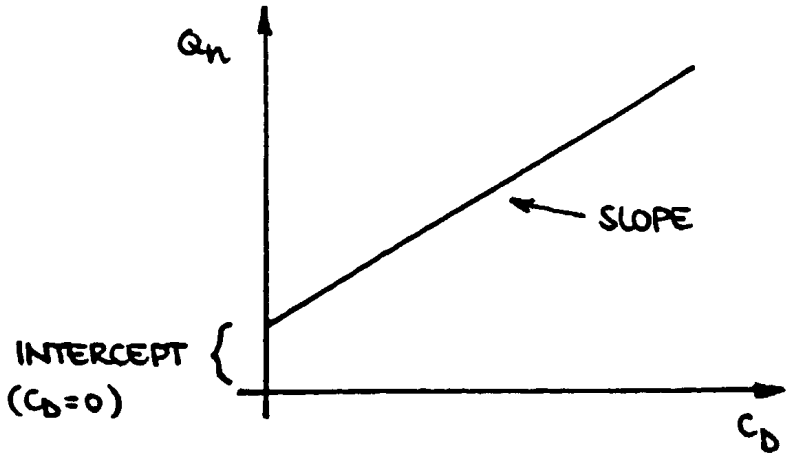

Noise slope is a convenient measure to compare preamplifiers and predict noise over a range of capacitance.

Caution: both noise slope and zero intercept depend on *both the preamplifier and the shaper*

Same preamplifier, but different shapers:

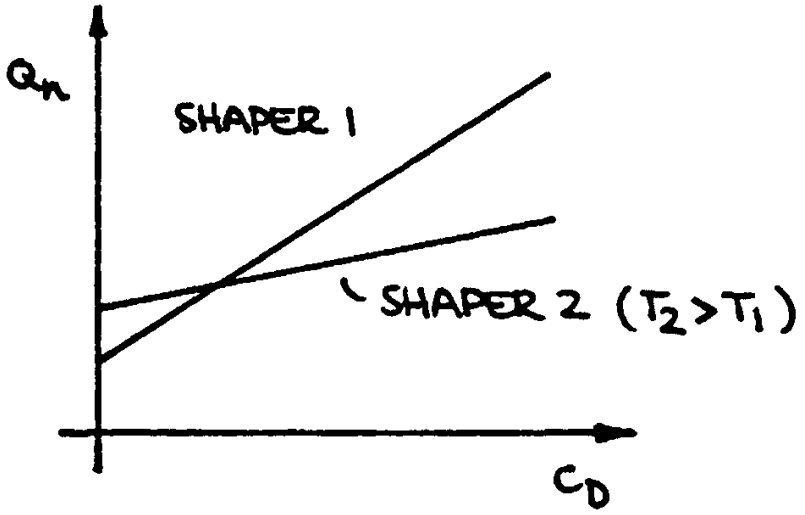

Caution: Noise slope is only valid when current noise negligible.

Current noise contribution may be negligible at high detector capacitance, but not for C_d=0 where the voltage noise contribution is smaller.

$$Q_n\big|_{C_d=0} = \sqrt{i_n^2 F_i T + C_a^2 e_n^2 F_v / T}$$

6. Noise in Transistors

a) Field Effect Transistors

Field Effect Transistors (FETs) utilize a conductive channel whose resistance is controlled by an applied potential.

1. Junction Field Effect Transistor (JFET)

In JFETs a conducting channel is formed of n or p-type semiconductor (GaAs, Ge or Si).
Connections are made to each end of the channel, the Drain and Source.

In the implementation shown below a pair of gate electrodes of opposite doping with respect to the channel are placed at opposite sides of the channel. Applying a reverse bias forms a depletion region that reduces the cross section of the conducting channel.

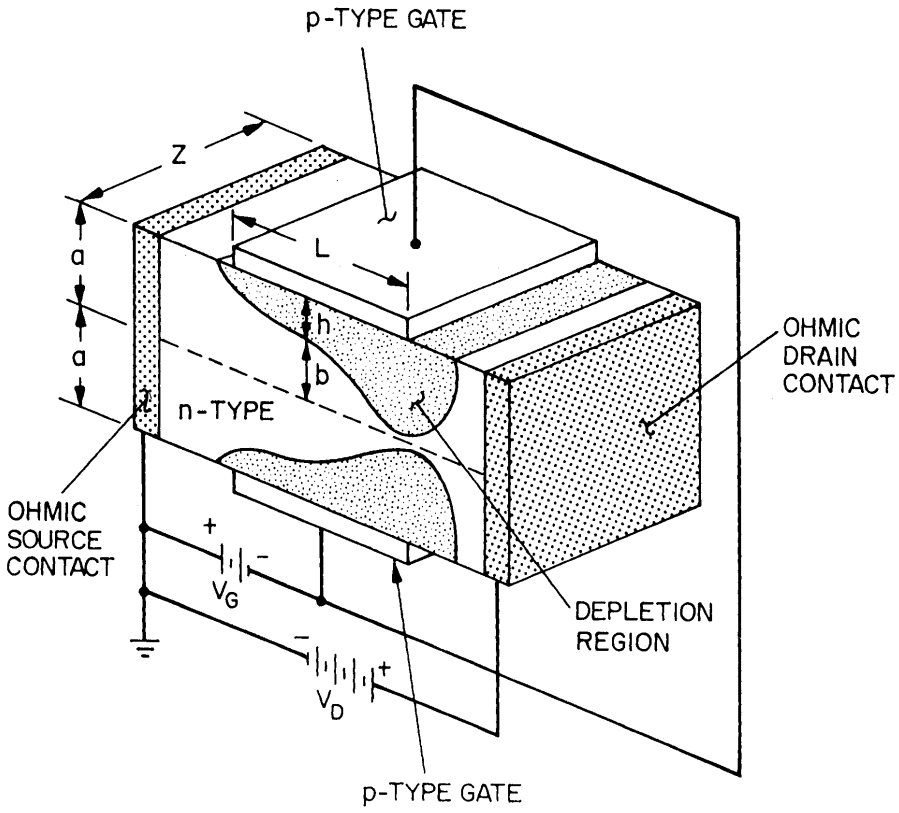

(from Sze)

Changing the magnitude of the reverse bias on the gate modulates the cross section of the channel.

2. Metal Oxide Field Effect Transistors (MOSFETs)

Both JFETs and MOSFETs are conductivity modulated devices, utilizing only one type of charge carrier. Thus they are called unipolar devices, unlike bipolar transistors, for which both electrons and holes are crucial.

Unlike a JFET, where a conducting channel is formed by doping and its geometry modulated by the applied voltages, the MOSFET changes the carrier concentration in the channel.

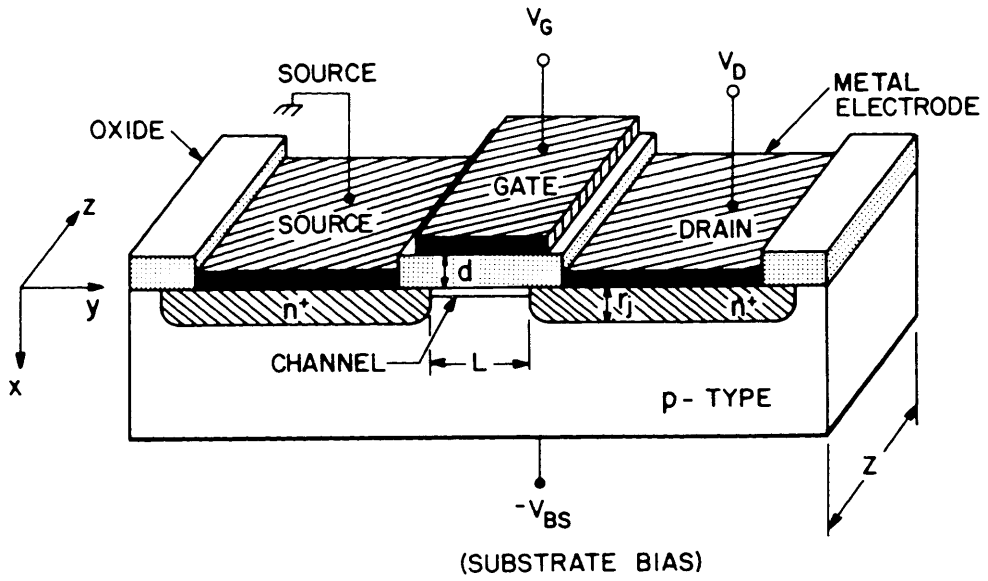

(from Sze)

The source and drain are n^+ regions in a p-substrate.

The gate is capacitively coupled to the channel region through an insulating layer, typically SiO_2.

Applying a positive voltage to the gate increases the electron concentration at the silicon surface beneath the gate.

- As in a JFET the combination of gate and drain voltages control the conductivity of the channel.

- Both JFETs and MOSFETs are characterized primarily by transconductance, i.e. the change in output current vs. input voltage

a) Noise in Field Effect Transistors

The primary noise sources in field effect transistors are

a) thermal noise in the channel

b) gate current in JFETs

Since the area of the gate is small, this contribution to the noise is very small and usually can be neglected.

Thermal velocity fluctuations of the charge carriers in the channel superimpose a noise current on the output current.

The spectral density of the noise current at the drain is

$$i_{nd}^2 = \frac{N_{C,tot} q_e}{L^2} m_0 \, 4k_B T_e$$

The current fluctuations depend on the number of charge carriers in the channel $N_{C,tot}$ and their thermal velocity, which in turn depends on their temperature T_e and low field mobility m_0. Finally, the induced current scales with 1/L because of Ramo's theorem.

To make practical use of the above expression it is necessary to express it in terms of directly measureable device parameters. Since the transconductance in the saturation region

$$g_m \propto \frac{W}{L} m N_{ch} d$$

one can express the noise current as

$$i_{nd}^2 = g_n g_m \, 4k_B T_0$$

where T_0= 300K and g_n is a semi-empirical constant that depends on the carrier concentration in the channel and the device geometry.

In a JFET the gate noise current is the shot noise associated with the reverse bias current of the gate-channel diode

$$i_{ng} = 2q_e I_G$$

The noise model of the FET

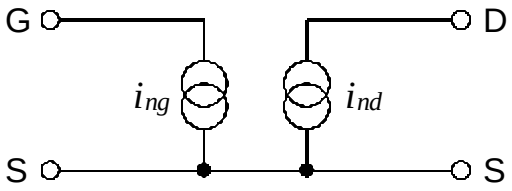

The gate and drain noise currents are independent of one another.

However, if an impedance Z is connected between the gate and the source, the gate noise current will flow through this impedance and generate a voltage at the gate

$$e_{ng} = Z\ i_{ng}$$

leading to an additional noise current at the output $g_m v_{ng}$, so that the total noise current at the output becomes

$$i_{no}^2 = i_{nd}^2 + (g_m Z i_{ng})^2$$

To allow a direct comparison with the input signal this cumulative noise will be referred back to the input to yield the equivalent input noise voltage

$$e_{ni}^2 = \frac{i_{no}^2}{g_m^2} = \frac{i_{nd}^2}{g_m^2} + Z i_{ng}^2 \equiv e_n^2 + Z i_n^2$$

i.e. referred to the input, the drain noise current i_{nd} translates into a noise voltage source

$$e_n^2 = 4k_B T_0 \frac{g_n}{g_m}$$

The noise coefficient g_n is usually given as 2/3, but is typically in the range 0.5 to 1 (exp. data will shown later).

This expression describes the noise of both JFETs and MOSFETs.

In this parameterization the noise model becomes

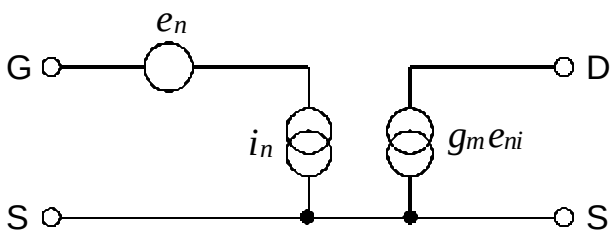

where e_n and i_n are the input voltage and current noise. As was shown above, these contribute to the input noise voltage e_{ni}, which in turn translates to the output through the transconductance g_m to yield a noise current at the output $g_m e_{ni}$.

The equivalent noise charge

$$Q_n^2 = i_n^2 F_i T + e_n^2 C_i^2 \frac{F_v}{T}$$

For a representative JFET g_m= 0.02, C_i= 10 pF and I_G < 150 pA. If F_i=F_v=1

$$Q_n^2 = 1.9 \cdot 10^9 T + \frac{3.25 \cdot 10^{-3}}{T}$$

As the shaping time T is reduced, the current noise contribution decreases and the voltage noise contribution increases. For T= 1 μs the current contribution is 43 el and the voltage contribution 3250 el, so the current contribution is negligible, except in very low frequency applications.

Optimization of Device Geometry

For a given device technology and normalized operating current I_D/W both the transconductance and the input capacitance are proportional to device width W

$$g_m \propto W \quad \text{and} \quad C_i \propto W$$

so that the ratio

$$\frac{g_m}{C_i} = const$$

Then the signal-to-noise ratio can be written as

$$\left(\frac{S}{N}\right)^2 = \frac{(Q_s/C)^2}{v_n^2} = \frac{Q_s^2}{(C_{\det} + C_i)^2}\frac{g_m}{4k_B T_0 \Delta f}$$

$$\left(\frac{S}{N}\right)^2 = \frac{Q_s^2}{\Delta f}\frac{1}{4k_B T_0}\left(\frac{g_m}{C_i}\right)\frac{1}{C_i\left(1+\frac{C_{\det}}{C_i}\right)^2}$$

S/N is maximized for $C_i = C_{det}$ (capacitive matching).

$C_i << C_{det}$: The detector capacitance dominates, so the effect of increased transistor capacitance is negligible.
As the device width is increased the transconductance increases and the equivalent noise voltage decreases, so S/N improves.

$C_i > C_{det}$: The equivalent input noise voltage decreases as the device width is increased, but only with $1/\sqrt{W}$, so the increase in capacitance overrides, decreasing S/N.

Bipolar Transistors

Consider the *npn* structure shown below.

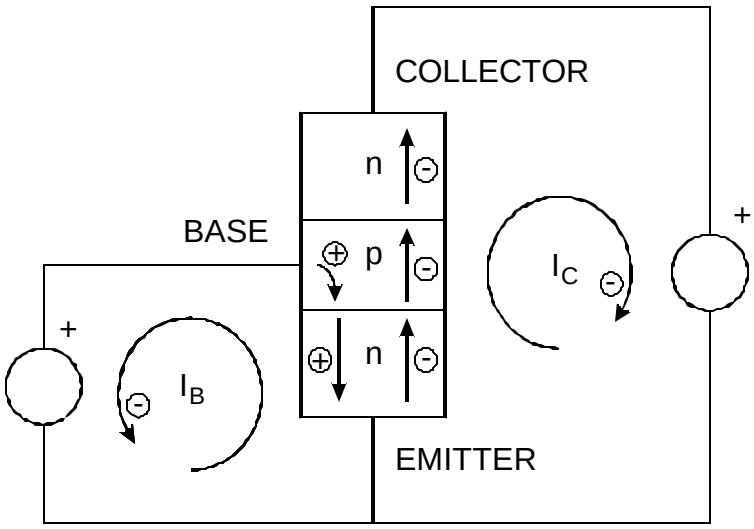

The base and emitter form a diode, which is forward biased so that a base current I_B flows.

The base current injects holes into the base-emitter junction.

As in a simple diode, this gives rise to a corresponding electron current through the base-emitter junction.

If the potential applied to the collector is sufficiently positive so that the electrons passing from the emitter to the base are driven towards the collector, an external current I_C will flow in the collector circuit.

The ratio of collector to base current is equal to the ratio of electron to hole currents traversing the base-emitter junction. In an ideal diode

$$\frac{I_C}{I_B} = \frac{I_{nBE}}{I_{pBE}} = \frac{D_n / N_A L_n}{D_p / N_D L_p} = \frac{N_D}{N_A} \frac{D_n L_p}{D_p L_n}$$

If the ratio of doping concentrations in the emitter and base regions N_D/N_A is sufficiently large, the collector current will be greater than the base current.

- DC current gain

Furthermore, we expect the collector current to saturate when the collector voltage becomes large enough to capture all of the minority carrier electrons injected into the base.

Since the current inside the transistor comprises both electrons and holes, the device is called a bipolar transistor.

Dimensions and doping levels of a modern high-frequency transistor (5 – 10 GHz bandwidth)

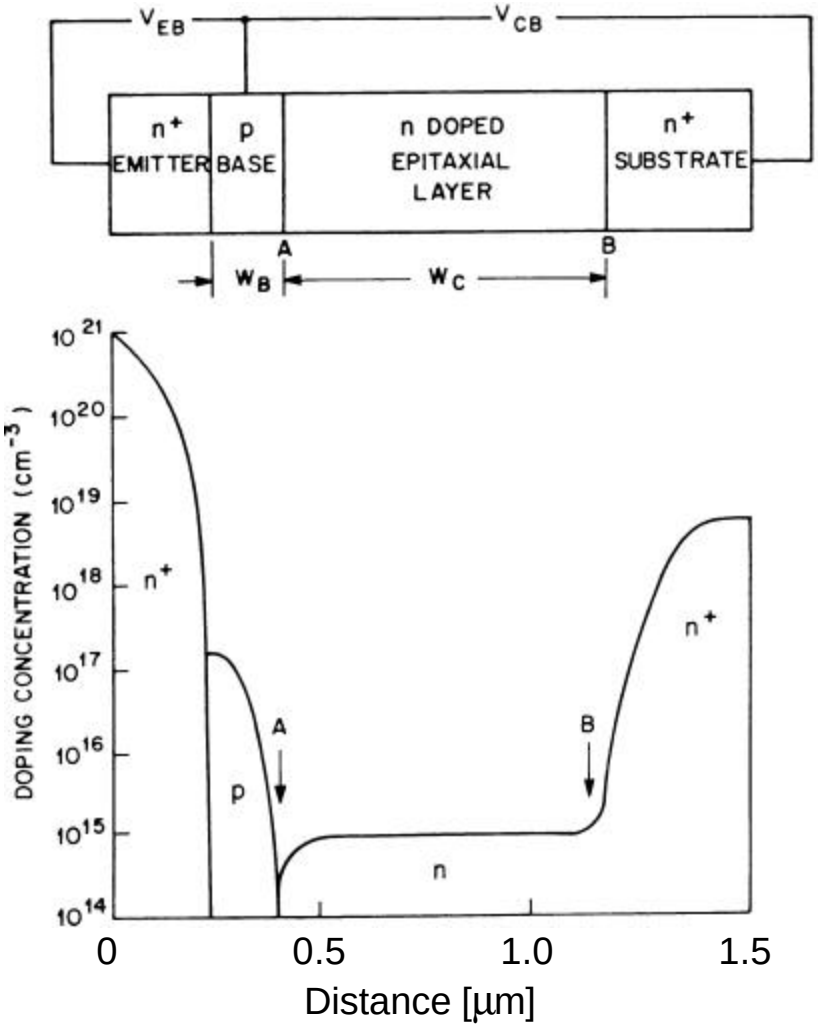

(adapted from Sze)

High-speed bipolar transistors are implemented as vertical structures.

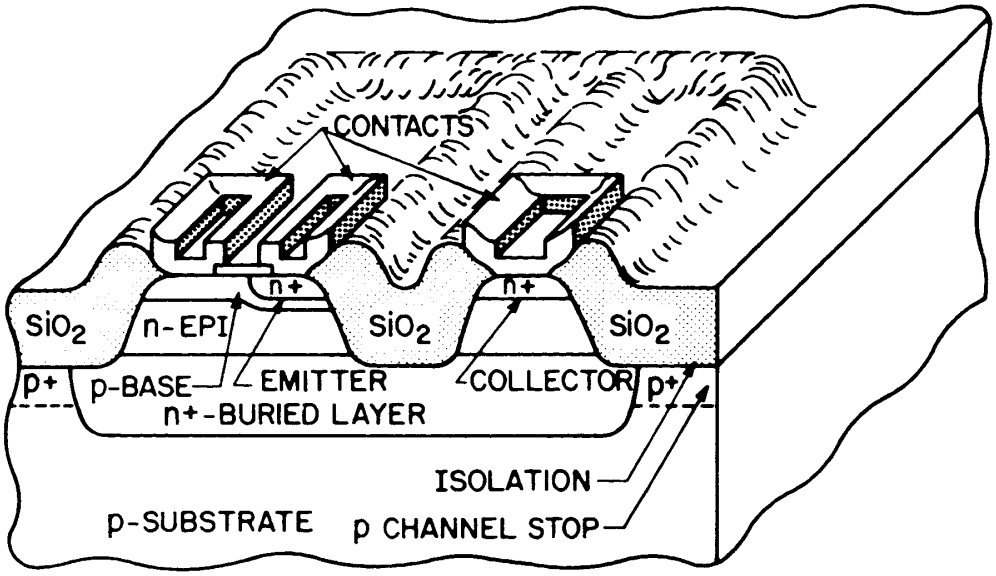

(from Sze)

The base width, typically 0.2 μm or less in modern high-speed transistors, is determined by the difference in diffusion depths of the emitter and base regions.

The thin base geometry and high doping levels make the base-emitter junction sensitive to large reverse voltages.

Typically, base-emitter breakdown voltages for high-frequency transistors are but a few volts.

As shown in the preceding figure, the collector region is usually implemented as two regions: one with low doping (denoted “epitaxial layer” in the figure) and the other closest to the collector contact with a high doping level. This structure improves the collector voltage breakdown characteristics.

b) Noise in Bipolar Transistors

In bipolar transistors the shot noise from the base current is important.

The basic noise model is the same as shown before, but the magnitude of the input noise current is much greater, as the base current will be 1 – 100 μA rather than <100 pA.

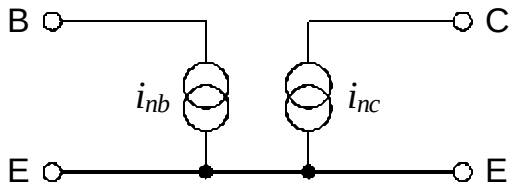

The base current noise is shot noise associated with the component of the emitter current provided by the base.

$$i_{nb}^2 = 2q_e I_B$$

The noise current in the collector is the shot noise originating in the base-emitter junction associated with the collector component of the emitter current.

$$i_{nc}^2 = 2q_e I_C$$

Following the same argument as in the analysis of the FET, the output noise current is equivalent to an equivalent noise voltage

$$e_n^2 = \frac{i_{nc}^2}{g_m^2} = \frac{2q_e I_C}{(q_e I_C / k_B T)^2} = \frac{2(k_B T)^2}{q_e I_C}$$

yielding the noise equivalent circuit

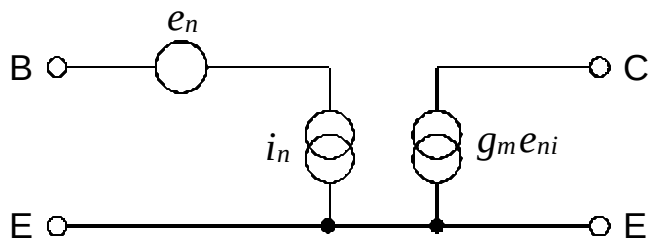

where i_n is the base current shot noise i_{nb}.

The equivalent noise charge

$$Q_n^2 = i_n^2 F_i T + e_n^2 C^2 \frac{F_v}{T} = 2q_e I_B F_i T + \frac{2(k_B T)^2}{q_e I_C} C^2 \frac{F_v}{T}$$

Since $I_B = I_C / b_{DC}$

$$Q_n^2 = 2q_e \frac{I_C}{b_{DC}} F_i T + \frac{2(k_B T)^2}{q_e I_C} C^2 \frac{F_v}{T}$$

The current noise term increases with I_C, whereas the second (voltage) noise term decreases with I_C.

Thus, the noise attains a minimum

$$Q_{n,\min}^2 = 4k_B T \frac{C}{\sqrt{b_{DC}}} \sqrt{F_i F_v}$$

at a collector current

$$I_C = \frac{k_B T}{q_e} C \sqrt{b_{DC}} \sqrt{\frac{F_v}{F_i}} \frac{1}{T} .$$

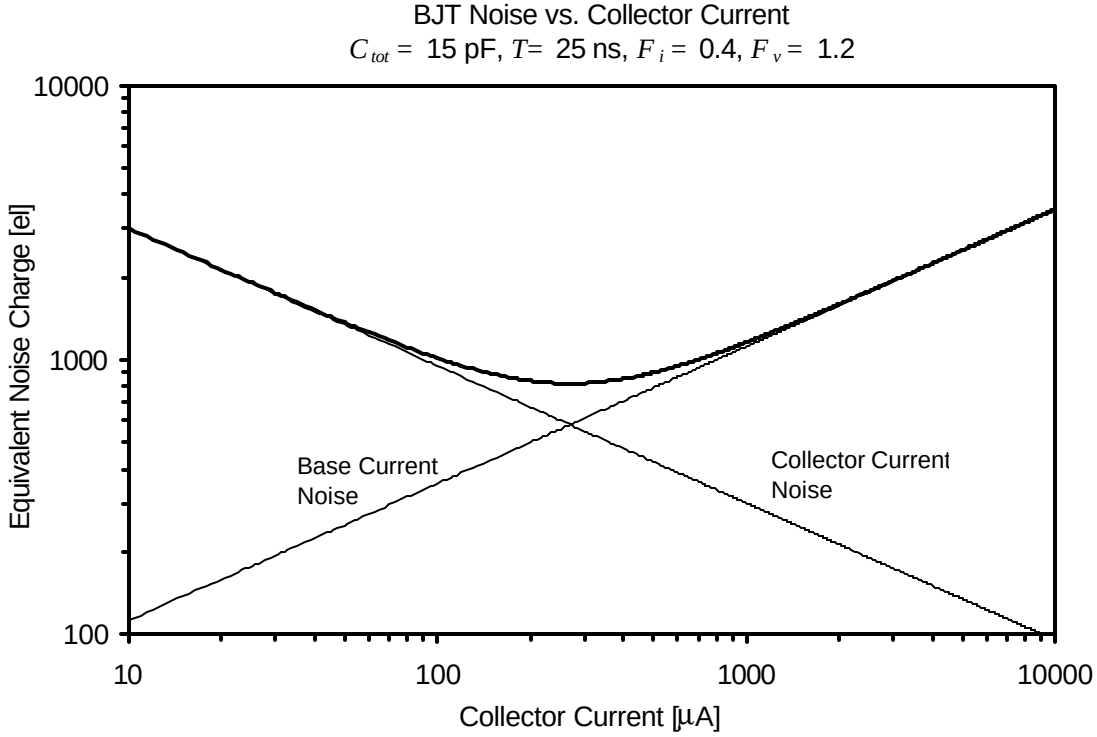

- For a given shaper, the minimum obtainable noise is determined only by the total capacitance at the input and the DC current gain of the transistor, *not by the shaping time*.

- The shaping time only determines the current at which this minimum noise is obtained

T= 100 ns

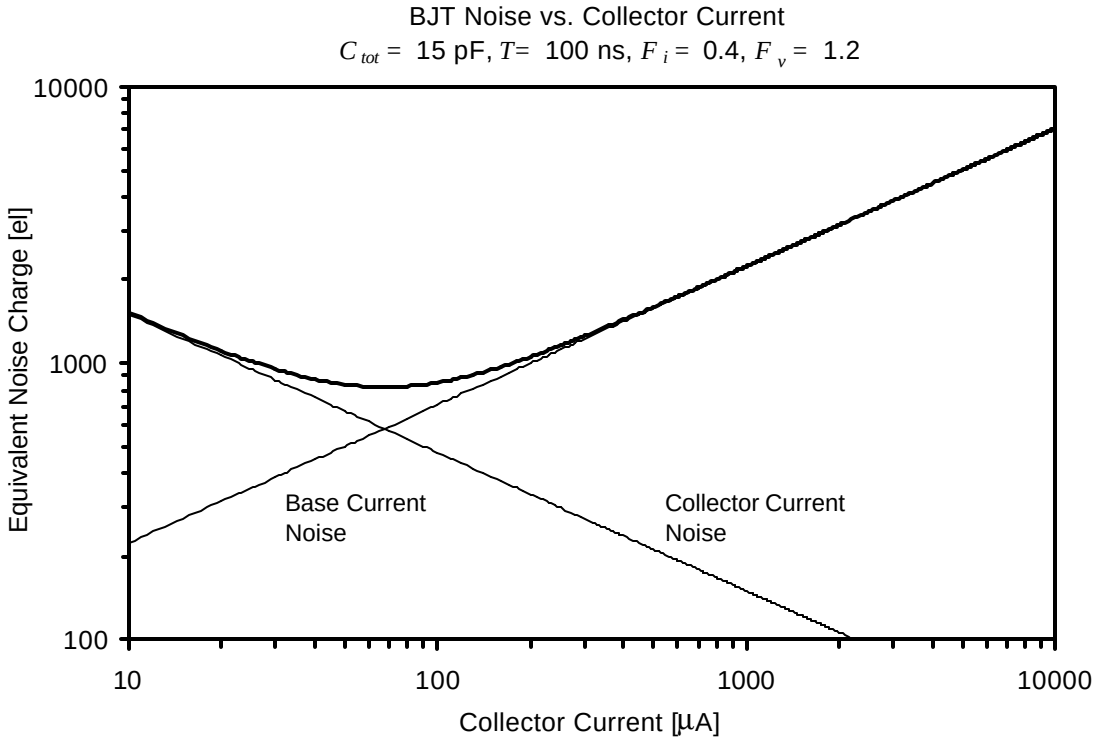

T= 10 ns

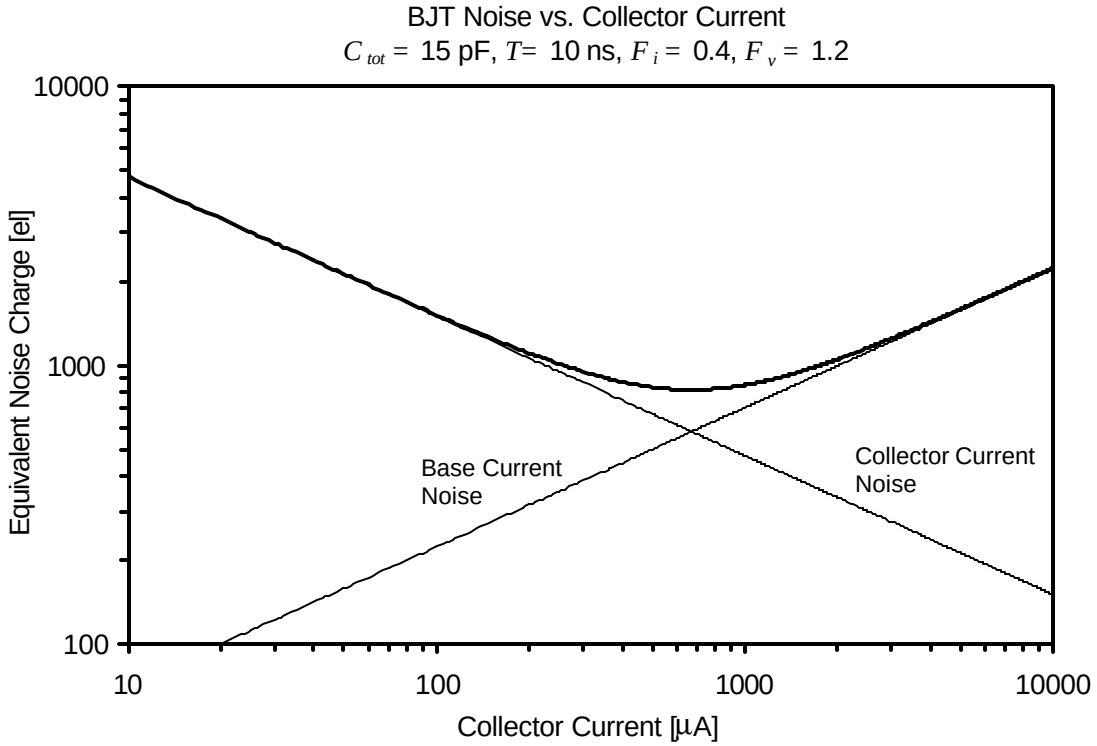

Increasing the capacitance at the input shifts the collector current noise curve upwards, so the noise increases and the minimum shifts to a higher current.

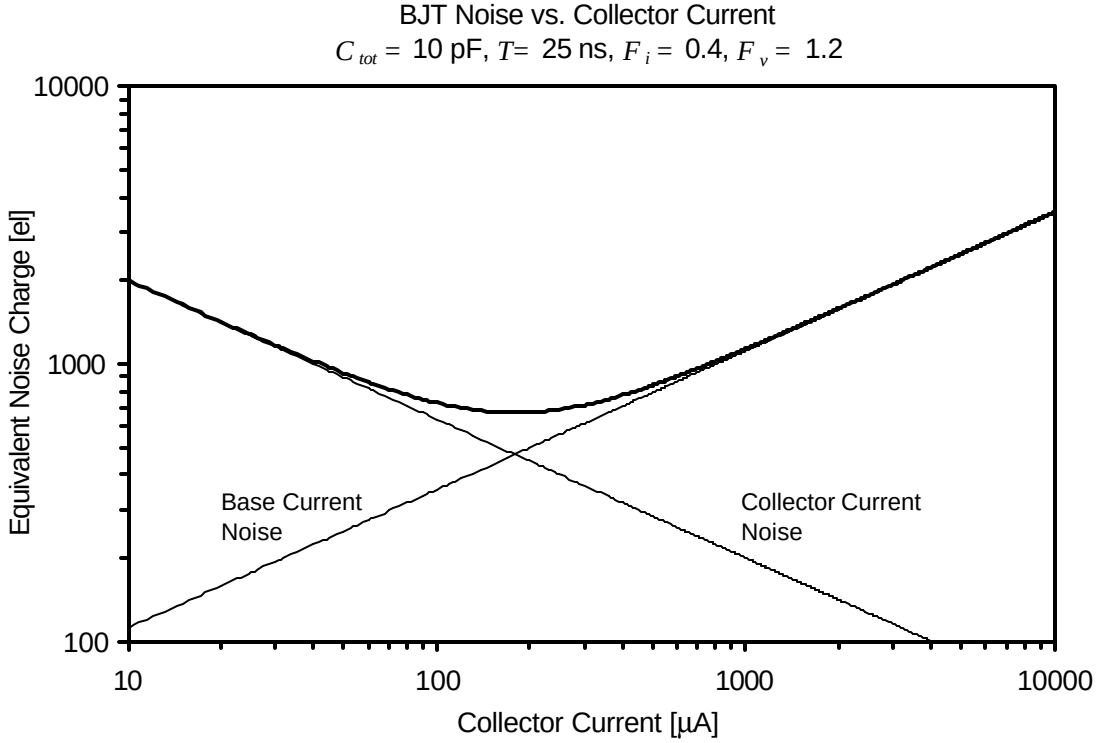

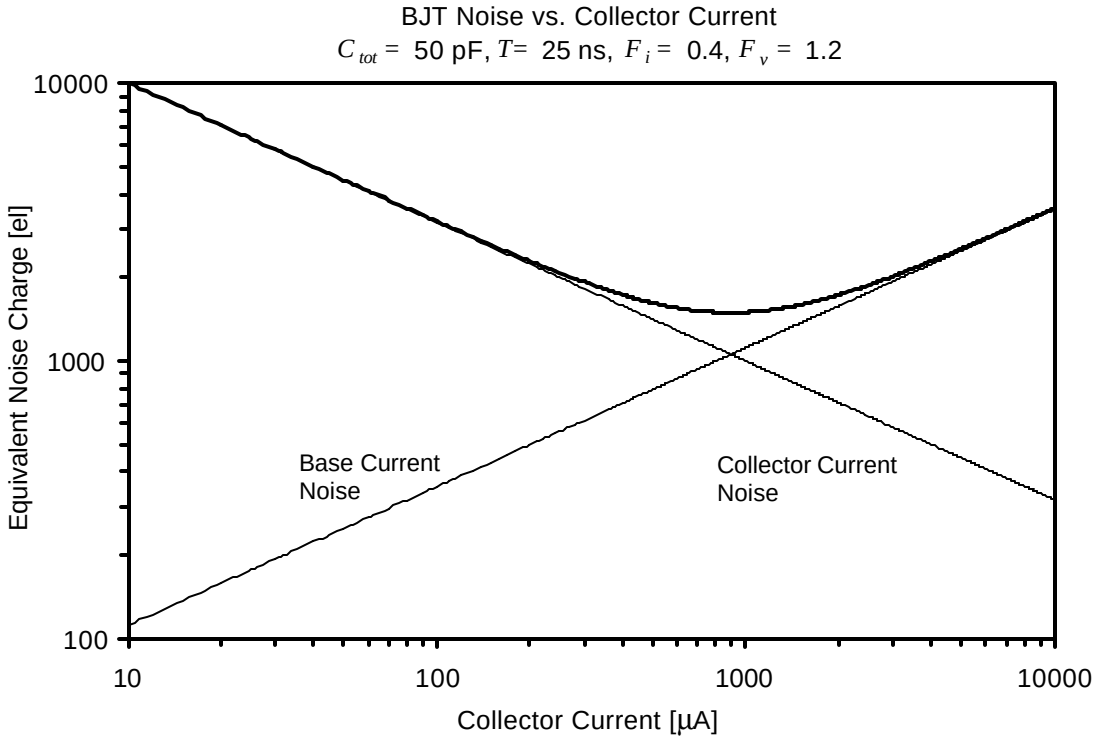

Simple Estimate of obtainable BJT noise

For a CR-RC shaper

$$Q_{n,\min} = 772\left[\frac{el}{\sqrt{pF}}\right]\cdot\frac{\sqrt{C}}{\sqrt[4]{b_{DC}}}$$

obtained at $$I_c = 26\left[\frac{mA\cdot ns}{pF}\right]\cdot\frac{C}{t}\sqrt{b_{DC}}$$

Since typically $b_{DC} \approx 100$, these expressions allow a quick and simple estimate of the noise obtainable with a bipolar transistor.

Note that specific shapers can be optimized to minimize either the current or the voltage noise contribution, so both the minimum obtainable noise and the optimum current will be change with respect to the above estimates.

The noise characteristics of bipolar transistors differ from field effect transistors in four important aspects:

1. The equivalent input noise current cannot be neglected, due to base current flow.
2. The total noise does not decrease with increasing device current.
3. The minimum obtainable noise does not depend on the shaping time.
4. The input capacitance is usually negligible.

The last statement requires some explanation.

The input capacitance of a bipolar transistor is dominated by two components,

1. the geometrical junction capacitance, or transition capacitance C_{TE}, and
2. the diffusion capacitance C_{DE}.

The transition capacitance in small devices is typically about 0.5 pF.

The diffusion capacitance depends on the current flow I_E through the base-emitter junction and on the base width W, which sets the diffusion profile.

$$C_{DE} = \frac{\partial q_B}{\partial V_{be}} = \frac{q_e I_E}{k_B T}\left(\frac{W}{2D_B}\right) \equiv \frac{q_e I_E}{k_B T} \cdot \frac{1}{w_{Ti}}$$

where D_B is the diffusion constant in the base and w_{Ti} is a frequency that characterizes carrier transport in the base. w_{Ti} is roughly equal to the frequency where the current gain of the transistor is unity.

Inserting some typical values, I_E=100 µA and w_{Ti} =10 GHz, yields C_{DE}= 0.4 pF. The transistor input capacitance $C_{TE}+C_{DE}$= 0.9 pF, whereas FETs providing similar noise values at comparable currents have input capacitances in the range 5 – 10 pF.

Except for low capacitance detectors, the current dependent part of the BJT input capacitance is negligible, so it will be neglected in the following discussion. For practical purposes the amplifier input capacitance can be considered constant at 1 ... 1.5 pF.

This leads to another important conclusion.

Since the primary noise parameters do not depend on device size and there is no significant linkage between noise parameters and input capacitance

- Capacitive matching does not apply to bipolar transistors.

Indeed, capacitive matching is a misguided concept for bipolar transistors. Consider two transistors with the same DC current gain but different input capacitances. Since the minimum obtainable noise

$$Q_{n,\min}^2 = 4k_B T \frac{C}{\sqrt{b_{DC}}} \sqrt{F_i F_v} \ ,$$

increasing the transistor input capacitance merely increases the total input capacitance C_{tot} and the obtainable noise.

When to use FETs and when to use BJTs?

Since the base current noise increases with shaping time, bipolar transistors are only advantageous at short shaping times.

With current technologies FETs are best at shaping times greater than 50 to 100 ns, but decreasing feature size of MOSFETs will improve their performance.

7. Rate of Noise Pulses in Threshold Discriminator Systems

Noise affects not only the resolution of amplitude measurements, but also the determines the minimum detectable signal threshold.

Consider a system that only records the presence of a signal if it exceeds a fixed threshold.

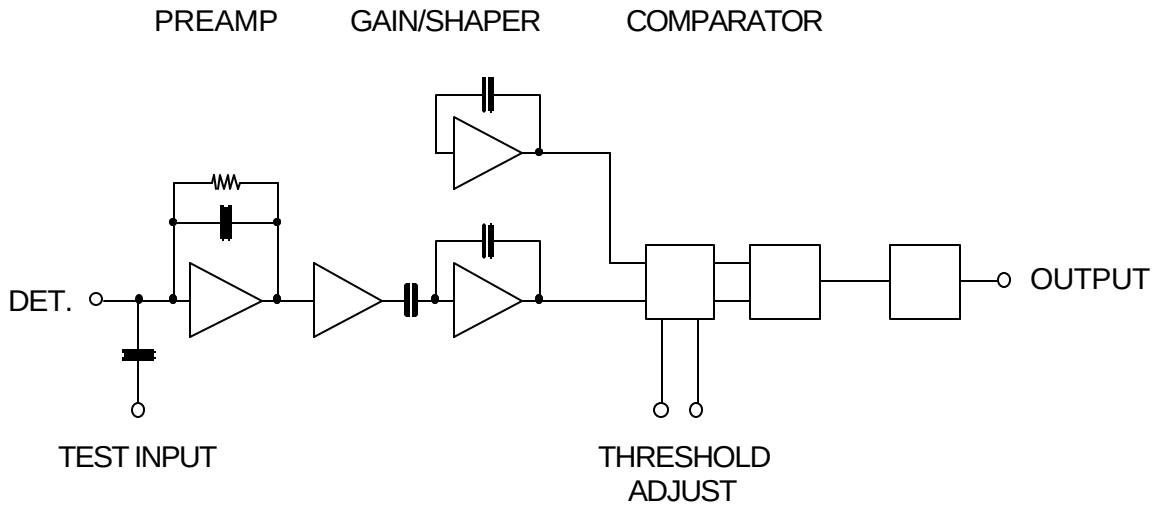

How small a detector pulse can still be detected reliably?

Consider the system at times when no detector signal is present.

Noise will be superimposed on the baseline.

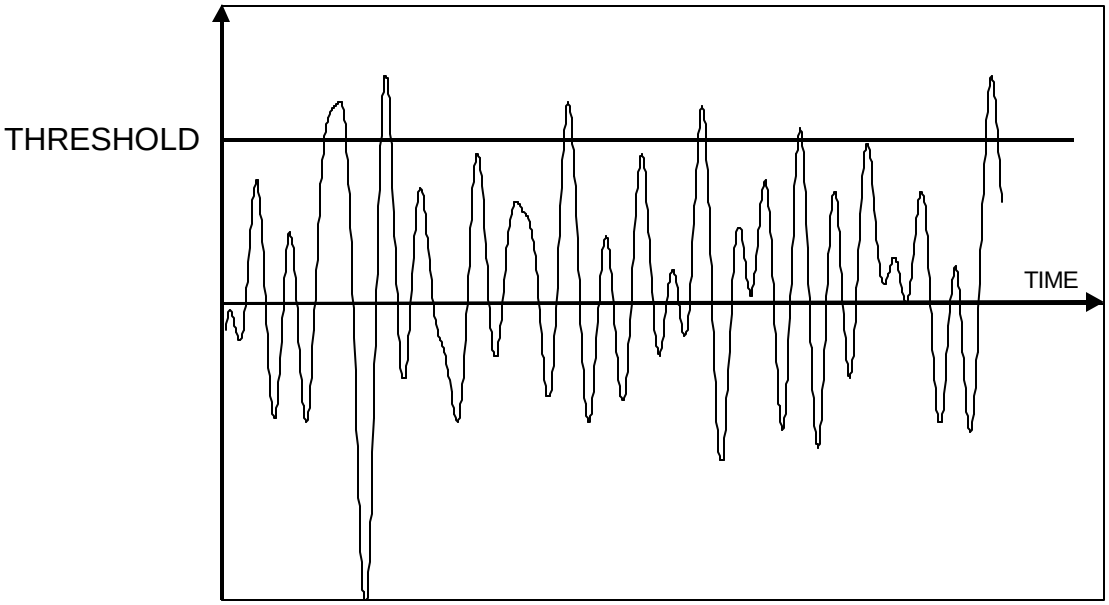

The amplitude distribution of the noise is gaussian.

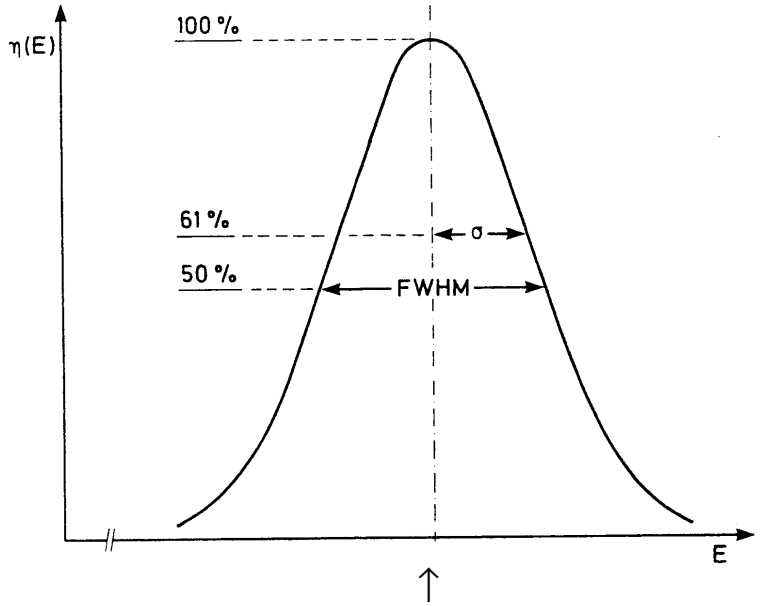

Baseline Level (E=0)

With the threshold level set to 0 relative to the baseline, all of the positive excursions will be recorded.

Assume that the desired signals are occurring at a certain rate.

If the detection reliability is to be >99%, then the rate of noise hits must be less than 1% of the signal rate.

The rate of noise hits can be reduced by increasing the threshold.

If the system were sensitive to pulse magnitude alone, the integral over the gaussian distribution (the error function) would determine the factor by which the noise rate f_{n0} is reduced.

$$\frac{f_n}{f_{n0}} = \frac{1}{Q_n\sqrt{2p}} \int_{Q_T}^{\infty} e^{-(Q/2Q_n)^2}\, dQ$$

where Q is the equivalent signal charge, Q_n the equivalent noise charge and Q_T the threshold level. However, since the pulse shaper broadens each noise impulse, the time dependence is equally important. For example, after a noise pulse has crossed the threshold, a subsequent pulse will not be recorded if it occurs before the trailing edge of the first pulse has dropped below threshold.

The **combined probability function** for gaussian time and amplitude distributions yields the expression for the noise rate as a function of threshold-to-noise ratio.

$$f_n = f_{n0} \cdot e^{-Q_T^2/2Q_n^2}$$

Of course, one can just as well use the corresponding voltage levels.

What is the noise rate at zero threshold f_{n0}?

Since we are interested in the number of positive excursions exceeding the threshold, f_{n0} is ½ the frequency of zero-crossings.

A rather lengthy analysis of the time dependence shows that the frequency of zero crossings at the output of an ideal band-pass filter with lower and upper cutoff frequencies f_1 and f_2 is

$$f_0 = 2\sqrt{\frac{1}{3}\frac{f_2^3 - f_1^3}{f_2 - f_1}}$$

(Rice, Bell System Technical Journal, **23** (1944) 282 and **24** (1945) 46)

For a CR-RC filter with $t_i = t_d$ the ratio of cutoff frequencies of the noise bandwidth is

$$\frac{f_2}{f_1} = 4.5$$

so to a good approximation one can neglect the lower cutoff frequency and treat the shaper as a low-pass filter, *i.e.* $f_1 = 0$. Then

$$f_0 = \frac{2}{\sqrt{3}} f_2$$

An ideal bandpass filter has infinitely steep slopes, so the upper cutoff frequency f_2 must be replaced by the noise bandwidth.

The noise bandwidth of an RC low-pass filter with time constant t is

$$\Delta f_n = \frac{1}{4t}$$

Setting $f_2 = Df_n$ yields the frequency of zeros

$$f_0 = \frac{1}{2\sqrt{3}\,t}$$

and the frequency of noise hits vs. threshold

$$f_n = f_{n0} \cdot e^{-Q_{th}^2/2Q_n^2} = \frac{f_0}{2} \cdot e^{-Q_{th}^2/2Q_n^2} = \frac{1}{4\sqrt{3}\,t} \cdot e^{-Q_{th}^2/2Q_n^2}$$

Thus, the required threshold-to-noise ratio for a given frequency of noise hits f_n is

$$\frac{Q_T}{Q_n} = \sqrt{-2\log(4\sqrt{3}\ f_n t)}$$

Note that the threshold-to-noise ratio determines the product of noise rate and shaping time, i.e. for a given threshold-to-noise ratio the noise rate is higher at short shaping times

- The noise rate for a given threshold-to-noise ratio is proportional to bandwidth.
- To obtain the same noise rate, a fast system requires a larger threshold-to-noise ratio than a slow system with the same noise level.

Frequently a threshold discriminator system is used in conjunction with other detectors that provide additional information, for example the time of a desired event.

In a collider detector the time of beam crossings is known, so the output of the discriminator is sampled at specific times.

The number of recorded noise hits then depends on

1. the sampling frequency (e.g. bunch crossing frequency) f_S

2. the width of the sampling interval Dt, which is determined by the time resolution of the system.

The product $f_S\, Dt$ determines the fraction of time the system is open to recording noise hits, so the rate of recorded noise hits is $f_S\, Dt\, f_n$.

Often it is more interesting to know the probability of finding a noise hit in a given interval, i.e. the occupancy of noise hits, which can be compared to the occupancy of signal hits in the same interval.

This is the situation in a storage pipeline, where a specific time interval is read out after a certain delay time (e.g. trigger latency)

The occupancy of noise hits in a time interval Dt

$$P_n = \Delta t \cdot f_n = \frac{\Delta t}{2\sqrt{3}\, t} \cdot e^{-Q_T^2/2Q_n^2}$$

i.e. the occupancy falls exponentially with the square of the threshold-to-noise ratio.

The dependence of occupancy on threshold can be used to measure the noise level.

$$\log P_n = \log\left(\frac{\Delta t}{2\sqrt{3}\,t}\right) - \frac{1}{2}\left(\frac{Q_T}{Q_n}\right)^2$$

so the *slope* of log P_n vs. Q_T^2 yields the noise level, *independently of the details of the shaper*, which affect only the offset.

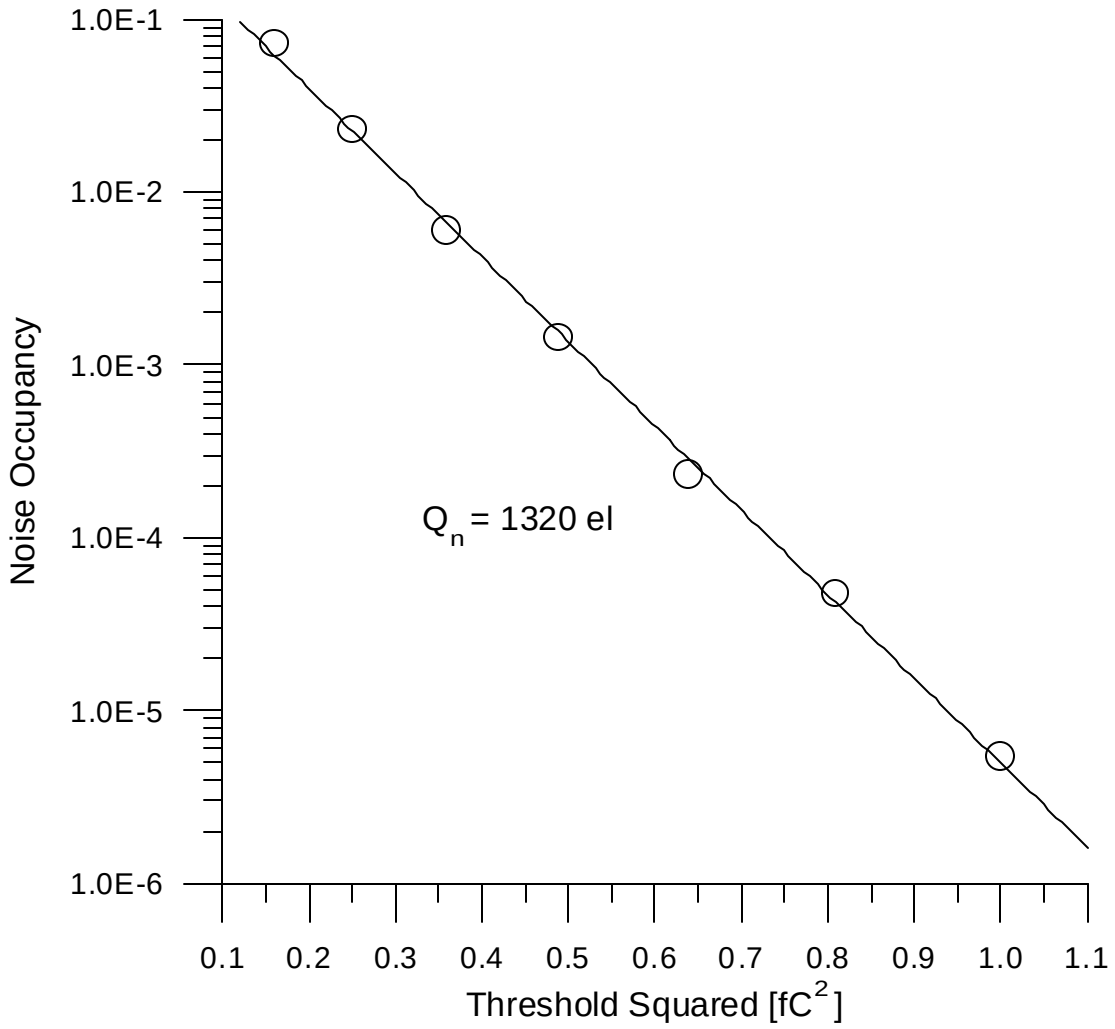

7. Some Other Aspects of Pulse Shaping

7.1 Baseline Restoration

Any series capacitor in a system prevents transmission of a DC component.

A sequence of unipolar pulses has a DC component that depends on the duty factor, i.e. the event rate.

- The baseline shifts to make the overall transmitted charge equal zero.

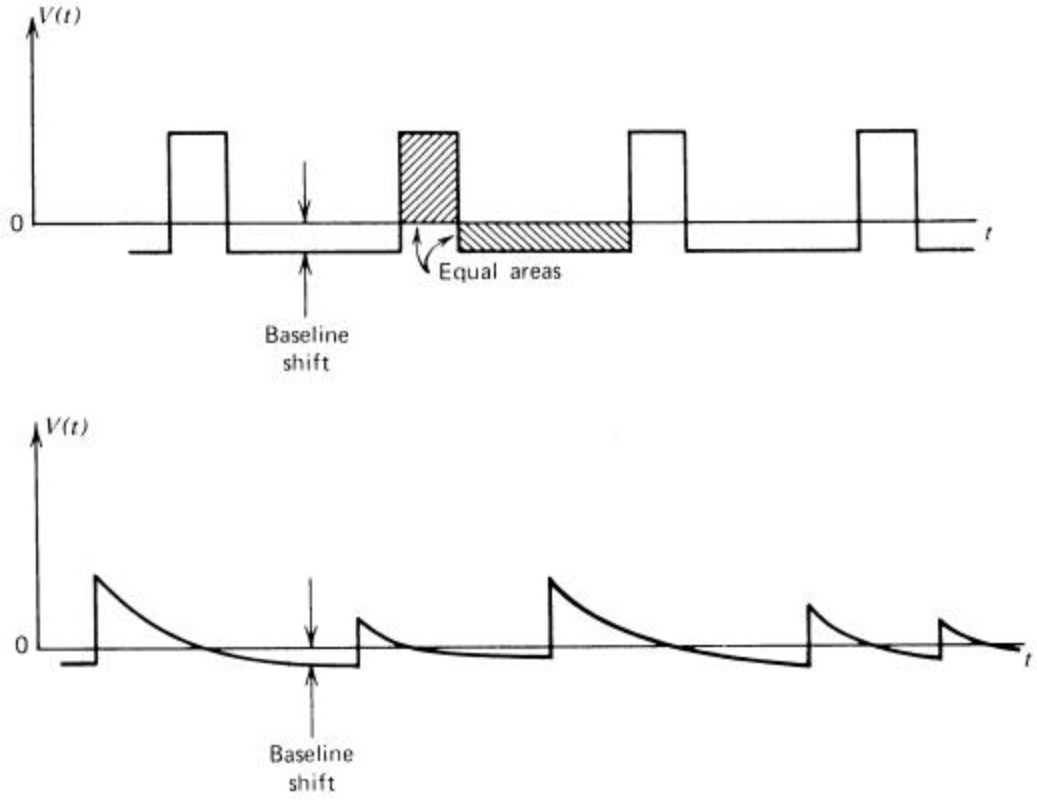

(from Knoll)

Random rates lead to random fluctuations of the baseline shift

- spectral broadening
- These shifts occur whenever the DC gain is not equal to the midband gain

The baseline shift can be mitigated by a baseline restorer (BLR).

Principle of a baseline restorer:

Connect signal line to ground during the absence of a signal to establish the baseline just prior to the arrival of a pulse.

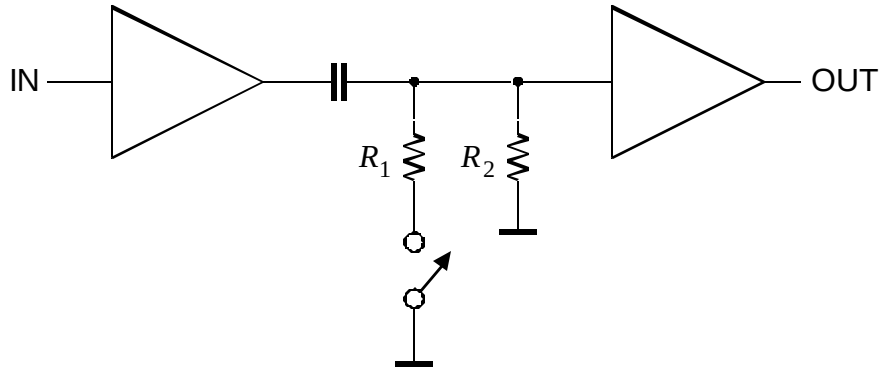

R_1 and R_2 determine the charge and discharge time constants. The discharge time constant (switch opened) must be much larger than the pulse width.

Originally performed with diodes (passive restorer), baseline restoration circuits now tend to include active loops with adjustable thresholds to sense the presence of a signal (gated restorer). Asymmetric charge and discharge time constants improve performance at high count rates.

- This is a form of time-variant filtering. Care must be exercized to reduce noise and switching artifacts introduced by the BLR.

- Good pole-zero cancellation (next topic) is crucial for proper baseline restoration.

3.2 Pole-Zero (Tail) Cancellation

Feedback capacitor in charge sensitive preamplifier must be discharged. Commonly done with resistor.

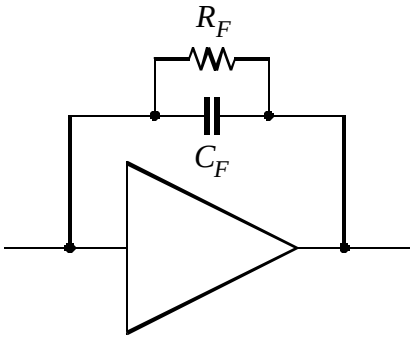

Output no longer a step, but decays exponentially

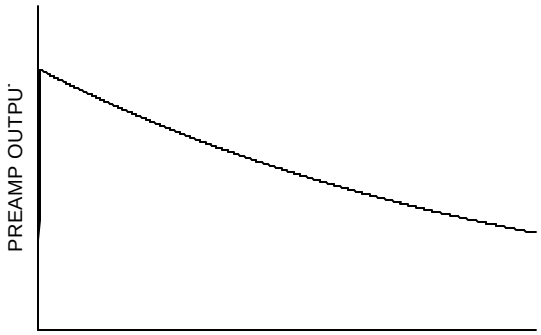

Exponential decay superimposed on shaper output.

$\Rightarrow$ undershoot

$\Rightarrow$ loss of resolution due to baseline variations

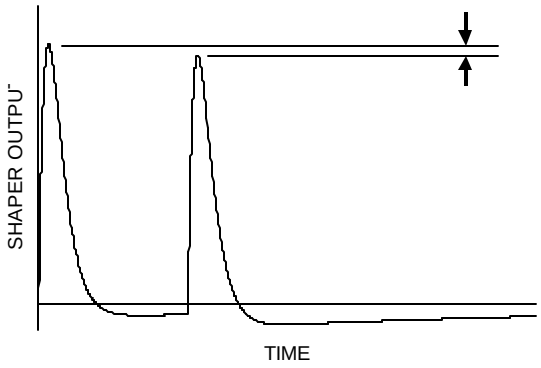

Add R_{pz} to differentiator:

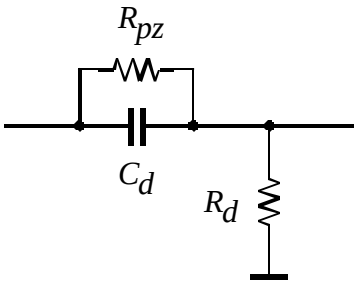

"zero" cancels "pole" of preamp when $R_F C_F = R_{pz} C_d$

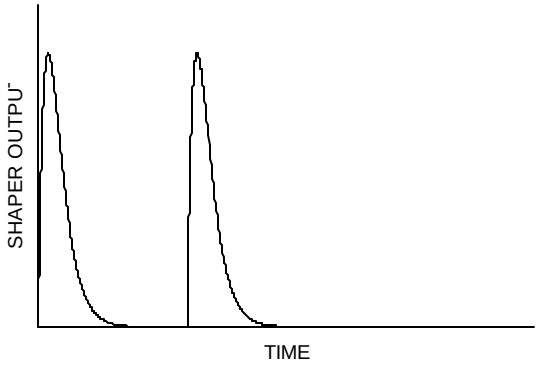

Not needed in pulsed reset circuits (optical or transistor)

Technique also used to compensate for "tails" of detector pulses: "tail cancellation"

Critical for proper functioning of baseline restorer.

3.3 Bipolar vs. Unipolar Shaping

Unipolar pulse + 2nd differentiator ® Bipolar pulse

Examples:

unipolar bipolar

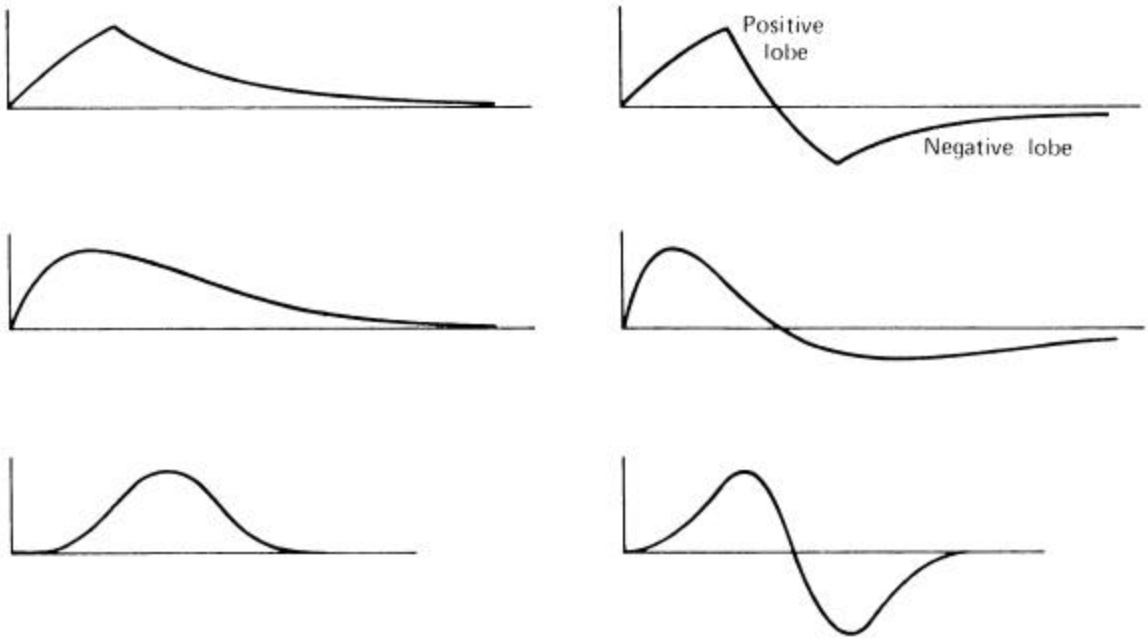

Electronic resolution with bipolar shaping typ. 25 – 50% worse than for corresponding unipolar shaper.

However …

- Bipolar shaping eliminates baseline shift (as the DC component is zero).
- Pole-zero adjustment less critical
- Added suppression of low-frequency noise (see Part 7).
- Not all measurements require optimum noise performance. Bipolar shaping is much more convenient for the user (important in large systems!) – often the method of choice.

3.4 Pulse Pile-Up and Pile-Up Rejectors

pile-up ⇒ false amplitude measurement

Two cases:

1.

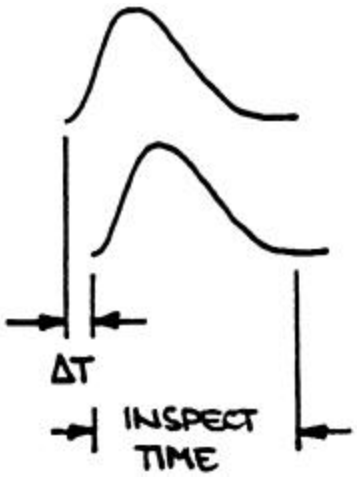

ΔT < time to peak

Both peak amplitudes are affected by superposition.

⇒ Reject both pulses

Dead Time: ΔT + inspect time
(~ pulse width)

2.

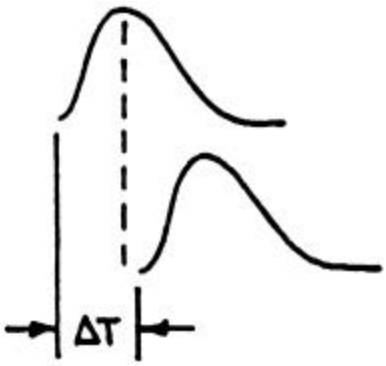

ΔT > time to peak and
ΔT < inspect time, i.e.
time where amplitude of first pulse << resolution

Peak amplitude of first pulse unaffected.

⇒ Reject 2nd pulse only

No additional dead time if first pulse accepted for digitization and dead time of ADC >
(DT + inspect time)

Typical Performance of a Pile-Up Rejector

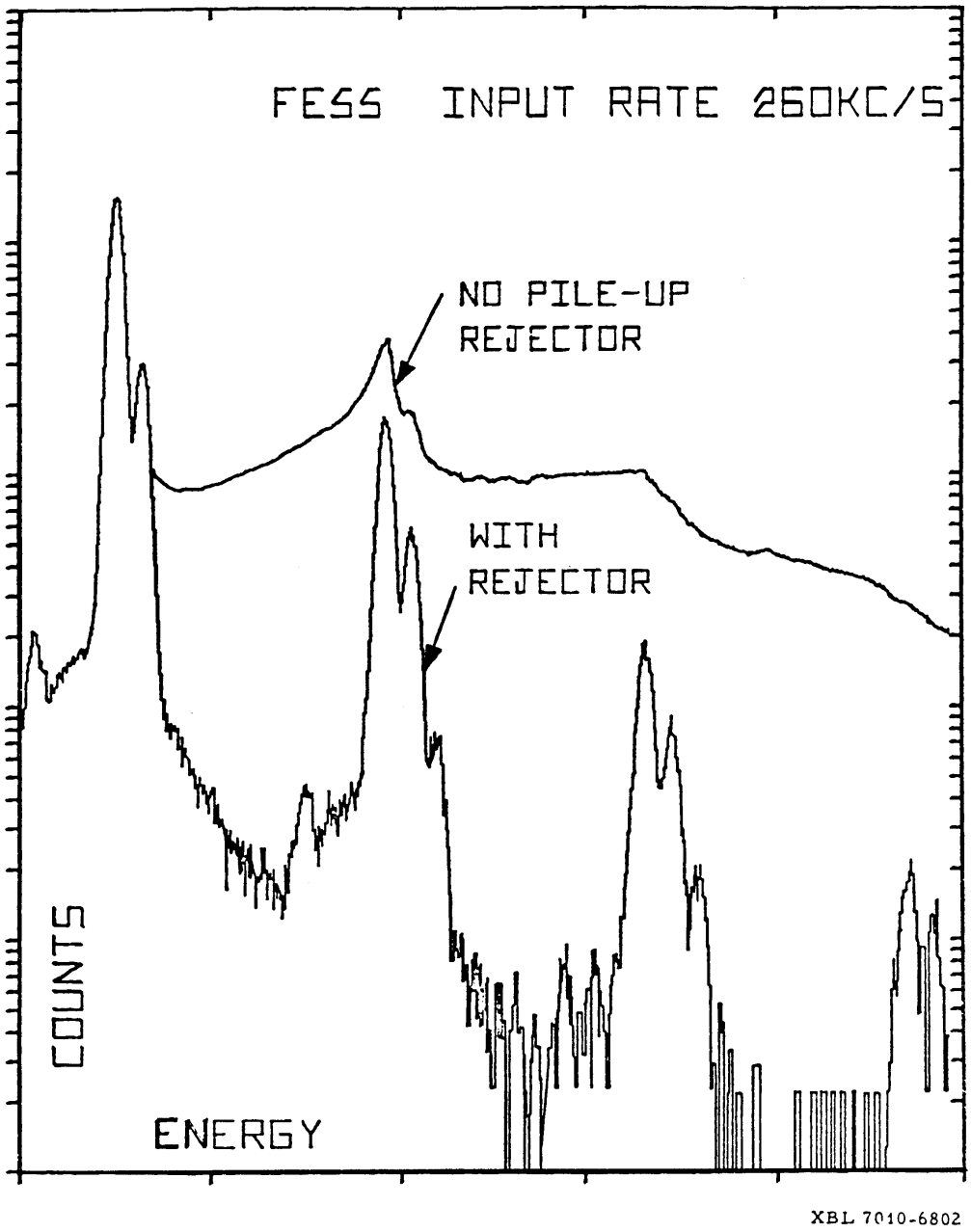

(Don Landis)

Dead Time and Resolution vs. Counting Rate

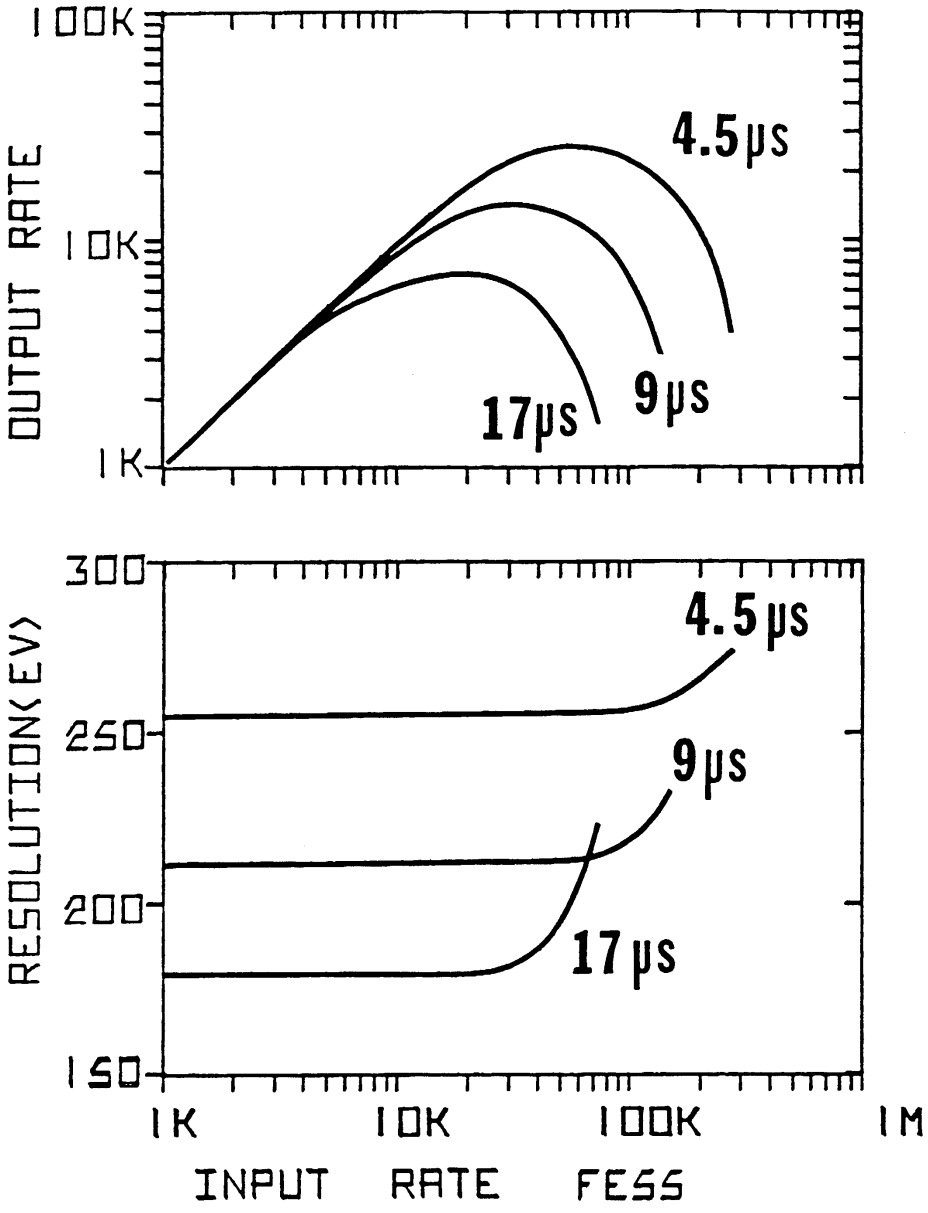

(Joe Jaklevic)

Throughput peaks and then drops as the input rate increases, as most events suffer pile-up and are rejected.

Resolution also degrades beyond turnover point.

- Turnover rate depends on pulse shape and PUR circuitry.
- Critical to measure throughput vs. rate!

Limitations of Pile-Up Rejectors

Minimum dead time where circuitry can't recognize second pulse

⇒ spurious sum peaks

Detectable dead time depends on relative pulse amplitudes

e.g. small pulse following large pulse

⇒ amplitude-dependent rejection factor

problem when measuring yields!

These effects can be evaluated and taken into account, but in experiments it is often appropriate to avoid these problems by using a shorter shaping time (trade off resolution for simpler analysis).

3.5 Delay-Line Clipping

In many instances, e.g. scintillation detectors, shaping is not used to improve resolution, but to increase rate capability.

Example: delay line clipping with NaI(Tl) detector

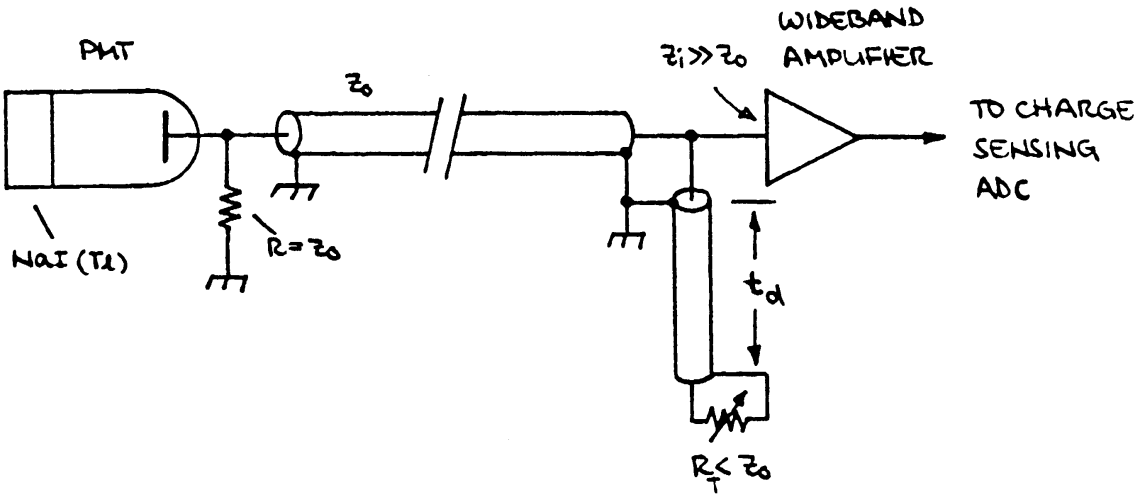

Reminder: Reflections on Transmission Lines

Termination < Line Impedance: Reflection with opposite sign
Termination > Line Impedance: Reflection with same sign

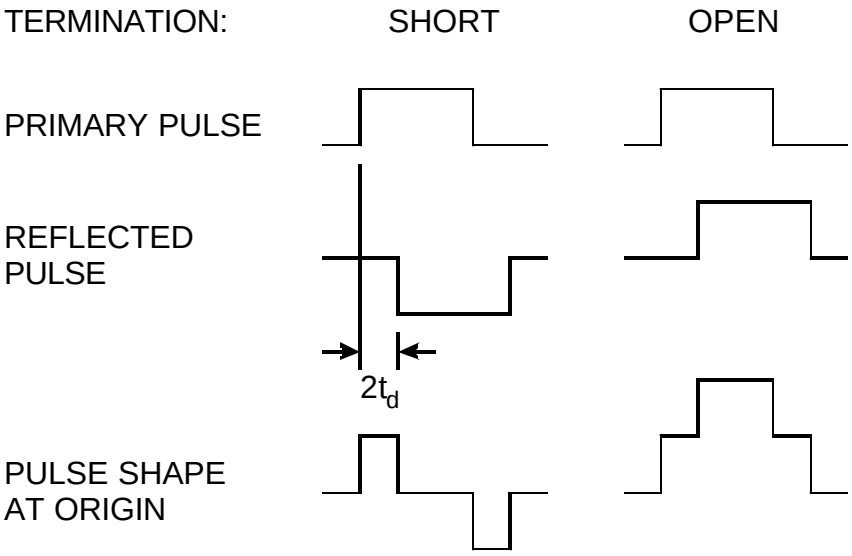

The scintillation pulse has an exponential decay.

PMT Pulse

Reflected Pulse

Sum

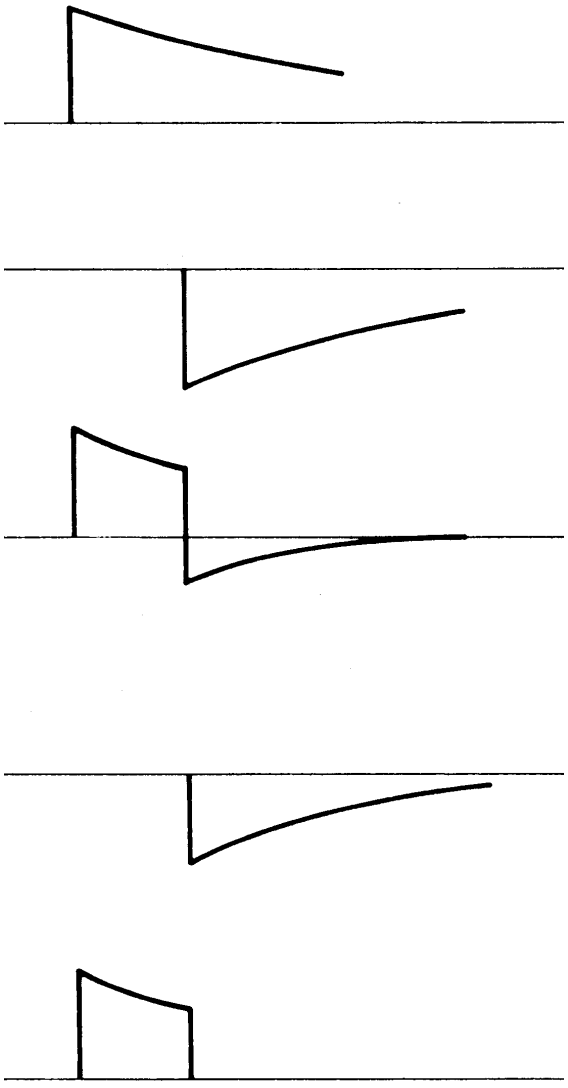

Eliminate undershoot by adjusting magnitude of reflected pulse

$R_T < Z_0$, but $R_T > 0$

magnitude of reflection = amplitude of detector pulse at $t = 2\ t_d$.

No undershoot at summing node ("tail compensation")

Only works perfectly for single decay time constant, but can still provide useful results when other components are much faster (or weaker).

9. Timing Measurements

Pulse height measurements discussed up to now emphasize accurate measurement of signal charge.

- Timing measurements optimize determination of time of occurrence.

- For timing, the figure of merit is not signal-to-noise, but slope-to-noise ratio.

Consider the leading edge of a pulse fed into a threshold discriminator (comparator).

The instantaneous signal level is modulated by noise.

Þ time of threshold crossing fluctuates

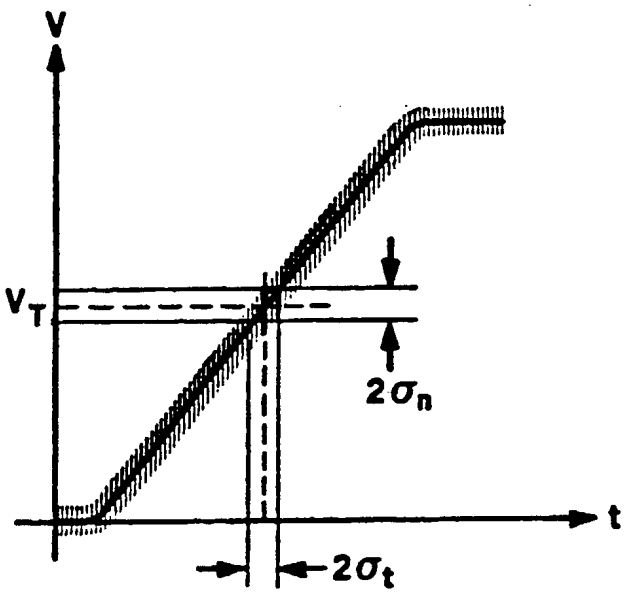

$$s_t = \frac{s_n}{\left.\frac{dV}{dt}\right|_{V_T}}$$

Typically, the leading edge is not linear, so the optimum trigger level is the point of maximum slope.

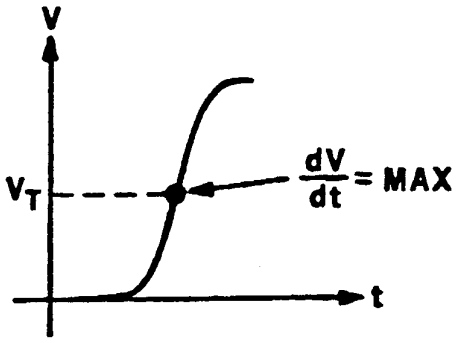

Pulse Shaping

Consider a system whose bandwidth is determined by a single RC integrator.

The time constant of the RC low-pass filter determines the

- rise time (and hence dV/dt)
- amplifier bandwidth (and hence the noise)

Time dependence: $V_o(t) = V_0(1 - e^{-t/t})$

The rise time is commonly expressed as the interval between the points of 10% and 90% amplitude

$$t_r = 2.2\, t$$

In terms of bandwidth

$$t_r = 2.2\, t = \frac{2.2}{2p\ f_u} = \frac{0.35}{f_u}$$

Example: An oscilloscope with 100 MHz bandwidth has 3.5 ns rise time.

For a cascade of amplifiers: $t_r \approx \sqrt{t_{r1}^2 + t_{r2}^2 + \ldots + t_{rn}^2}$

Choice of Rise Time in a Timing System

Assume a detector pulse with peak amplitude V_0 and a rise time t_c passing through an amplifier chain with a rise time t_{ra}.

If the amplifier rise time is longer than the signal rise time,

$$\text{Noise} \propto \sqrt{f_u} \propto \sqrt{\frac{1}{t_{ra}}}$$

$$\frac{dV}{dt} \propto \frac{1}{t_{ra}} \propto f_u$$

increase in bandwidth ⇒ gain in dV/dt outweighs increase in noise.

In detail …

The cumulative rise time at the amplifier output (discriminator output) is

$$t_r = \sqrt{t_c^2 + t_{ra}^2}$$

The electronic noise at the amplifier output is

$$V_{no}^2 = \int e_{ni}^2 \, df = e_{ni}^2 \, \Delta f_n$$

For a single RC time constant the noise bandwidth

$$\Delta f_n = \frac{p}{2} f_u = \frac{1}{4t} = \frac{0.55}{t_{ra}}$$

As the number of cascaded stages increases, the noise bandwidth approaches the signal bandwidth. In any case

$$\Delta f_n \propto \frac{1}{t_{ra}}$$

The timing jitter

$$s_t = \frac{V_{no}}{dV/dt} \approx \frac{V_{no}}{V_0/t_r} = \frac{1}{V_0} V_{no} t_r \propto \frac{1}{V_0} \frac{1}{\sqrt{t_{ra}}} \sqrt{t_c^2 + t_{ra}^2} = \frac{\sqrt{t_c}}{V_0} \sqrt{\frac{t_c}{t_{ra}} + \frac{t_{ra}}{t_c}}$$

The second factor assumes a minimum when the rise time of the amplifier equals the collection time of the detector $t_{ra} = t_c$.

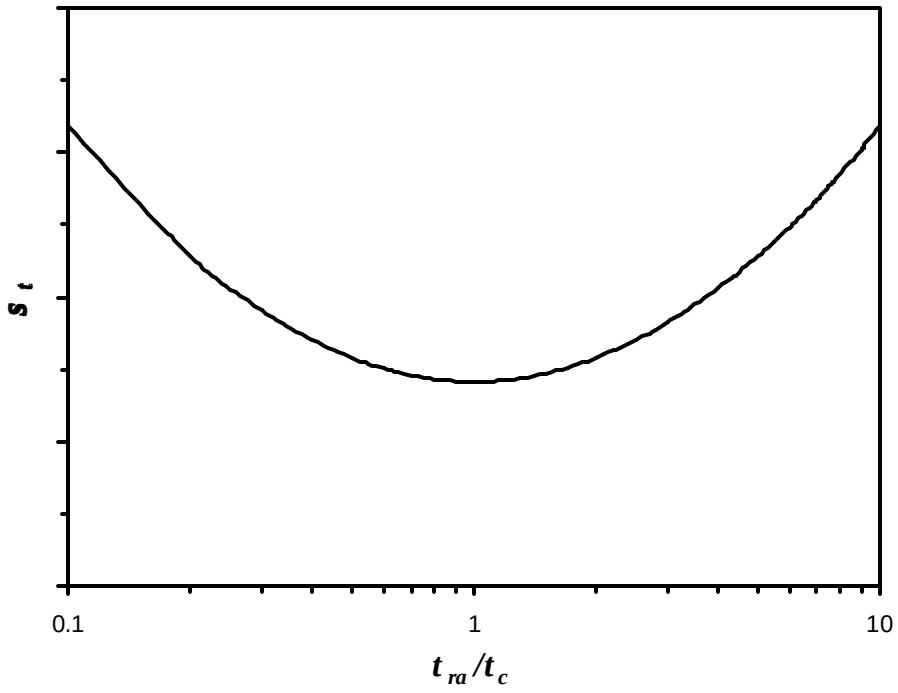

At amplifier rise times greater than the collection time, the time resolution suffers because of rise time degradation. For smaller amplifier rise times the electronic noise dominates.

The timing resolution improves with decreasing collection time $\sqrt{t_c}$ and increasing signal amplitude V_0.

The integration time should be chosen to match the rise time.

How should the differentiation time be chosen?

As shown in the figure below, the loss in signal can be appreciable even for rather large ratios t_{diff}/t_{int}, e.g. >20% for $t_{diff}/t_{int} = 10$.

Since the time resolution improves directly with increasing peak signal amplitude, the differentiation time should be set to be as large as allowed by the required event rate.

CR-RC SHAPER
FIXED INTEGRATOR TIME CONSTANT = 10 ns
DIFFERENTIATOR TIME CONSTANT = ∞ , 100, 30 and 10 ns

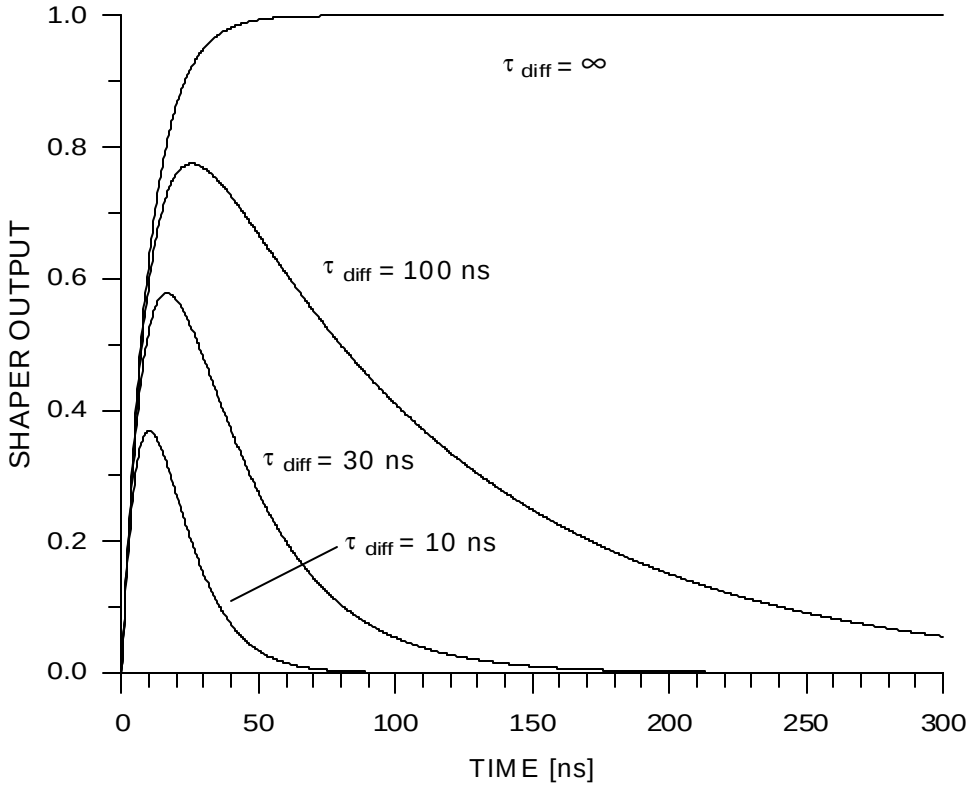

Time Walk

For a fixed trigger level the time of threshold crossing depends on pulse amplitude.

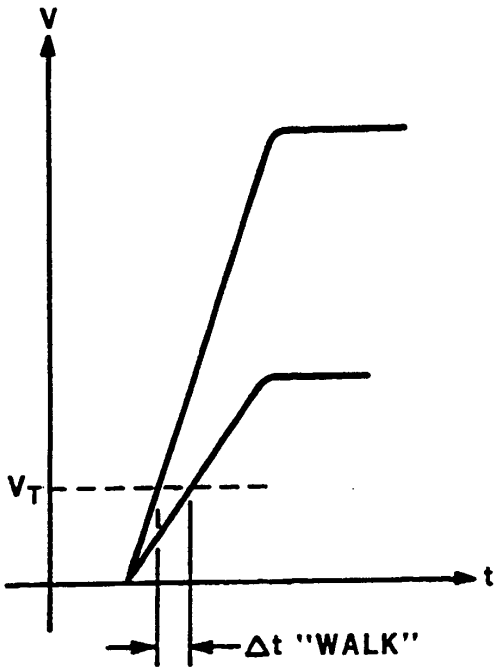

- Accuracy of timing measurement limited by
  - jitter (due to noise)
  - time walk (due to amplitude variations)

If the rise time is known, “time walk” can be compensated in software event-by-event by measuring the pulse height and correcting the time measurement.

This technique fails if both amplitude and rise time vary, as is common.

In hardware, time walk can be reduced by setting the threshold to the lowest practical level, or by using amplitude compensation circuitry, e.g. constant fraction triggering.

Lowest Practical Threshold

Single RC integrator has maximum slope at $t = 0$.

$$\frac{d}{dt}(1 - e^{-t/t}) = \frac{1}{t} e^{-t/t}$$

However, the rise time of practically all fast timing systems is determined by multiple time constants.

For small t the slope at the output of a single RC integrator is linear, so initially the pulse can be approximated by a ramp $a\ t$.

Response of the following integrator

$$V_i = a\ t \quad \rightarrow \quad V_o = a(t - t) - a\ t\ e^{-t/t}$$

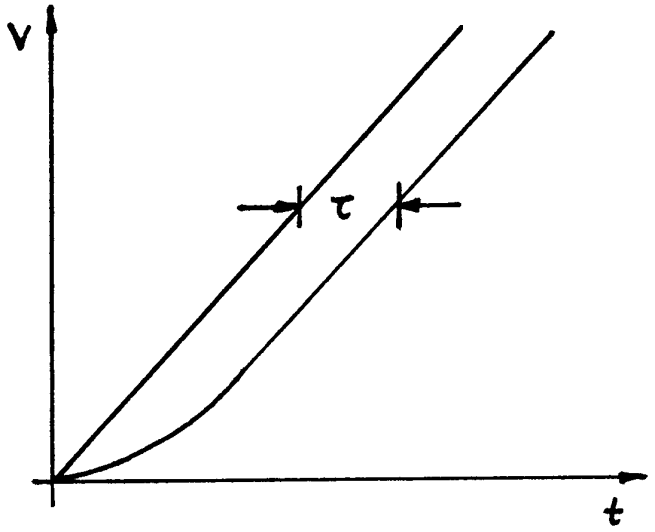

$\Rightarrow$ The output is delayed by t and curvature is introduced at small t.

Output attains 90% of input slope after $t = 2.3\,t$.

Delay for n integrators= $n\,t$

Additional RC integrators introduce more curvature at the beginning of the pulse.

Output pulse shape for multiple RC integrators

(normalized to preserve the peaking time $t_n = t_{n=1}/n$)

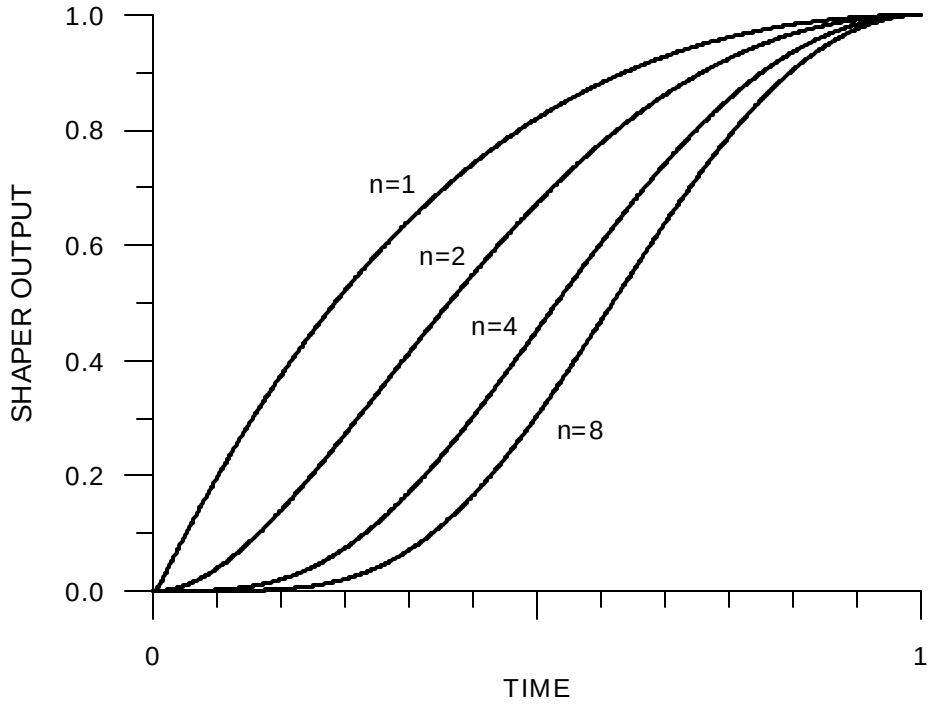

Increased curvature at beginning of pulse limits the minimum threshold for good timing.

- One dominant time constant best for timing measurements

Unlike amplitude measurements, where multiple integrators are desirable to improve pulse symmetry and count rate performance.

Constant Fraction Timing

Basic Principle:

make the threshold track the signal

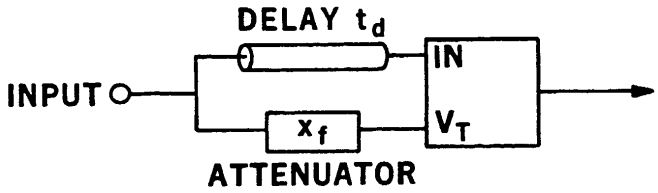

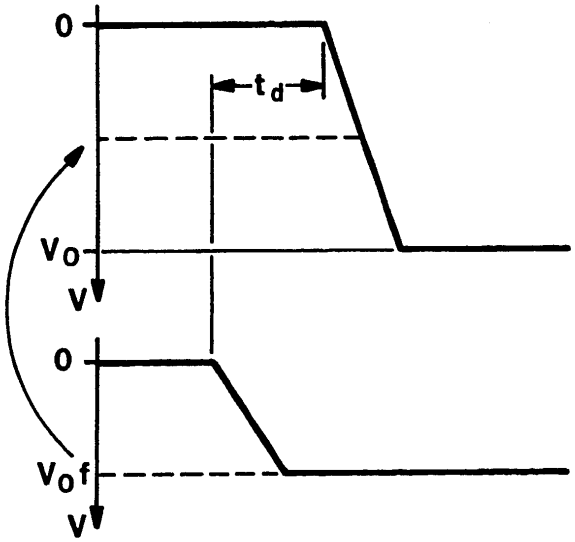

The threshold is derived from the signal by passing it through an attenuator $V_T = f\, V_s$.

The signal applied to the comparator input is delayed so that the transition occurs after the threshold signal has reached its maximum value $V_T = f\, V_0$.

For simplicity assume a linear leading edge

$$V(t) = \frac{t}{t_r} V_0 \quad \text{for } t \le t_r \qquad \text{and} \qquad V(t) = V_0 \quad \text{for } t > t_r$$

so the signal applied to the input is

$$V(t) = \frac{t - t_d}{t_r} V_0$$

When the input signal crosses the threshold level

$$f\, V_0 = \frac{t - t_d}{t_r} V_0$$

and the comparator fires at the time

$$t = f\, t_r + t_d \qquad (t_d > t_r)$$

at a constant fraction of the rise time independent of peak amplitude.

If the delay t_d is reduced so that the pulse transitions at the signal and threshold inputs overlap, the threshold level

$$V_T = f \frac{t}{t_r} V_0$$

and the comparator fires at

$$f \frac{t}{t_r} V_0 = \frac{t - t_d}{t_r} V_0$$

$$t = \frac{t_d}{1 - f} \qquad (t_d < (1 - f)\, t_r)$$

independent of both amplitude and rise time (amplitude and rise-time compensation).

The circuit compensates for amplitude and rise time if pulses have a sufficiently large linear range that extrapolates to the same origin.

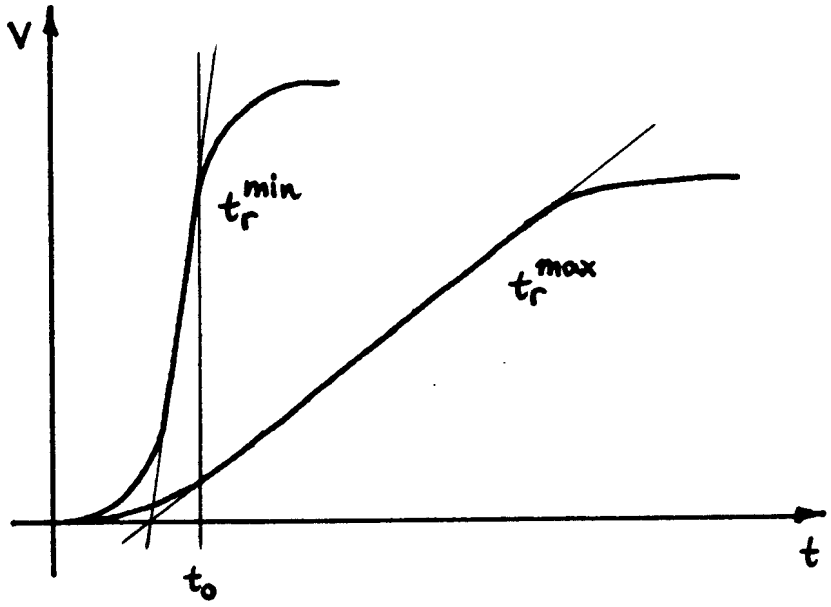

The condition for the delay must be met for the minimum rise time:

$$t_d \leq (1-f)\, t_{r,\min}$$

In this mode the fractional threshold V_T/V_0 varies with rise time.

For all amplitudes and rise times within the compensation range the comparator fires at the time

$$t_0 = \frac{t_d}{1-f}$$

Another View of Constant Fraction Discriminators

The constant fraction discriminator can be analyzed as a pulse shaper, comprising the

- delay
- attenuator
- subtraction

driving a trigger that responds to the zero crossing.

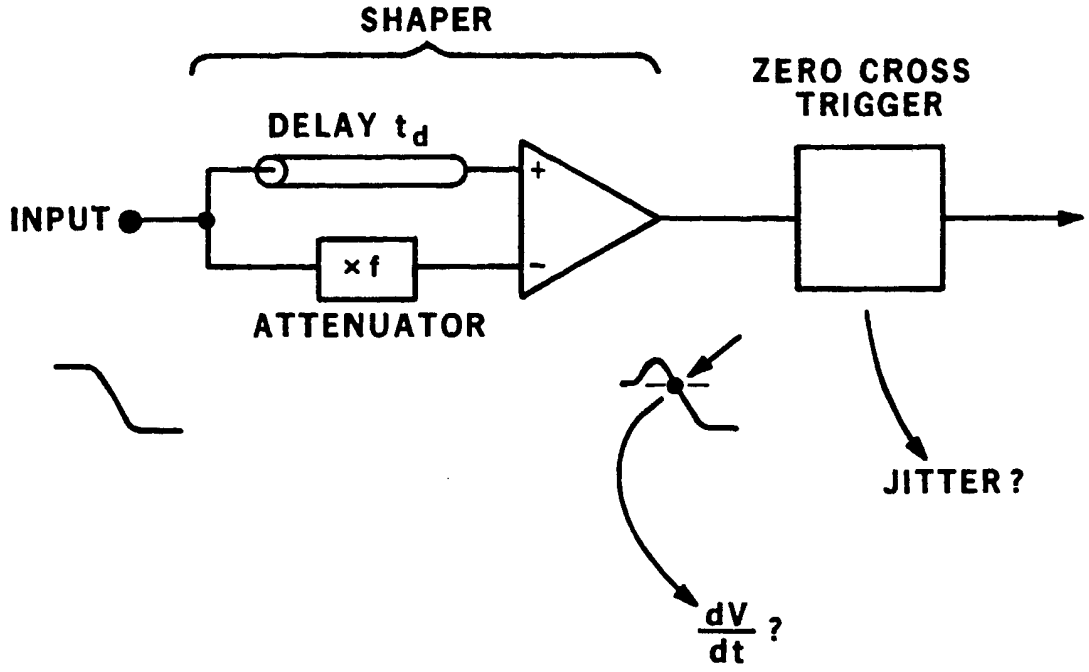

The timing jitter depends on

- the slope at the zero-crossing
  (depends on choice of f and t_d)
- the noise at the output of the shaper
  (this circuit increases the noise bandwidth)

Examples

1. g -g coincidence (as used in positron emission tomography)

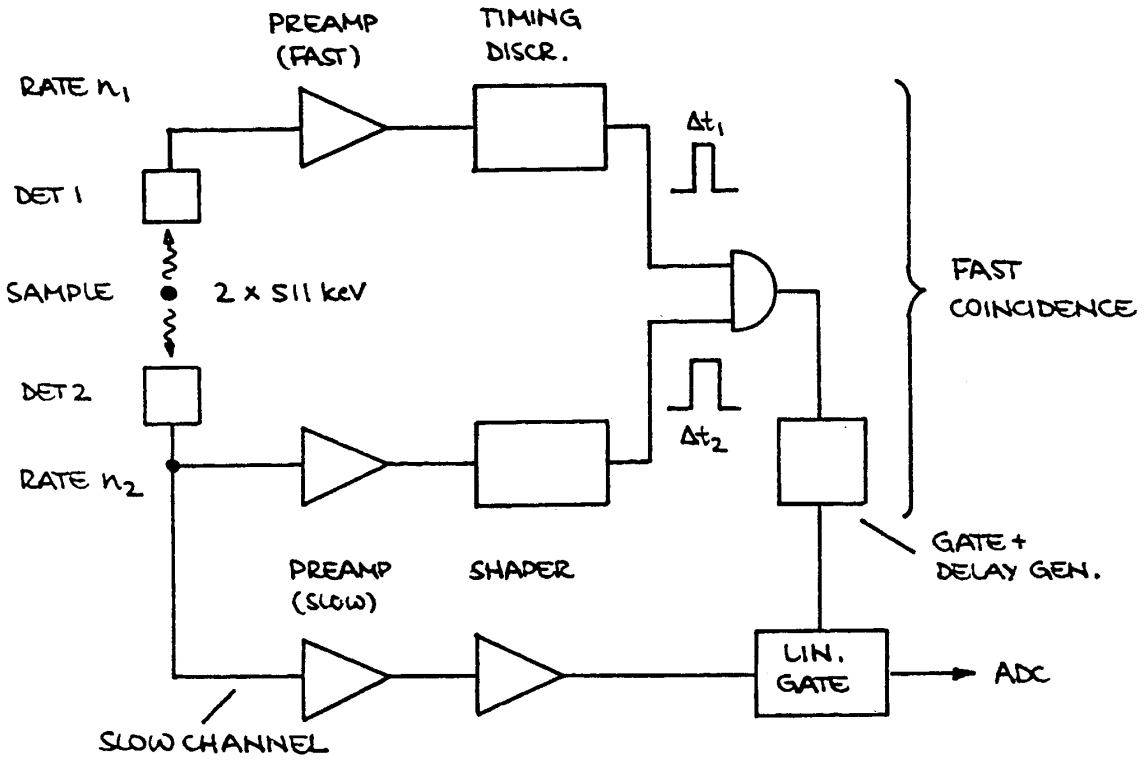

Positron annihilation emits two collinear 511 keV photons.

Each detector alone will register substantial background.

Non-coincident background can be suppressed by requiring simultaneous signals from both detectors.

- Each detector feeds a fast timing channel.
- The timing pulses are combined in an AND gate (coincidence unit). The AND gate only provides an output if the two timing pulses overlap.
- The coincidence output is used to open a linear gate, that allows the energy signal to pass to the ADC.

This arrangement accommodates the contradictory requirements of timing and energy measurements. The timing channels can be fast, whereas the energy channel can use slow shaping to optimize energy resolution ("fast-slow coincidence").

Chance coincidence rate

Two random pulse sequences have some probability of coincident events.

If the event rates in the two channels are n_1 and n_2, and the timing pulse widths are Dt_1 and Dt_2, the probabality of a pulse from the first source occuring in the total coincidence window is

$$P_1 = n_1 \cdot (\Delta t_1 + \Delta t_2)$$

The coincidence is "sampled" at a rate n_2 , so the chance coincidence rate is

$$n_c = P_1 \cdot n_2$$

$$n_c = n_1 \cdot n_2 \cdot (\Delta t_1 + \Delta t_2)$$

i.e. in the arrangement shown above, the chance coincidence rate increases with the square of the source strength.

Example: $n_1 = n_2 = 10^6\ s^{-1}$

$Dt_1 = Dt_1 = 5$ ns

Þ $n_c = 10^4\ s^{-1}$

2. Nuclear Mass Spectroscopy by Time-of-Flight

Two silicon detectors

First detector thin, so that particle passes through it (transmission detector)

$\Rightarrow$ differential energy loss DE

Second detector thick enough to stop particle

$\Rightarrow$ Residual energy E

Measure time-of-flight Dt between the two detectors

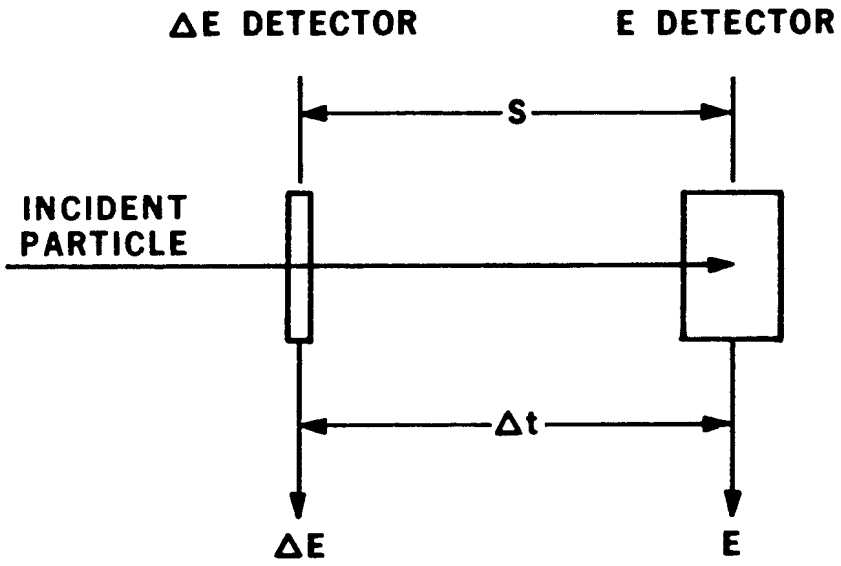

$\Delta E + E \rightarrow E_{TOT}$
$\Delta E, E \rightarrow Z$
$\Delta t, E \rightarrow A$

$$E_{tot} = \Delta E + E \qquad Z \propto \sqrt{\Delta E \cdot E_{tot}} \qquad A \propto E \cdot (\Delta t / s)^2$$

"Typical" Results

Example 1

Flight path 20 cm, $Dt \approx 50$ ps FWHM

$s_t = 21$ ps

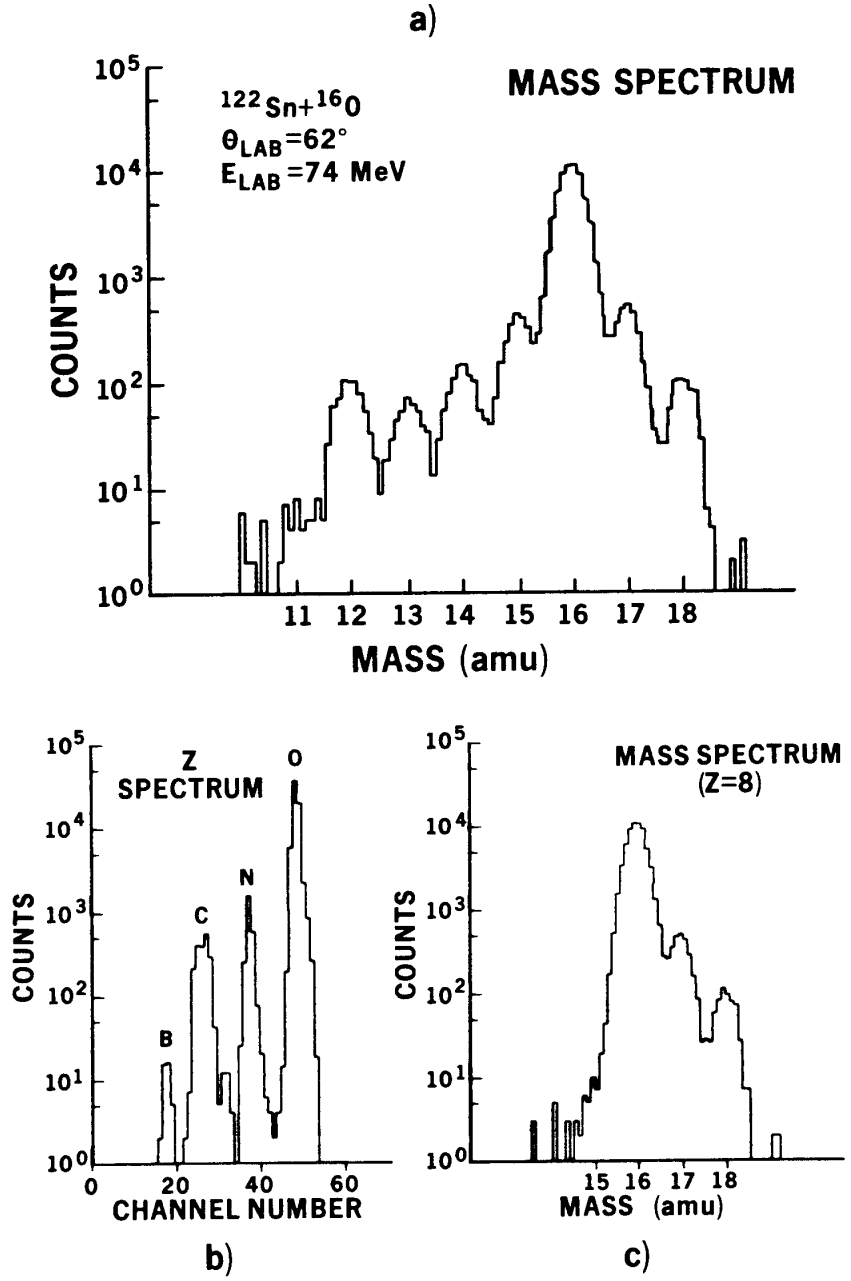

(H. Spieler et al., Z. Phys. **A278** (1976) 241)

Example 2

1. DE-detector: 27 μm thick, A= 100 mm^2, $<E>$=1.1·10^4 V/cm

2. E-detector: 142 μm thick, A= 100 mm^2, $<E>$=2·10^4 V/cm

For 230 MeV ^{28}Si: DE = 50 MeV ⇒ V_s= 5.6 mV
E = 180 MeV ⇒ V_s= 106 mV

⇒ Dt = 32 ps FWHM
s_t = 14 ps

Example 3

Two transmission detectors,

each 160 μm thick, A= 320 mm^2

For 650 MeV/u ^{20}Ne: DE = 4.6 MeV ⇒ V_s= 800 μV

⇒ Dt = 180 ps FWHM
s_t = 77 ps

For 250 MeV/u ^{20}Ne: DE = 6.9 MeV ⇒ V_s= 1.2 mV

⇒ Dt = 120 ps FWHM
s_t = 52 ps

Fast Timing: Comparison between theory and experiment

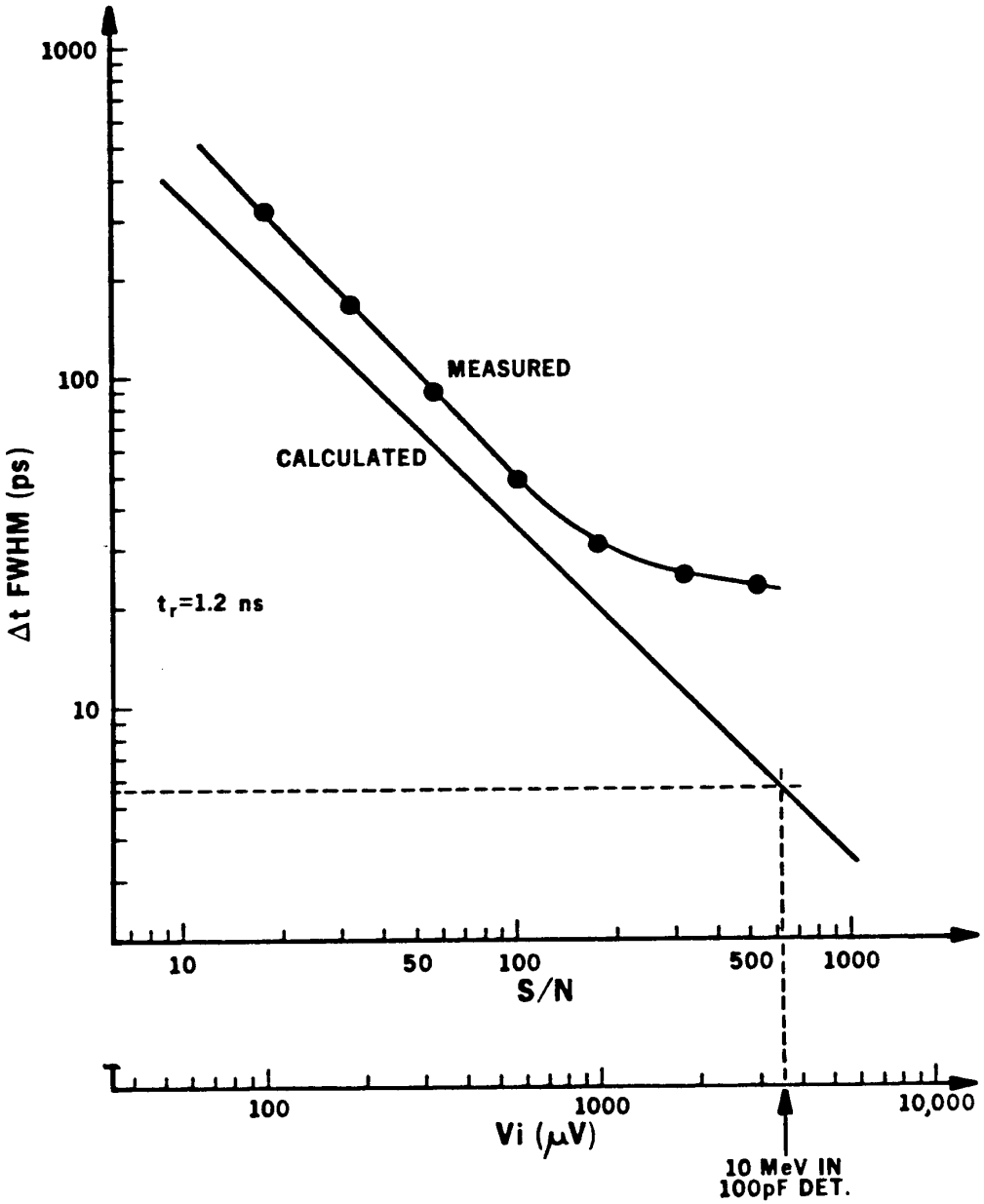

At $S/N<100$ the measured curve lies above the calculation because the timing discriminator limited the rise time.
At high S/N the residual jitter of the time digitizer limits the resolution.

For more details on fast timing with semiconductor detectors, see H. Spieler, IEEE Trans. Nucl. Sci. **NS-29/3** (1982) 1142.

10. Digitization of Pulse Height and Time – Analog to Digital Conversion

For data storage and subsequent analysis the analog signal at the shaper output must be digitized.

Important parameters for ADCs used in detector systems:

1. Resolution
   The "granularity" of the digitized output

2. Differential Non-Linearity
   How uniform are the digitization increments?

3. Integral Non-Linearity
   Is the digital output proportional to the analog input?

4. Conversion Time
   How much time is required to convert an analog signal to a digital output?

5. Count-Rate Performance
   How quickly can a new conversion commence after completion of a prior one without introducing deleterious artifacts?

6. Stability
   Do the conversion parameters change with time?

Instrumentation ADCs used in industrial data acquisition and control systems share most of these requirements. However, detector systems place greater emphasis on differential non-linearity and count-rate performance. The latter is important, as detector signals often occur randomly, in contrast to measurement systems where signals are sampled at regular intervals.

9.1 ADC Parameters

1. Resolution

Digitization incurs approximation, as a continuous signal distribution is transformed into a discrete set of values. To reduce the additional errors (noise) introduced by digitization, the discrete digital steps must correspond to a sufficiently small analog increment.

Simplistic assumption:

Resolution is defined by the number of output bits, e.g.

13 bits ® $\frac{\Delta V}{V} = \frac{1}{8192} = 1.2 \cdot 10^{-4}$

True Measure: Channel Profile

Plot probability vs. pulse amplitude that a pulse height corresponding to a specific output bin is actually converted to that address.

Ideal ADC:

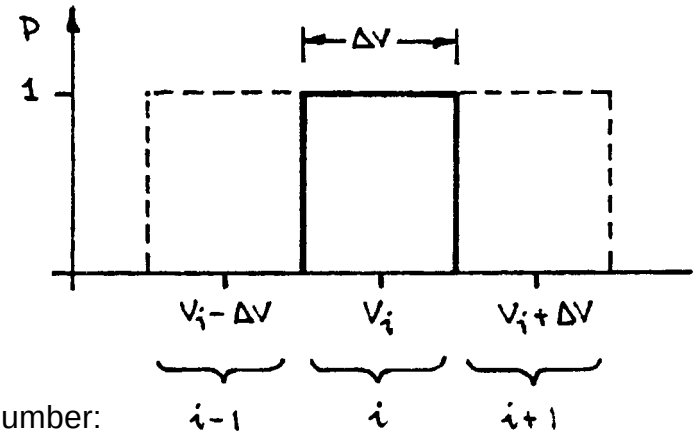

output bin number:

Measurement accuracy:

- If all counts of a peak fall in one bin, the resolution is ΔV.
- If the counts are distributed over several (>4 or 5) bins, peak fitting can yield a resolution of $10^{-1} – 10^{-2}\ \Delta V$, *if the distribution is known and reproducible* (not necessarily a valid assumption for an ADC).

In reality, the channel profile is not rectangular as sketched above.

Electronic noise in the threshold discrimination process that determines the channel boundaries “smears” the transition from one bin to the next.

Measured channel profile (13 bit ADC)

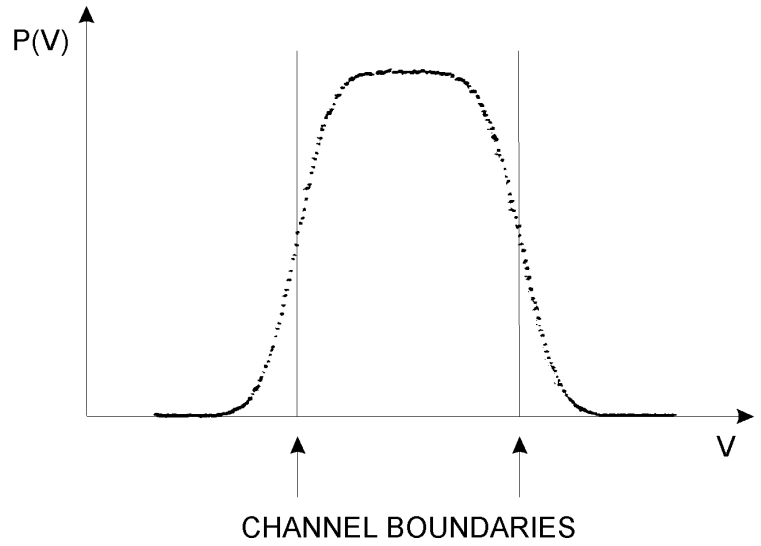

The profiles of adjacent channels overlap

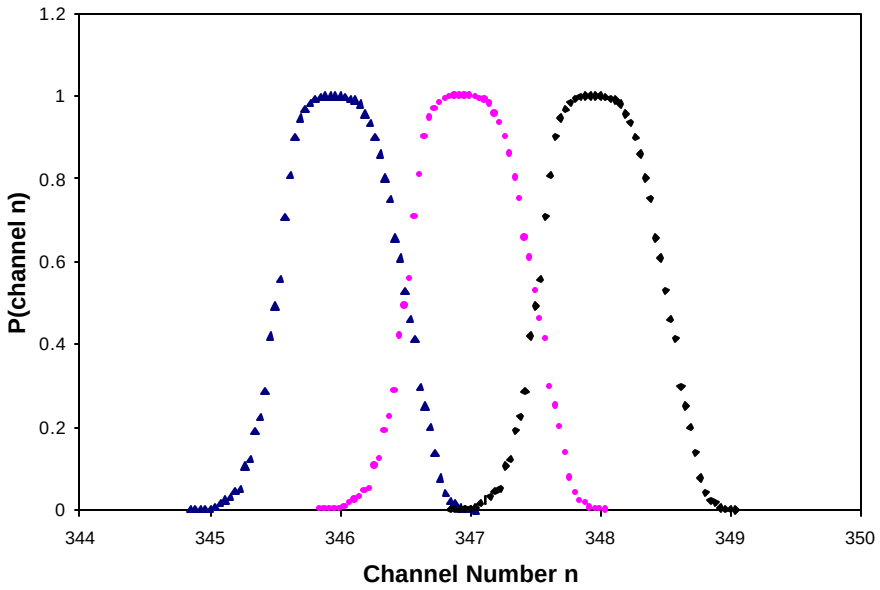

Channel profile can be checked quickly by applying the output of a precision pulser to the ADC.

If the pulser output has very low noise, i.e. the amplitude jitter is much smaller than the voltage increment corresponding to one ADC channel or bin, all pulses will be converted to a single channel, with only a small fraction appearing in the neighbor channels.

Example of an ADC whose digital resolution is greater than its analog resolution:

8192 ch conversion range (13 bits)

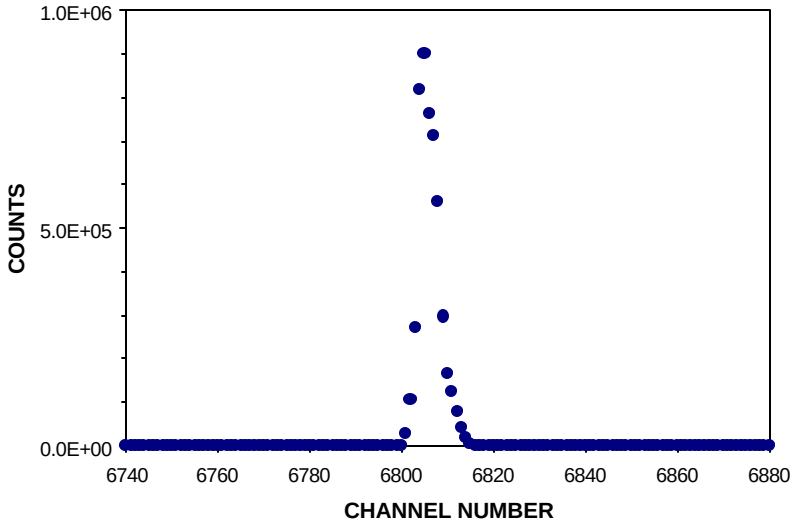

2048 ch conversion range (11 bits)

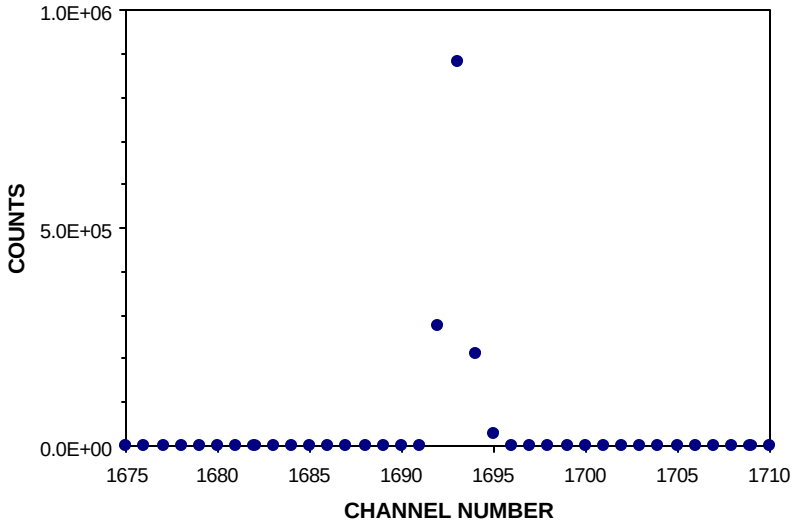

2K range provides maximum resolution – higher ranges superfluous.

How much ADC Resolution is Required?

Example:

Detector resolution
1.8 keV FWHM

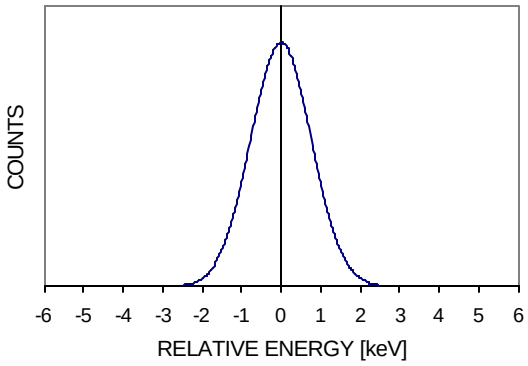

Digitized spectra for various ADC resolutions (bin widths) ΔE:

ΔE= 1.8 keV = 1 x FWHM

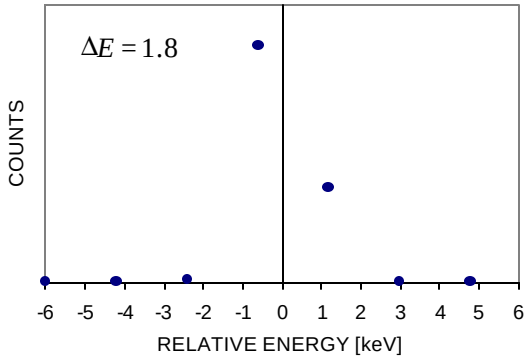

ΔE= 0.72 keV = 0.4 x FWHM

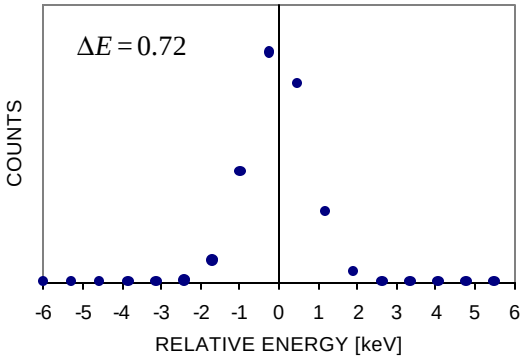

ΔE= 0.36 keV = 0.2 x FWHM

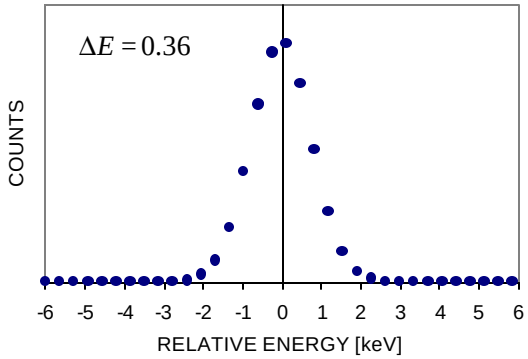

ΔE= 0.18 keV = 0.1 x FWHM

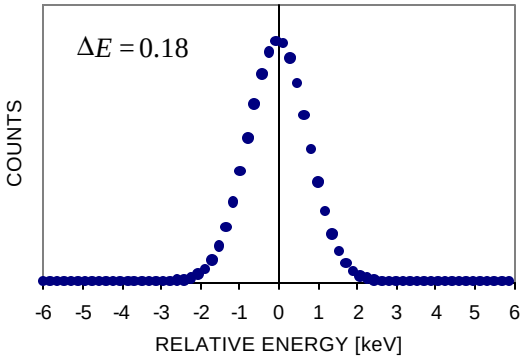

Fitting can determine centroid position to fraction of bin width even with coarse digitization, **if the line shape is known**.

Five digitizing channels within a linewidth (FWHM) allow robust peak fitting and centroid finding, even for imperfectly known line shapes and overlapping peaks.

2. Differential Non-Linearity

Differential non-linearity is a measure of the inequality of channel profiles over the range of the ADC.

Depending on the nature of the distribution, either a peak or an rms specification may be appropriate.

$$DNL = \max\left\{\frac{\Delta V(i)}{\langle \Delta V \rangle} - 1\right\}$$

or

$$DNL = \text{r.m.s.}\left\{\frac{\Delta V(i)}{\langle \Delta V \rangle} - 1\right\}$$

where $\langle \Delta V \rangle$ is the average channel width and $\Delta V(i)$ is the width of an individual channel.

Differential non-linearity of < ±1% max. is typical, but state-of-the-art ADCs can achieve 10^{-3} rms, i.e. the variation is comparable to the statistical fluctuation for 10^6 random counts.

Note: Instrumentation ADCs are often specified with an accuracy of ±0.5 LSB (least significant bit), so the differential non-linearity may be 50% or more.

Typical differential non-linearity patterns ("white" input spectrum).

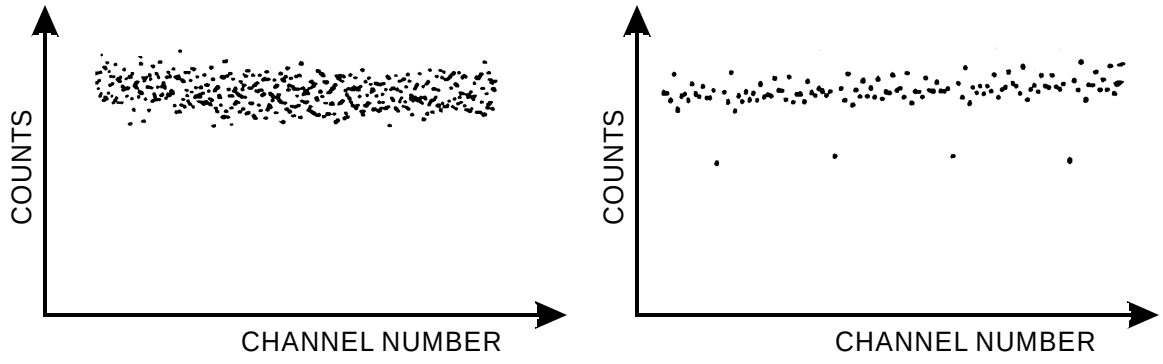

An ideal ADC would show an equal number of counts in each bin.

The spectrum to the left shows a random pattern, but note the multiple periodicities visible in the right hand spectrum.

3. Integral Non-Linearity

Integral non-linearity measures the deviation from proportionality of the measured amplitude to the input signal level.

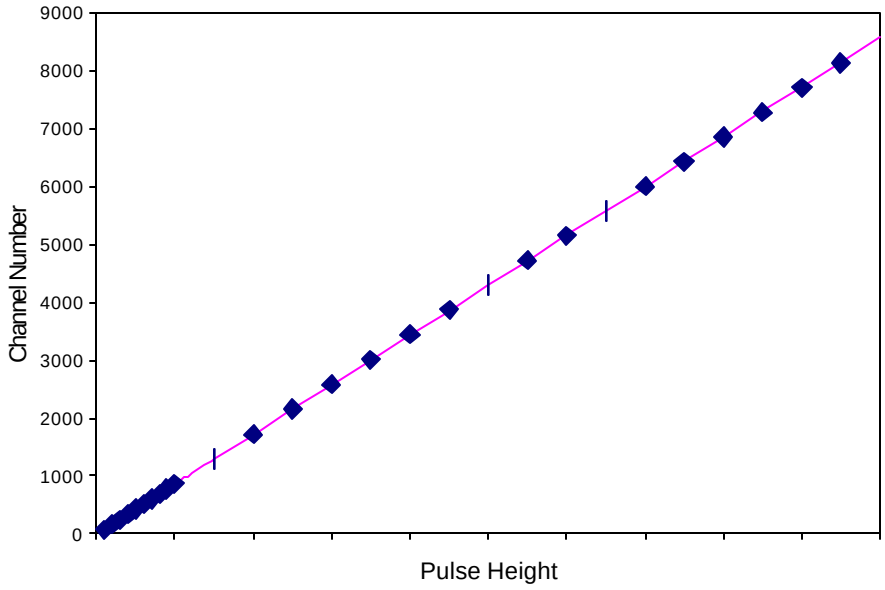

The dots are measured values and the line is a fit to the data.

This plot is not very useful if the deviations from linearity are small.

Plotting the deviations of the measured points from the fit yields:

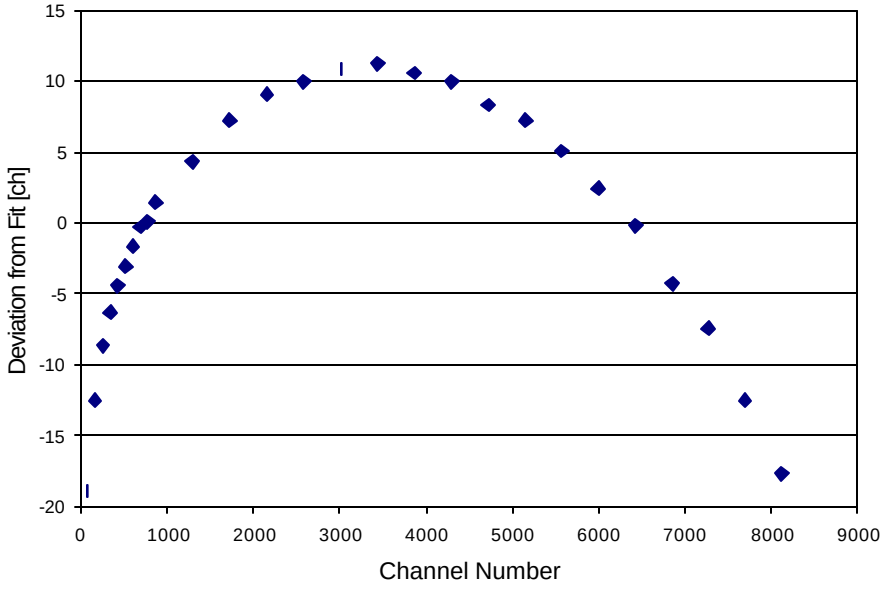

The linearity of an ADC can depend on the input pulse shape and duration, due to bandwidth limitations in the circuitry.

The differential non-linearity shown above was measured with a 400 ns wide input pulse.

Increasing the pulse width to 3 μs improved the result significantly:

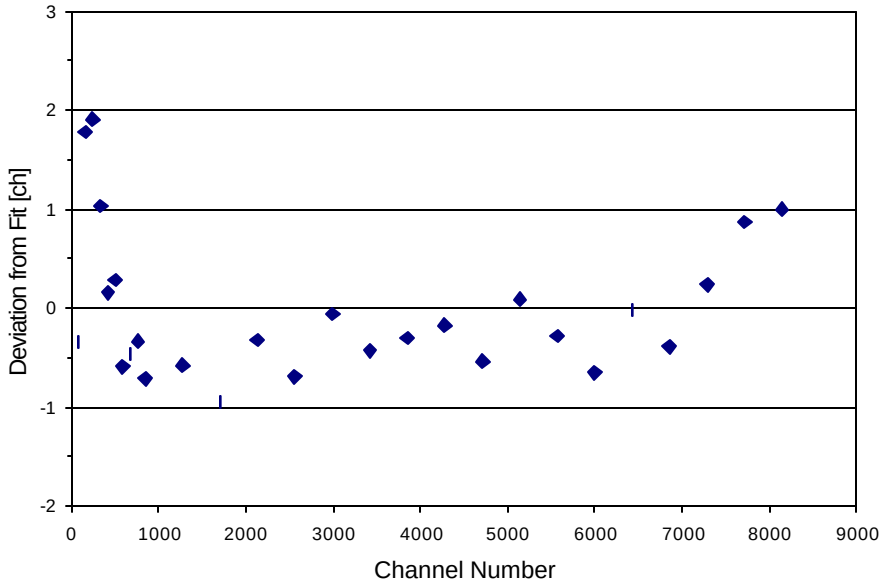

4. Conversion Time

During the acquisition of a signal the system cannot accept a subsequent signal ("dead time")

Dead Time =

signal acquisition time	→	time-to-peak + const.
+ conversion time	→	can depend on pulse height
+ readout time to memory	→	depends on speed of data transmission and buffer memory access - can be large in computer-based systems

Dead time affects measurements of yields or reaction cross-sections. Unless the event rate << 1/(dead time), it is necessary to measure the dead time, e.g. with a reference pulser fed simultaneously into the spectrum.

The total number of reference pulses issued during the measurement is determiend by a scaler and compared with the number of pulses recorded in the spectrum.

Does a pulse-height dependent dead time mean that the correction is a function of pulse height?

Usually not. If events in different part of the spectrum are not correlated in time, i.e. random, they are all subject to the same average dead time (although this average will depend on the spectral distribution).

- Caution with correlated events!
  Example: Decay chains, where lifetime is < dead time.
  The daughter decay will be lost systematically.

5. Count Rate Effects

Problems are usually due to internal baseline shifts with event rate or undershoots following a pulse.

If signals occur at constant intervals, the effect of an undershoot will always be the same.

However, in a random sequence of pulses, the effect will vary from pulse to pulse.

- spectral broadening

Baseline shifts tend to manifest themselves as a systematic shift in centroid position with event rate.

Centroid shifts for two 13 bit ADCs vs. random rate:

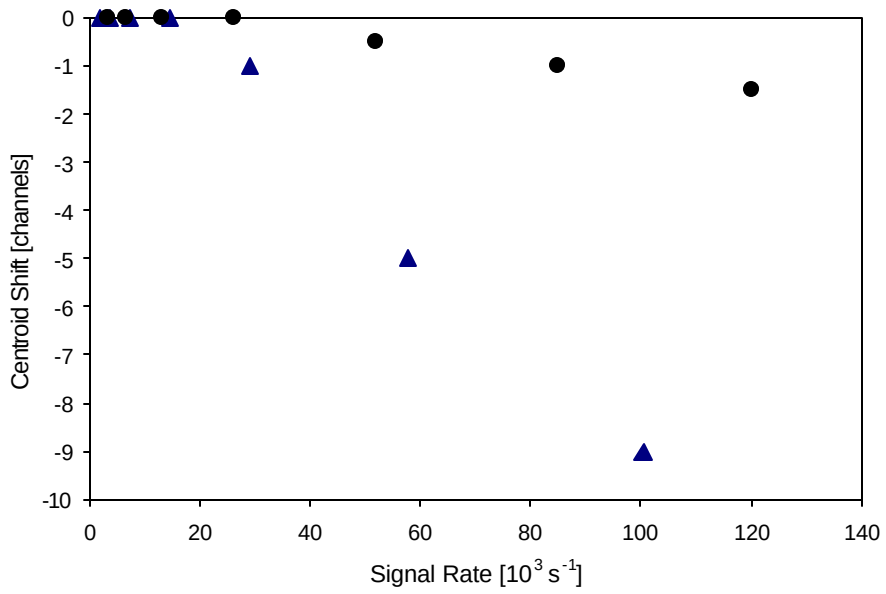

6. Stability

   Stability vs. temperature is usually adequate with modern electronics in a laboratory environment.

- Note that temperature changes within a module are typically much smaller than ambient.

  However: Highly precise or long-term measurements require spectrum stabilization to compensate for changes in gain and baseline of the overall system.

  Technique: Using precision pulsers place a reference peak at both the low and high end of the spectrum.

  (Pk. Pos. 2) – (Pk. Pos. 1) $\rightarrow$ Gain, … then

  (Pk. Pos. 1) or (Pk. Pos. 2) $\rightarrow$ Offset

  Traditional Implementation: Hardware, spectrum stabilizer module

  Today, it is more convenient to determine the corrections in software. These can be applied to calibration corrections or used to derive an electrical signal that is applied to the hardware (simplest and best in the ADC).

10.2 Analog to Digital Conversion Techniques

1. Flash ADC

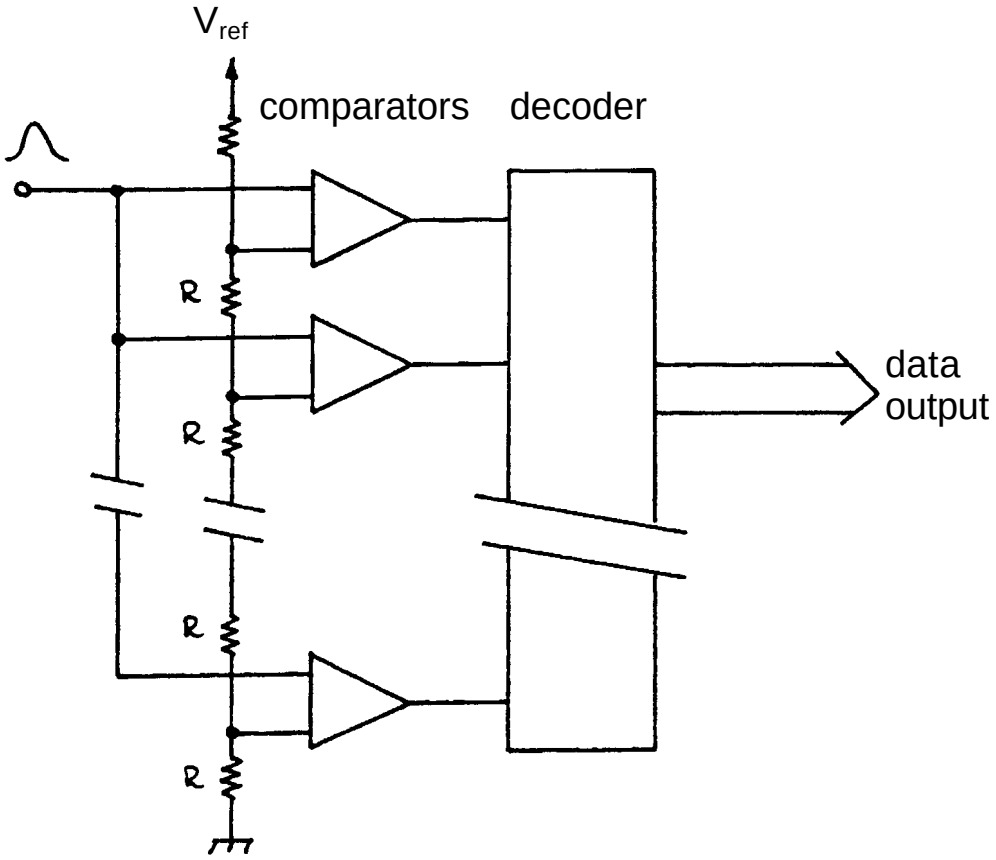

The input signal is applied to *n* comparators in parallel. The switching thresholds are set by a resistor chain, such that the voltage difference between individual taps is equal to the desired measurement resolution.

2^n comparators for *n* bits (8 bit resolution requires 256 comparators)

Feasible in monolithic ICs since the absolute value of the resistors in the reference divider chain is not critical, only the relative matching.

Advantage: short conversion time (<10 ns available)
Drawbacks: limited accuracy (many comparators)
power consumption
Differential non-linearity ~ 1%
High input capacitance (speed is often limited by the analog driver feeding the input)

2. Successive Approximation ADC

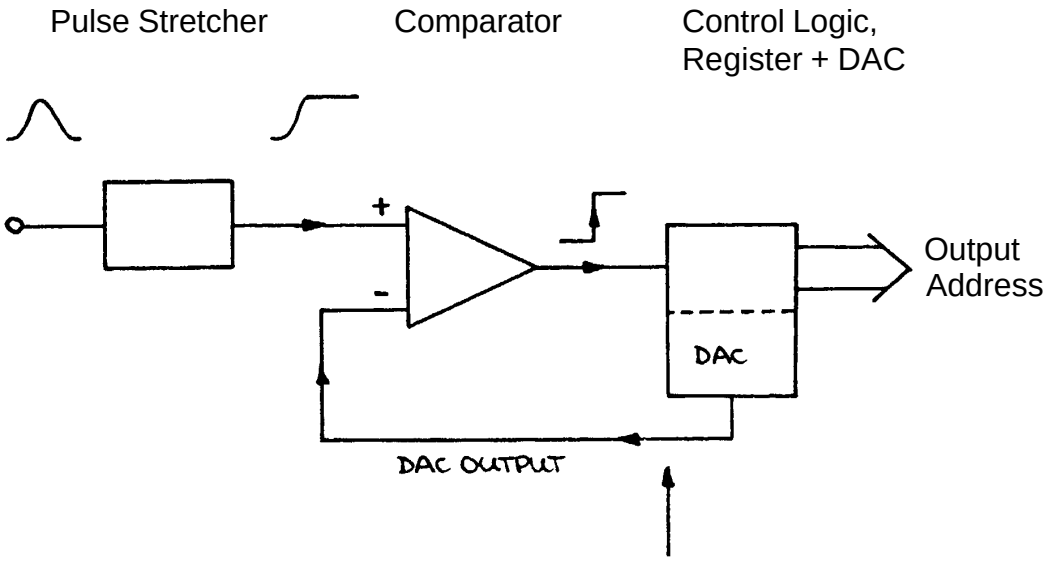

Sequentially add levels proportional to 2^n, 2^{n-1}, … 2^0 and set corresponding bit if the comparator output is high (DAC output < pulse height)

n conversion steps yield 2^n channels,
i.e. 8K channels require 13 steps

Advantages: speed (~ μs)
high resolution
ICs (monolithic + hybrid) available

Drawback: Differential non-linearity (typ. 10 – 20%)

Reason: Resistors that set DAC output must be extremely accurate.

For DNL < 1% the resistor determining the 2^{12} level in an 8K ADC must be accurate to < $2.4 \cdot 10^{-6}$.

DNL can be corrected by various techniques:

- averaging over many channel profiles for a given pulse amplitude ("sliding scale" or "Gatti principle")
- correction DAC ("brute force" application of IC technology)

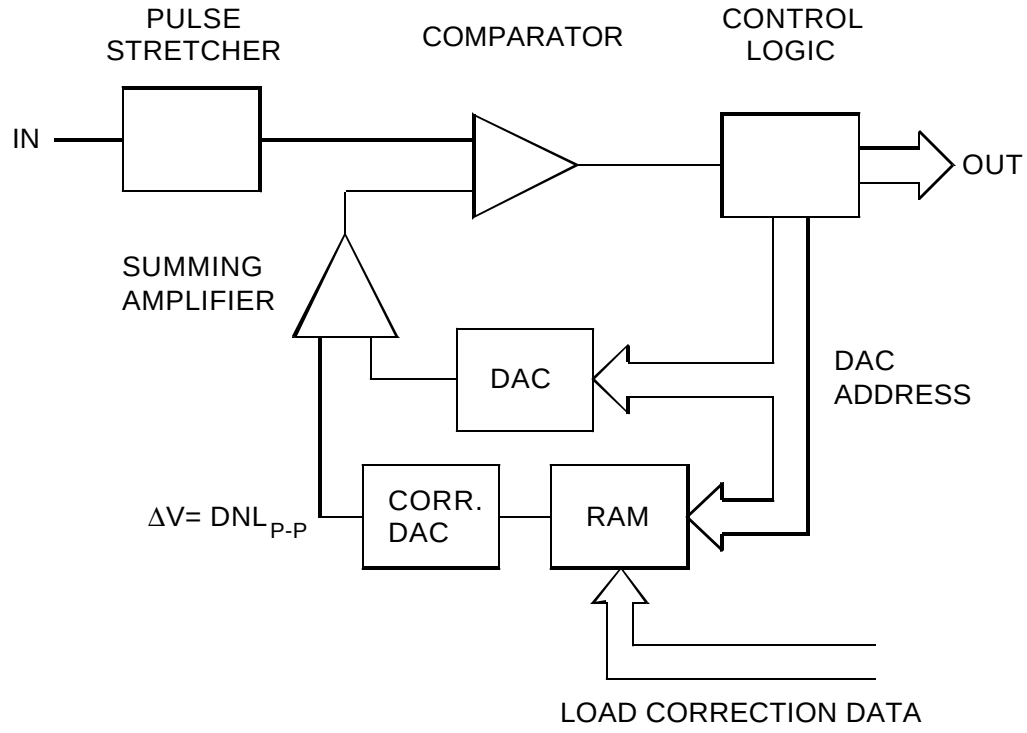

The primary DAC output is adjusted by the output of a correction DAC to reduce differential non-linearity.

Correction data are derived from a measurement of DNL. Corrections for each bit are loaded into the RAM, which acts as a look-up table to provide the appropriate value to the correction DAC for each bit of the main DAC.

The range of the correction DAC must exceed the peak-to-peak differential non-linearity.

If the correction DAC has N bits, the maximum DNL is reduced by $2^{-(N-1)}$ (if deviations are symmetrical).

3. Wilkinson ADC

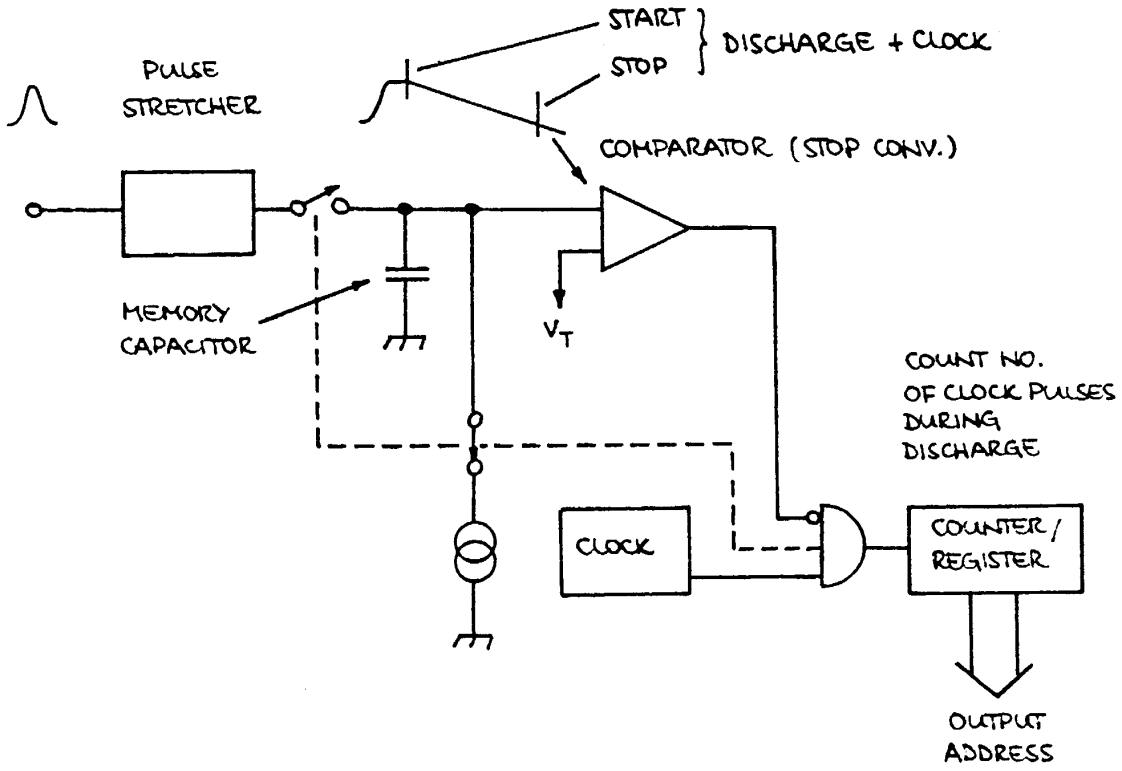

The peak signal amplitude is acquired by a pulse stretcher and transferred to a memory capacitor. Then, simultaneously,

1. the capacitor is disconnected from the stretcher,
2. a current source is switched to linearly discharge the capacitor,
3. a counter is enabled to determine the number of clock pulses until the voltage on the capacitor reaches the baseline.

Advantage: excellent differential linearity
(continuous conversion process)

Drawbacks: slow – conversion time = $n \cdot T_{clock}$
(n = channel number $\propto$ pulse height)
T_{clock} = 10 ns $\rightarrow T_{conv}$ = 82 µs for 13 bits
Clock frequencies of 100 MHz typical, but >400 MHz possible with excellent performance

"Standard" technique for high-resolution spectroscopy.

Hybrid Analog-to-Digital Converters

Conversion techniques can be combined to obtain high resolution and short conversion time.

1. Flash + Successive Approximation or
   Flash + Wilkinson (Ramp Run-Down)

   Utilize fast flash ADC for coarse conversion
   (*e.g.* 8 out of 13 bits)

   Successive approximation or Wilkinson converter to provide fine resolution. Limited range, so short conversion time:

   256 ch with 100 MHz clock $\Rightarrow$ 2.6 μs

   Results: 13 bit conversion in < 4 μs
   with excellent integral and differential linearity

2. Flash ADCs with Sub-Ranging

   Not all applications require constant absolute resolution over the full range. Sometimes only *relative* resolution must be maintained, especially in systems with a very large dynamic range.

   Precision binary divider at input to determine coarse range + fast flash ADC for fine digitization.

   Example: Fast digitizer that fits in phototube base.
   Designed at FNAL.

   17 to 18 bit dynamic range
   Digital floating point output
   (4 bit exponent, 8+1 bit mantissa)
   16 ns conversion time

10.3 Time Digitizers

1. Counter

Simplest arrangement.

Count clock pulses between start and stop.

Limitation: Speed of counter

Current technology limits speed of counter system to about 1 GHz

➧ Δt = 1 ns

Multi-hit capability

2. Analog Ramp

Commonly used in high-resolution digitizers (Δt = 10 ps)

Principle: charge capacitor through switchable current source

Start pulse: turn on current source

Stop pulse: turn off current source

➧ Voltage on storage capacitor

Use Wilkinson ADC with smaller discharge current to digitize voltage.

Drawbacks: No multi-hit capability
Deadtime

3. Digitizers with Clock Interpolation

Most experiments in HEP require multi-hit capability, no deadtime

Commonly used technique for time digitization (Y. Arai, KEK)

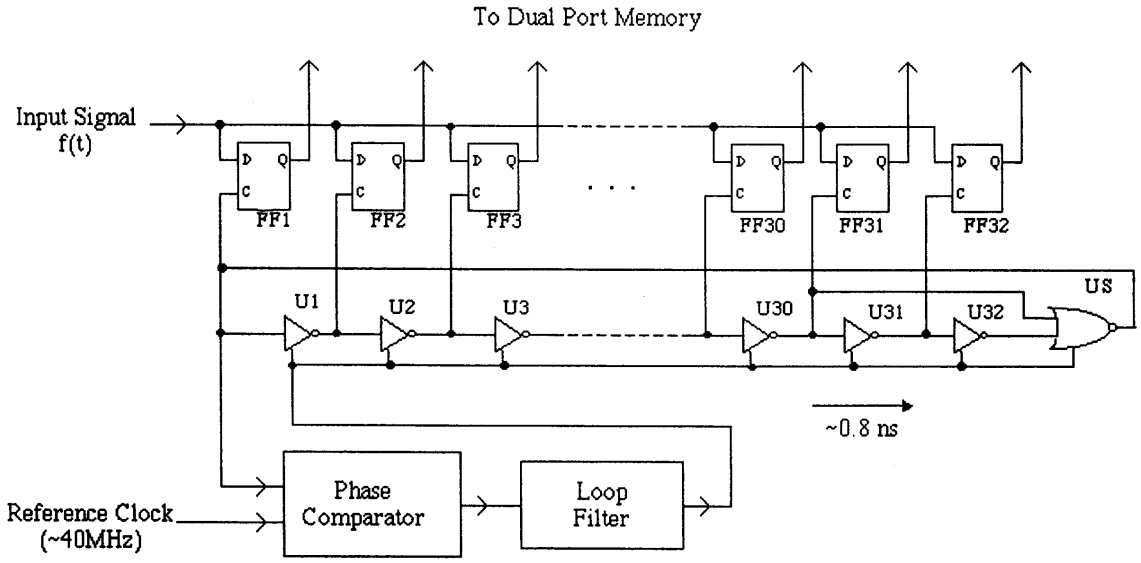

- Digitiging an external signal at a period of internal gate delay of ~0.8ns.
- High Stability with a Phase Locked Loop.
- Long time range (>3 us) & No deadtime by a Dual Port Memory.
- High precision, High Density & Low Cost LSI.

Patent Pending
- S63-067314 (JP)
- H3-133169 (JP)
- H6-69507 (JP)
- 95300652.5 (EU)

Clock period interpolated by inverter delays (U1, U2, …).
Delay can be fine-tuned by adjusting operating point of inverters.

Delays stabilized by delay-locked loop

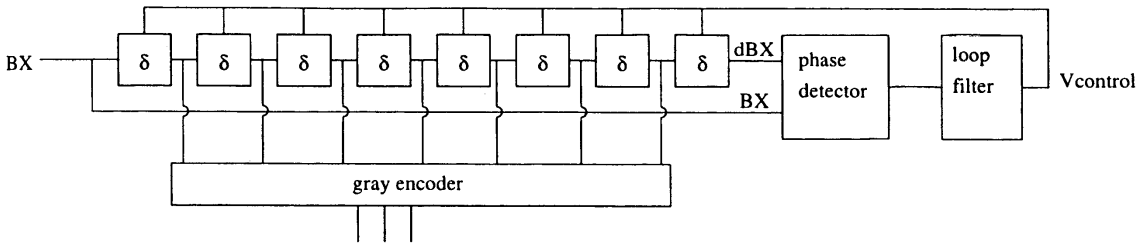

Devices with 250 ps resolution fabricated and tested.

see Y. Arai et al., IEEE Trans. Nucl. Sci. **NS-45/3** (1998) 735-739
and references therein.

11. Digital Signal Processing

Sample detector signal with fast digitizer to reconstruct pulse:

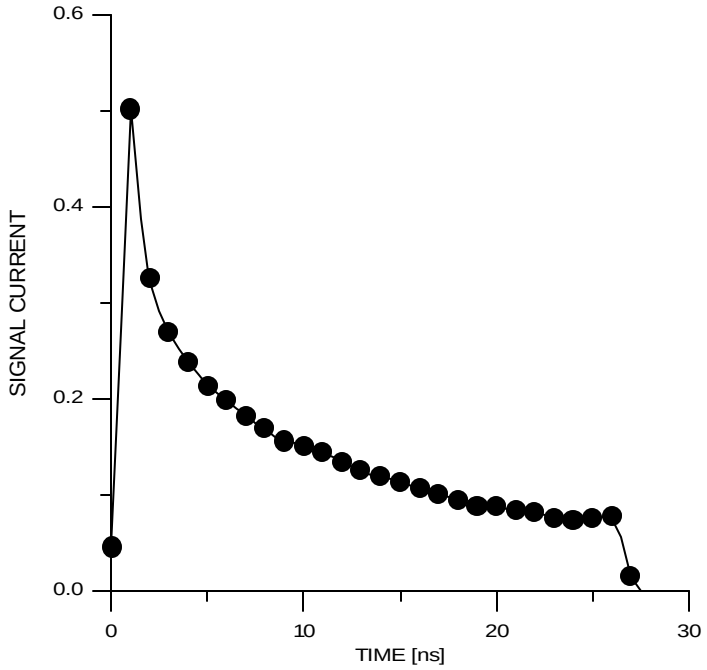

Then use digital signal processor to perform mathematical operations for desired pulse shaping.

Block Diagram

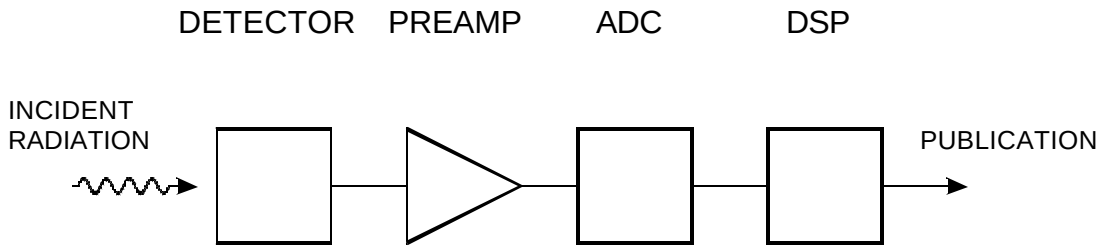

DSP allows great flexibility in implementing filtering functions

However: increased circuit complexity
increased demands on ADC,
compared to traditional shaping.

Example:

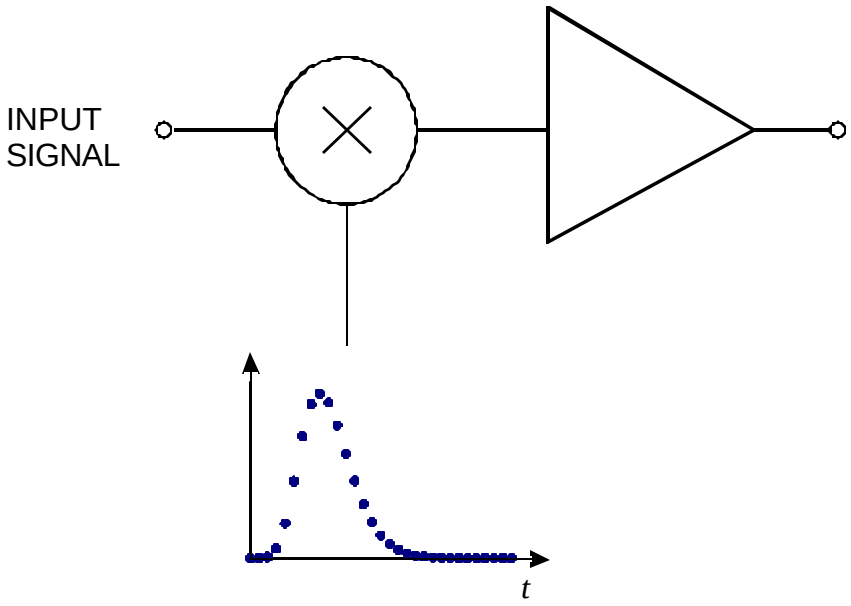

FILTER WEIGHTING FUNCTION

The amplitude of the input signal is multiplied at each discrete time step by a filter weighting function.

The filter function can be calculated in real time by the DSP or it can be stored as values in a look-up table.

This process could be applied to either a continuous or a digitized input signal.

Important to choose sample interval sufficiently small to capture pulse structure.

Sampling interval of 4 ns misses initial peak.

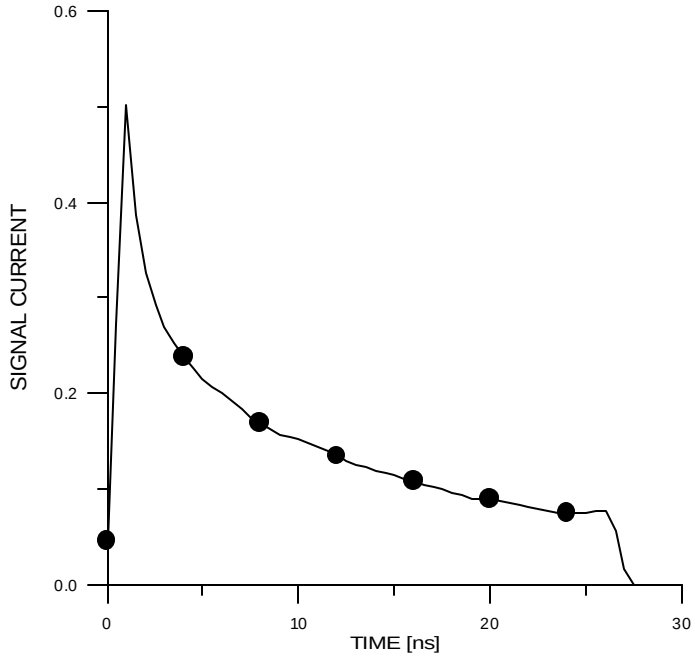

ADC must be capable of digitizing at greater than twice the rate of the highest frequency component in the signal (Nyquist criterion).

With too low a sampling rate high frequency components will be "aliased" to lower frequencies:

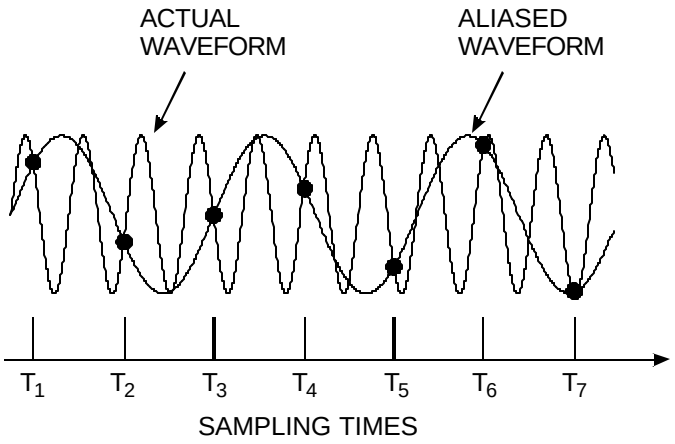

"Aliasing" occurs in any sampling process – i.e. also in 2D or 3D image processing.

Þ Fast ADC required + Pre-Filter to limit signal bandwidth

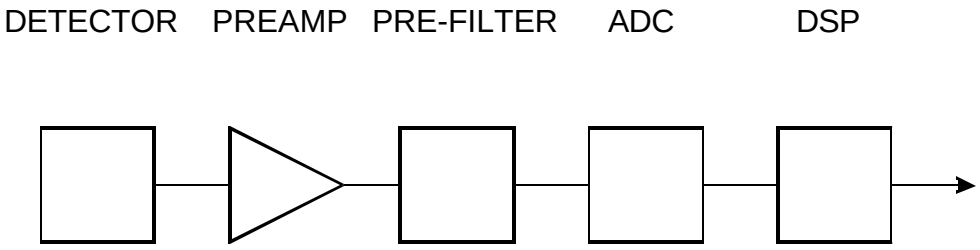

- Dynamic range requirements for ADC may be more severe than in analog filtered system (depending on pulse shape and pre-filter).

- ADC introduces additional noise
  quantization introduces quasi-random noise

$$s_n = \frac{\Delta V_C}{\sqrt{12}}$$

  where ΔV is the signal increment corresponding to 1 bit.
  – increased by differential non-linearity)

- Electronics preceding ADC and front-end of ADC must exhibit same precision as analog system, i.e.

  baseline and other pulse-to-pulse amplitude fluctuations less than order Q_n/10, i.e. typically 10^{-4} in high-resolution systems.

  For 10 V FS at the ADC input in a high-resolution gamma-ray detector system, this corresponds to < 1 mV.

Þ ADC must provide high performance at short conversion times

Today this is technically feasible for some applications, e.g. detectors with moderate to long collection times (γ and x-ray detectors).

Systems commercially available.

Benefits of digital signal processing:

- Flexibility in implementing filter functions
- Filters possible that are impractical in hardware
- Simple to change filter parameters
- Tail cancellation and pile-up rejection easily incorporated
- Adaptive filtering can be used to compensate for pulse shape variations.

Where is digital signal processing appropriate?

- Systems highly optimized for
  - Resolution
  - High counting rates
- Variable detector pulse shapes

Where is analog signal processing best (most efficient)?

- Fast shaping
- Systems not sensitive to pulse shape (fixed shaper constants)
- High density systems that require
  - small circuit area
  - low power

Both types of systems require careful analog design.

Progress in fast ADCs (precision, reduced power) will expand range of DSP applications